The Influence of Power Ultrasound on Setting and Strength Development of Cement Suspensions

DISSERTATION

zur Erlangung des akademischen Grades
Doktor-Ingenieur (Dr.-Ing.)

an der Fakultät Bauingenieurwesen
der Bauhaus-Universität Weimar

vorgelegt von

Simone Peters

Gutachter: Prof. Dr.-Ing. Horst-Michael Ludwig
Prof. Dr. H.F. Reinhard Trettin
Prof.dr.ir. H.J.H (Jos) Brouwers

Die öffentliche Disputation der Arbeit fand am 20.01.2016 in Weimar statt.

Dank

Diese Dissertation entstand während meiner Zeit als wissenschaftliche Mitarbeiterin an der Bauhaus-Universität in Weimar.

Ich möchte mich insbesondere bei Herrn Prof. Dr.-Ing. Horst-Michael Ludwig und Dr. rer. nat. Bernd Möser für die Möglichkeit zur Erarbeitung der vorliegenden Arbeit bedanken.
Besonderer Dank geht darüber hinaus an alle Mitarbeiter des F.A. Finger - Instituts, die mich bei der Durchführung der zahlreichen Untersuchungen unterstützt haben und mit vielfältigen, fachlich interessanten Diskussionen zum Gelingen dieser Arbeit beigetragen haben.

Herzlichen Dank auch an meine Kollegen der Arbeitsgruppe Elektronenmikroskopie/ Zementchemie – es war immer eine Freude, mit euch zu arbeiten!

Meiner Familie danke ich für die ungestörten Stunden im Arbeitszimmer.

Table of Contents

List of Abbreviations

Notations

AFm	Group of calcium aluminate hydrates (Al_2O_3-Fe_2O_3-mono)
ASR	Alkali silica reaction
Aq.	Aqueous
bmoc	By mass of cement
C-S-H	Calcium-silicate-hydrate
CH	Calcium hydroxide, Portlandite
C_3A	Tricalcium aluminate ($3CaO*Al_2O_3$)
C_3S	Tricalcium silicate ($3CaO*SiO_2$)
DEF	Delayed Ettringite formation
El.	Elektrical
Eq.	Equation
FEG	Field Emissions Gun
GGBFS	Grounded granulated blast-furnace slag
HH	Hemihydrate, Bassanite
ICP-OES	Inductively Coupled Plasma-Optical Emissions Spectroskopy
l/s	Liquid to solid ratio
LSP	Limestone Powder
Max.	Maximum
(M)/ (H)PEG	(Methoxy)/ (Hydroxyl)Polyethylene glycol
MZW	Metastable zone width
No.	Number
OPC	Ordinary Portland cement
PC	Polycarboxylate
PUS	Power ultrasound
QXRD	Quantitative X-Ray Diffraction
SCC	Self compacting concrete
SCF	Supercritical fluid
SCM	Secondary cementitious materials
SEM-(SE)	Scanning Electron Microskopy – (Secondary Elektron)
SP	Superplasticizer
TEA	Triethanolamine
TIP	Triisopopanolamine
TLD	Trough the Length Detector
w/b	Water to binder ratio
w/c	Water to cement ratio
7-ACDA	7-amino-3-desacetoxy cephalosporanic acid

Symbols

A	Pre-exponential factor
A	(Surface) Area
a	Radius of spherical particle
α	Hydration degree
E	Energy
E_A	Activation energy
E_v	Specific Energy
f	Frequency of sound
g	Earth´ gravity
$\dot{\gamma}$	Rate of shear
I	Intensity
η	Viscosity
η_{pl}	Plastic viscosity
k	Rate constant
l	Sample width
P_A	Pressure amplitude
P_a	Acoustic pressure
P_{ac}	Acoustic Power
P_h	Hydrostatic pressure
P_{tot}	Total pressure
Q	Reaction heat
R	Universal gas constant (8.314 J/(K*mol))
T	Absolute temperature
t	Time
$t_{ind.}$	Induction Time
ρ'	Density of particle
ρ	Density of fluid
τ	Shear stress
τ_0	Yield stress
x	Displacement
x_0	Maximum displacement
v_p	P-wave velocity
v	Sedimentation velocity
$\Delta_r H^\circ$	Reaction enthalpy

Kurzfassung

Ein aktuelles Thema in der Forschung der Betonindustrie ist die gezielte Steuerung des Erstarrens und der Entwicklung der (Früh)Festigkeit von Betonen und Mörteln. Aus ökonomischer Sicht sind außerdem die Reduktion der CO_2-Emission und die Schonung von Ressourcen und Energie wichtige Forschungsschwerpunkte. Eine Möglichkeit zum Erreichen dieser Ziele ist es, die Reaktivität/Hydratation der silikatischen Klinkerphasen gezielt anzuregen. Neben den bereits bekannten Möglichkeiten der Hydratationsbeschleunigung (u.a. Wärmebehandlung, Zugabe von Salzen) bietet die Anwendung von Power-Ultraschall (PUS) eine weitere Alternative zur Beschleunigung der Zementhydratation. Da bis zum jetzigen Zeitpunkt noch keine Erfahrungen zum Einsatz von PUS in der Zementchemie vorliegen, sollen mit der vorliegenden Arbeit grundlegende Kenntnisse zum Einfluss von PUS auf das Fließ- und Erstarrungsverhalten von Zementsuspensionen erarbeitet werden. Dazu wurde die Arbeit in fünf Hauptuntersuchungsabschnitte aufgeteilt.

Im **ersten Teil** wurden optimale PUS-Parameter wie Amplitude und Energieeintrag ermittelt, die eine effiziente Beschleunigung der Portlandzement(CEM I)hydratation bei kurzen Beschallzeiten und begrenzter Zementleimtemperaturerhöhung erlauben. Mit Hilfe unabhängiger Untersuchungsmethoden (Bestimmung des Erstarrungsbeginns, der Festigkeitsentwicklung, zerstörungsfreier Ultraschallprüfung, isothermer Wärmeflusskalorimetrie, hochauflösender Rasterelektronmikroskopie (REM) wurde die Wirkung von PUS auf den Hydratationsverlauf von CEM I-Suspensionen charakterisiert. Die Ergebnisse zeigen, dass die Behandlung von CEM I-Suspensionen mit PUS grundsätzlich ein beschleunigtes Erstarren und eine beschleunigte (Früh)Festigkeitsentwicklung hervorruft. Anhand von REM-Untersuchungen konnte eindeutig nachgewiesen werden, dass die Beschleunigung der CEM I-Hydratation mit einer beschleunigten Hydratation der Hauptklinkerphase Alit korreliert. Auf Grundlage dieser Erkenntnisse wurden die Ursachen der Aktivierung der Alithydratation untersucht. Dazu wurden Untersuchungen an Einzelsystemen des CEM I (silikatische Klinkerphase) durchgeführt.
Es ist bekannt, das die Hydratation der Hauptklinkerphase Alit (in der reinen Form Tricalciumsilikat $3CaO*SiO_2$; C_3S) durch Lösungs-/Fällungsreaktionen (Bildung von Calcium-Silikat-Hydrat Phasen, C-S-H Phasen) bestimmt wird. Mit Hilfe von Untersuchungen zur Auflösung (C_3S) und Kristallbildung (C-S-H Phasen) in Lösungen und Suspensionen (Aufzeichnung der elektrischen Leitfähigkeit sowie Bestimmung der Ionenkonzentrationen der wässrigen Phase, REM-Charakterisierung der Präzipitate) wurde die Beeinflussung dieser durch eine PUS-Behandlung charakterisiert. Die Ergebnisse zeigen, dass in partikelfreien Lösungen (primäre Keimbildung) eine PUS-Behandlung keinen Einfluss auf die Kinetik der Kristallisation von C-S-H Phasen hervorruft. Das heißt, auch die durch PUS eingetragene Energie reicht offensichtlich nicht aus, um in Abwesenheit von Oberflächen die C-S-H Phasen Bildung zu beschleunigen. Das weist darauf hin, dass die Bildung von C-S-H Phasen nicht durch eine Beschleunigung von Ionen in der Lösung (erhöhte Diffusion durch Anwendung von PUS) hervorgerufen wird. Eine Beschleunigung des Kristallisationsprozesses (Keimbildung und Wachstum von C-S-H Phasen) durch PUS wird

nur in Anwesenheit von Partikeln in der Lösung (Suspension) erzielt. Das belegen Ergebnisse, bei denen die Bildung erster C-S-H Phasen bei geringer Übersättigung (heterogene Keimbildung, in Anwesenheit von Oberflächen) erfolgt. Unter diesen Bedingungen konnte gezeigt werden, dass PUS innerhalb der ersten 30 Minuten der Hydratation eine erhöhte Fällung von ersten C-S-H Phasen bewirkt. Diese fungieren dann vermutlich während der Haupthydratation als Keim bzw. geeignete Oberfläche zum beschleunigten Aufwachsen von weiteren C-S-H Phasen. Weiterhin ist vorstellbar, dass (in Analogie zu anderen Bereichen der Sonochemie) PUS durch Kavitation Schockwellen hervorruft[i], welche Partikel und wässriges Medium beschleunigen und damit erhöhte Partikelbewegungen und -kollisionen induziert. Dies wiederum bewirkt, dass die anfänglich auf der C_3S-Oberfläche gebildeten C-S-H Phasen teilweise wieder entfernt werden. Damit ist das Inlösunggehen von Ca- und Si-Ionen aus dem C_3S weiterhin möglich. Um den genauen Mechanismus weiter zu charakterisieren sollten mit geeigneten Methoden weitere Untersuchungen durchgeführt werden.

Im **zweiten Teil** der Arbeit wurde der Einfluss von PUS auf das Fließverhalten von CEM I-Suspensionen untersucht. Aus der Anwendung von PUS in anderen technischen Bereichen sind unter anderem Effekte wie das Entlüften, das Homogenisieren und das Dispergieren von Suspensionen und Emulsionen mittels PUS bekannt. Mit Hilfe der Bestimmung des Luftporengehaltes, Sedimentationsversuchen und cryo-SEM Untersuchungen wurde der Einfluss von PUS auf CEM I-Suspensionen charakterisiert. Die Ergebnisse belegen, dass durch PUS eine verbesserte Homogenität und Dispergierung der CEM I-Suspension erzielt wird. Damit wird für CEM I-Suspensionen unterschiedlichster w/z-Werte eine verbesserte Fließfähigkeit festgestellt. Ergebnisse der Bestimmung von Ausbreitmaßen und Trichterauslaufzeiten zeigen, dass PUS einen direkten Einfluss vor allem auf die Viskosität der CEM I-Suspensionen besitzt. Werden Fließmitteln (FM) der CEM I-Suspension zugegeben, wird nicht in jedem Fall eine verbesserte Fließfähigkeit festgestellt. Hier scheint unter bestimmten Voraussetzungen (w/z-Wert, FM-Gehalt, PUS) die Reaktion zwischen Aluminat- und Sulfatphase des Klinkers gestört. Zur eindeutigen Klärung dieses Sachverhaltes bedarf es jedoch weiterer quantitativer Untersuchungen zum Reaktionsumsatz.

Im **dritten Teil** der Arbeit wurden die am CEM I gewonnenen Erkenntnisse zum Einfluss von PUS auf die Hydratation an Portland-Hüttensand(HÜS)-Zement-Systemen verifiziert. Dafür wurden auch in diesem Teil der Arbeit zunächst die optimalen PUS-Parameter festgelegt und der Einfluss auf das Erstarrung- und Erhärtungsverhalten dokumentiert. Untersuchungsmethoden sind unter anderem die Bestimmung des Erstarrungsbeginns und der (Früh)Festigkeitsentwicklung, Temperaturaufzeichnungen und isothermale Wärmeflusskalorimetrie sowie REM. Die Ergebnisse zeigen, dass auch die Reaktion von HÜS-Zementen durch PUS beschleunigt wird. Weiterführende Untersuchungen belegen,

[i] Mason, T.J.; Lorimer, J.P (2002): *Applied Sonochemistry*. Wiley-VCH Verlag GmbH, Weinheim.

dass die erzielte Beschleunigung vorwiegend auf der Beschleunigung der Alitkomponente des CEM I beruht.

Im Fokus der **Teile vier und fünf** dieser Arbeit stand die Anwendbarkeit der PUS-Technik unter praktischen Bedingungen. Zum einen wurde die Anwendbarkeit von PUS in fertig gemischten Mörteln beurteilt. Anhand des Vergleichs wichtiger Frisch- und Festmörteleigenschaften unterschiedlich hergestellter Mörtel (beschallt im Anschluss an konventionelle Mischtechnik, beschallt im Anschluss an Suspensionsmischtechnik mit anschließender Zumischung der Gesteinskörnung und nicht beschallt) wird gezeigt, dass im Fall von Mörteln mit hohem Leimanteil eine durch PUS induzierte beschleunigte Festigkeitsentwicklung auch mit herkömmlichen Mischabläufen (ohne aufwendige Umstellung des Mischprozesses) möglich ist.
Abschließend wird untersucht, ob der Herstellungsprozess von Wandbauteilen im Fertigteilwerk durch den Einsatz von PUS optimiert werden kann und ob eine Einbindung der PUS-Technik in den Fertigungsprozess ohne größeren Aufwand möglich ist. Dazu wurden in einem ersten Schritt die Frisch- und Festbetoneigenschaften eines aktuell angewendeten selbstverdichtenden Betons im Labormaßstab (Mörtel) in Abhängigkeit einer PUS-Behandlung dokumentiert und mit der seiner unbeschallten Referenz verglichen. Aufgrund der durch PUS verursachten verbesserten Fließ- und Festigkeitseigenschaften kann die beschallte Mörtelrezeptur hinsichtlich Fließmittelgehalt und Dauer der Wärmebehandlung optimiert werden. Somit werden ca. 30 % der Fließmittelzugabe und 40 % der Dauer der Wärmebehandlung eigespart. Eine Einbindung der PUS-Technik in das betrachtete Fertigteilwerk ist nach Überprüfung der konstruktiven Gegebenheiten der Fertigungsstrukturen ohne größeren Aufwand möglich.

Abstract

A current topic in the field of cement research is to influence setting and early strength development of concretes and mortars in a target manner. Furthermore, from an economical point of view another challenging aim is to reduce CO_2 emission and to save energy and resources. One possibility to achieve these ambiguous goals is to activate/accelerate the reactivity/hydration of the silicate phase of clinker. Besides usually applied approaches to enhance hydration process (amongst others addition of admixtures, heat treatment), power ultrasound (PUS) provides another alternative to accelerate cement hydration. However, up to now there exist no experiences in using PUS in the field of cements chemistry. Thus, the subject of this thesis is to gain a fundamental knowledge of how PUS influences the fluidity and strength development of cement suspensions. Therefore the study is divided in five main parts.

In the **first part**, optimum PUS parameters (amplitude, specific energy input) were determined attaining efficient acceleration of ordinary Portland cement (OPC) hydration taking account applicational aspects (short PUS duration, constrained suspension temperature). Using independent tests (determination of setting time, strength development, non-destructive ultrasound measurements, isothermal heat conduction calorimetry, high resolution scanning electron microscopy SEM) the influence of PUS on hydration of OPC suspensions was characterized. Results show that PUS application generally causes an accelerated setting and strength development of OPC suspensions/mortars. SEM investigations clearly evidence that accelerated cement hydration correlates with an accelerated hydration of the main clinker phase of OPC that is alite. On the basis of these findings the reason for the activated alite hydration was investigated. For that purpose investigations on pure systems (silicate phase) were performed.
It is known that the hydration process of the main clinker phase alite (as pure substance tricalciumsilicate $3CaO*SiO_2$; C_3S) is governed by dissolution/precipitation processes (precipitation of calcium-silicate-hydrate phases, C-S-H phases). Based on experimental studies (recording development of electrical conductivity, determination of ion concentration in aqueous phase, SEM characterization of precipitates) the influence of sonication on dissolution (C_3S) and precipitation (C-S-H phases) in solutions and suspensions was characterized. Results clearly show that PUS application has no effect on crystallization kinetics of C-S-H phases in particle-free solutions (primary nucleation). In other words, even with the energy input induced by sonication the formation of C-S-H phases could not be accelerated in the absence of particle surfaces. This indicates that formation of C-S-H phases is not initiated by the acceleration of ions in the solution (increased diffusion by PUS application). An accelerated crystallization process (nucleation and growth of C-S-H phases) due to PUS treatment is only observed when particles are present in solutions (suspension). This is confirmed by results where precipitation of first C-S-H phases is obtained at low supersaturation (heterogeneous nucleation, in presence of particle surfaces). Under these conditions it was demonstrated that applied PUS causes increased precipitation of very first C-S-H phases during first 30 minutes of hydration. In the following these very first C-S-H

phases probably serve as nucleation sites and/or provide appropriate surfaces for additional C-S-H phases to grow. Moreover it is also conceivable that (analogous to other research areas of sonochemistry) cavitation, induced by PUS, accelerates particles and aqueous media and thus initiate accelerated particle movements and increased particle collisions. Consequently first C-S-H phases grown on C_3S surfaces are partially removed again. This enables a continuous release of Ca and Si ions from C_3S dissolution. To characterize this mechanism in more detail further investigations should be done.

In the **second part** the influence of PUS on fluidity of OPC suspensions was investigated. Amongst others the de-airing effect, homogenizing and dispersing of suspensions and emulsions by PUS is known from wide spread technical applications. Based on the determination of air void content, sedimentation experiments and cryo-SEM conductions the influence of PUS on OPC suspensions was characterized. Results evidence an increased homogeneity and dispersion caused by PUS treatment. As a consequence, increased fluidity was determined for OPC suspensions at diverse water to cement ratios (w/c ratio). Results of the determination of spread flow diameters and V-funnel flow time reveal that PUS influences primarily viscosity of OPC suspensions. When superplasticizer (SP) is added to the mix liquefaction is not generally observed. Based on actual results it is deduced that under certain conditions (w/c ratio, SP content, PUS) the reaction between aluminate phase and sulfate phase (set regulator) is disturbed. However, clarification of observed reduction in fluidity requires further quantitative analyses.

In the **third part**, results obtained for OPC system should be verified for slag cement systems. Hence, comparable to the procedure described above (in OPC system) firstly optimum PUS Parameters were defined. The influence of PUS application on setting and strength development was documented. Analogous to previous investigations setting time and strength development were determined. Additionally development of sample temperature, isothermal heat conduction calorimetry and SEM examination were performed. Results clearly show that PUS application causes accelerated slag cement hydration. However, in-depth investigations reveal that obtained acceleration of slag cement hydration mainly accounts on the accelerated alite hydration of remaining OPC.

Practical aspects applying PUS in concrete production were in focus of **part four and five** of this thesis. Assumed that the effect of PUS is most effective in cement suspensions (sufficient availability of liquid phase) the question was, if PUS can also be applied to ready mixed mortars. Comparing important properties of fresh and hardened mortars produced by divers mixing designs (sonication follows conventional mixing, sonication of suspension with subsequent addition of aggregates, unsonicated reference) it becomes obvious that accelerated strength development is observed even when PUS is applied after conventional mixing process. Prerequisite is the existence of sufficiently high lime content.
Finally, it was verified if the precast production process of wallboards can be optimized by PUS application. Moreover, ways to implement the PUS technique in concrete production were discussed. For this reason the commercial used self compacting concrete (SCC)

mixture was downscaled to mortar. Properties of fresh and hardened mortars were documented in dependence of PUS application. Due to increased fluidity and strength development induced by PUS treatment mixture was optimized in view of SP addition and heat treatment duration. In consequence this enables to save 30 % of SP addition and 40 % of heat treatment duration. At last, the expertise of the plant construction reveals the possibility to implement the PUS technique without many efforts.

1. Introduction

Since more than 100 years concrete is the most important building material in human life. Nowadays building concrete structures are not only simple blocks but frequently have high aesthetic demands. Hence, more and more tailor made concretes with optimal concrete performances are required. A convenient opportunity to ensure sophisticated concrete elements with constant high quality is precast production. Of course, conditional on current market situation, an efficient economic and ecological (reduction of CO_2 emission, preserving resources) production process is essential.

The most important requirement for precast production is a fast early strength development coupled with adequate workability of fresh concrete. Besides applying appropriate concrete mixtures (i.e. low water to cement ratio, high cement content, cement with high strength class) accelerating admixtures and heat treatment are available to achieve sufficient early strength development. Adversely inappropriate application of both methods may induce durability risks (corrosion effects, delayed ettringite formation). Furthermore heating of formworks disagrees with recent economic (efficient and low cost production) and ecologic (reduction of CO_2 emission, preserving natural and/ or energy resources) requirements.

For the same economic and ecological reasons another challenging aim considering sustainability of concrete is to substitute Portland cement clinker by appropriate secondary cementitious materials (SCM, e.g. ground granulated blast-furnace slag: GGBFS, limestone, metakaolin). A prerequisite is that properties (strength development, durability) of resulting concretes were just equivalent, if not better, than concrete made of pure ordinary Portland cement (OPC). Since the major problem in this content seems to be the very early strength development, the focus is to accelerate cement hydration of blended cements. However, all methods that enhance strength development in OPC did not succeed to accelerate SCM content in composite cements satisfactorily (i.e. mainly alite hydration is influenced). Nevertheless, accelerated hydration of fly ash and alkali activated slag paste at early ages by novel acceleration admixtures (nano-sized SiO_2, synthetic C-S-H) was proven for pure SCM systems[1,2].

A further promising method to influence setting and strength development is the application of power ultrasound (PUS). Results of previous investigations in the field of sonochemistry prove the influence of PUS on chemical reactions[112,113,114,115,111,107,116,117,103,130,109,110,105,108,106,92,102]. Therefore present work investigates the effects on cement hydration induced by PUS application. Besides the identification of suitable PUS parameter, the influence of sonication on setting, strength development and workability (fluidity) of various cement suspensions/ mortars is evaluated. Additionally, since alite is the most important clinker phase for cement hydration, more detailed investigations are performed using the model substance tricalcium silicate (C_3S) to gain a basic understanding on how PUS influences hydration progress. Furthermore, the capability to accelerate hydration of SCM induced by PUS is investigated for grounded granulated blast-furnace slag (GGBFS). Finally, to estimate the capability to use the PUS technique in concrete production a feasibility study was performed.

2. State of the art

2.1. Acceleration of cement hydration

2.1.1. Cement hydration in general

Generally setting and hardening of concrete is linked with the hydration of cement paste ("glue" between aggregates). Since cement is a composition of several compounds (clinker phases, set regulator, additives and/ or admixtures) the hydration is a complex process that is in focus of numerous studies (summarized in books[34,3] and review articles[4,8,5]). Whereas certain aspects are still under debate it is generally agreed that the hydration of clinker phases/ C_3S proceeds via dissolution and precipitation reactions[52,48,34] with concurrent heat release. Therefore one commonly used method to investigate cement (respectively C_3S) hydration kinetics is heat flow calorimetry. Thereby, every single clinker compound possesses characteristic hydration kinetics. Consequently, the heat release rate during (Portland) cement hydration monitored by isothermal conductivity is a non-monotonic process (**Figure 1**).

As shown in **Figure 1** different stages of (Portland) cement hydration are distinguished in dependence of the current heat release rate. These periods are known to be I) the initial period, II) the dormant/ induction period (period of low reaction rate), III) the acceleration period, IV) the deceleration period, and sometimes additionally V) the constant period (**Figure 1**).[3,18,6,7,8]

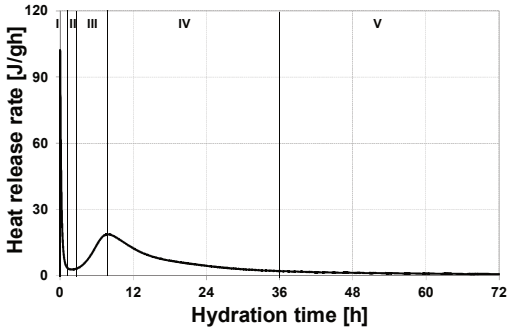

Figure 1: General heat release rate of cement hydration in dependence of time measured by isothermal calorimetry.

When cement gets in contact with water, a first exothermic peak can be observed in the heat flow diagram. This initial reaction (period I, **Figure 1**) is attributed to several simultaneous processes: a) the wetting of the cement particles, b) the heat release due to the reaction of free lime, c) the dissociation of alkali sulfates, and d) the precipitation of primary hydration products (especially ettringite).[9] Ettringite precipitates due to the reaction of the calcium aluminate clinker phase (C_3A) with sulfate ions provided by the dissolution of setting regulator ($CaSO_4*nH_2O$) or soluble alkali sulfates (K_2SO_4, Na_2SO_4). Additionally, in dependence of cement composition (alkali sulphates, free lime) other hydration products are observed (secondary gypsum, syngenite, portlandite)[3,9,10,11,12,13]. However, for the initial period a significant percentage to the heat release due to calcium

silicate hydrate (C-S-H) formation (from alite hydration) was excluded by Stark et al.[9]. Subsequent to the impetuous initial reaction, all reactions are slowed down. Significant heat release cannot be determined during this so called induction period of hydration (period II, **Figure 1**). The onset of the acceleration period (period with major heat release rate, period III, **Figure 1**) for cement hydration is associated with the hydration of the main clinker phase alite[14,15] and thus with the formation and growth of C-S-H phases. Subsequent deceleration period (period IV, **Figure 1**) is characterized by reducing heat release rate with time. With ongoing reaction process cement particles become covered with precipitates (especially C-S-H phases). This, on the one hand reduces the available surface for growth. On the other hand continuous supply of ions from dissolving solids becomes hindered[18,7]. Thus, at later age, deceleration period becomes diffusion controlled[1] and enters in a steady state (period V, **Figure 1**).

The strength determining and thus most important Portland cement clinker phase is alite (50 m.-% to 70 m.-% of OPC). Alite can be represented by the model substance tricalcium silicate (C_3S). This phase, due to its importance for concretes strength and durability properties, occupies an outstanding position in the field of cement hydration research. Understanding the fundamental principles of physico/ chemical processes during C_3S hydration is the basis to understand the more complex process of overall cement hydration. Consequently, numerous investigations focus on C_3S hydration, especially on the origin of the induction period (period of low reaction that enables workability of concrete). From a lively debate to this topic (origin of induction period) two hypotheses becomes most important (latest reviewed by Sowoidnich[136]), being the formation of a metastable hydrate layer[16,17,18,19,39] and the slow dissolution step hypothesis[5,20,52] (developed from the concept of "superficially hydroxylated C_3S" [21]).

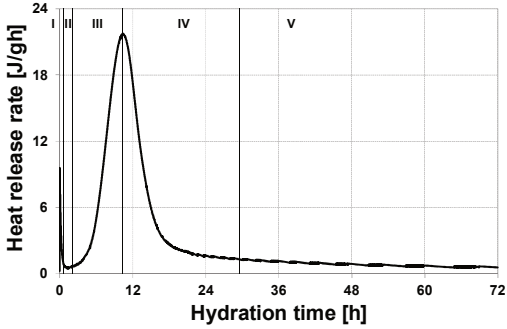

Figure 2: General heat release rate of C_3S hydration in dependence of time measured by isothermal calorimetry.

The development of heat release during C_3S hydration proceeds similar to that of OPC (**Figure 2**): The first exothermic peak during C_3S hydration (period I, **Figure 2**) is due to the wetting and the initial congruent dissolution of C_3S (less than 1 %[22])[3,8]. Subsequently, similar as for cement hydration, a period of slow reaction rate (induction period) is observed (period II, **Figure 2**). As mentioned before, the origin of the induction period is not fully clarified yet. Afterwards the third period (acceleration period, period III,

Figure 2) is related to a nucleation and growth mechanism where the hydration rate increases[8].
Analogous to autocatalytic chemical reactions the rate-controlling step is related to the heterogeneous nucleation/ growth of C-S-H on C_3S surfaces and other suitable mineral surfaces[18,8]. During the deceleration period (period IV, **Figure 2**) reaction rate declines again until a steady reaction rate is reached (period V, **Figure 2**), governed by diffusion controlled processes.

Another suitable method to investigate C_3S hydration process is the determination of electrical conductivity in diluted suspensions. Diluted conditions (i.e. w/s > 10[134]) lengthen the very early reaction steps and thus more detailed information can be obtained. According to Damidot et al.[134] the development of the electrical conductivity (el. conductivity) in diluted suspensions during C_3S hydration can be divided into five periods (**Figure 3**).

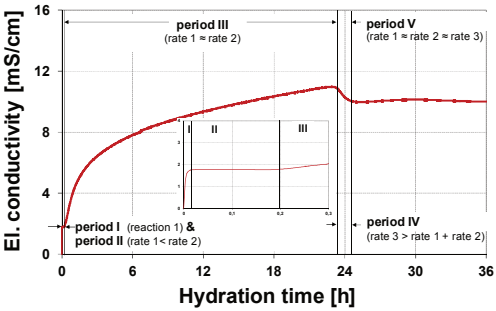

Figure 3: Reaction stages (I-V) as defined by the el. conductivity curve during the hydration process of C_3S in diluted suspension according to Damidot[134], inlet detailed period I & II. (rate 1 = rate reaction of C_3S dissolution, rate 2 = rate reaction of C-S-H precipitation, rate 3 = rate reaction of portlandite precipitation).

Immediately after the contact with water C_3S initially dissolves congruently (**Eq. 1**)[3] and solution is enriched by Ca and Si ions until it becomes supersaturated with respect to C-S-H (increase of the el. conductivity, period I, **Figure 3**).

C_3S ($3Ca^{2+}$:O^{2-}:SiO_4) + excess water → $3Ca^{2+}$(aq.) + $4OH^-$(aq.) + $H_2SiO_4^{2-}$(aq.) **Eq. 1**

Subsequently first C-S-H nuclei are formed during induction period (period II, see inset in **Figure 3**). While Ca ion consumption due to C-S-H precipitation equals release of Ca ions due to dissolution of C_3S (C-S-H precipitation rate is greater than C_3S dissolution rate) the el. conductivity of diluted suspension remains constant during this period of time. In the third period (period III, **Figure 3**) growth of C-S-H phases proceeds whereas the precipitation rate equals the C_3S dissolution rate. Since not all Ca ions are consumed during C-S-H precipitation, suspension becomes enriched with Ca and OH ions (the el. conductivity increases again). After supersaturation with regard to portlandite is reached, this phase precipitates as indicated by a significant decrease of the el. conductivity (period IV, **Figure 3**). Finally equilibrium of dissolution and precipitation is reached (period V, **Figure 3**). For this period (V) the reaction rate of dissolution of C_3S, precipitation of C-S-H and portlandite, respectively are all the same.[134]

2.1.2. Acceleration of cement hydration by salts, heat treatment, and seeds

There are various methods to accelerate cement hydration. Most commonly used are the addition of chemical admixtures and heat treatment (especially in precast production), respectively. As mentioned before, these methods may induce disadvantages concerning durability if they are not properly applied. Additionally, poor long term properties as reduced compressive strength and reduced elastic modulus at later ages have been reported[6,23,(24),25,46].

As summarized by Cheung et.al[26] common chemical accelerators are the group of soluble inorganic salts (chlorides, bromides, fluorides, carbonates, thiocyanates, nitrites, nitrates, thiosulfates, silicates, aluminates, and alkali hydroxides), soluble organic compounds (triethanolamine: TEA – known from the use as grinding aid for Portland cement clinker, triisopropanolamine: TIP), and admixtures for shotcrete production (alkali aluminates, aluminum chloride, alkali-free acid solutions of aluminum salts), respectively.
Most effective and cheapest inorganic salt for accelerating cement and C_3S hydration is calcium chloride[27,28.29]. Generally, the addition of calcium chloride (most commonly 2 m.-% $CaCl_2$ by mass of cement)[34] significantly accelerates main reaction[27], i.e. the rate of C-S-H formation/ growth is increased[30,34,31] that is essential for strength development. However, chloride ions cause depassivation of steel in reinforced concrete even in the alkaline environment of the cement matrix[32,33]. Consequently, corrosion effects (formation of expanding corrosion products) cause cracking of concrete[32,34]. Thus the application of $CaCl_2$ as accelerator is not longer used in reinforced concrete production. Besides $CaCl_2$, calcium formate and calcium nitrate are also commonly used accelerators. In fact they also may promote corrosion and thus are not suitable for pre-stressed concrete constructions.
Alkali-free accelerators such as aluminum sulfates and aluminum hydroxide are used as accelerators for shotcrete production[35,36], because they accelerate the setting of cement. As given by Xu[36] the formation of C-A-H phases and additional ettringite formation could be proven to be the reason for accelerated set of concrete. Thereby, the long prismatic habitus of precipitating ettringite was shown to be disadvantageous for the development of a dense microstructure[36]. As a result durability and final strength[36] may be reduced. Furthermore high alkali contents harbor the risk of alkali-silica reactions (ASR) and excess aluminum may cause secondary ettringite formation in the case of sulfate attack.[36]

In precast concrete production systematic heating of formworks is the most common method to accelerate strength development. Due to thermal treatment the overall hydration is accelerated as illustrated by the Arrhenius equation (**Eq.2**).

$$k = A \cdot e^{-E_A/(R \cdot T)}, \qquad \textbf{Eq. 2}$$

where k is the rate constant, A is the pre-exponential factor, E_A is the activation energy given in J/mol, R is the universal gas constant (8.314 J/(K*mol)) and T is the absolute temperature given in Kelvin. From **Eq. 2** it can be inferred that either an increased temperature or decreased activation energy leads to an increased rate of reaction. Currently in precast concrete production this is the most widely used approach to decrease the induction period of cement hydration and thus increase the early strength of concrete.
In fact, the accelerating effects by heating include all components of cement and, therefore, C-S-H formation. Mayor disadvantage linked to heat treatment is the phenomenon known as delayed ettringite formation (DEF): At increasing temperatures (> 60°C dependent on the alkali content) the chemical stability of ettringite ($3CaO \cdot Al_2O_3 \cdot 3CaSO_4 \cdot 32H_2O$) decreases and monosulfate ($3CaO \cdot Al_2O_3 \cdot CaSO_4 \cdot 12H_2O$) is becoming the thermodynamically more stable phase[34,37]. If temperature is later on decreased again this process is reversed (transition from monosulfate to ettringite). This transition is related to significant volume changes. This process of concrete damage is known as DEF (delayed ettringite formation[38]). To avoid this durability risk heating of concrete has to be limited to a maximal temperature of 55 °C (according to DBS 918 143: 03/2010).

Recent investigations show that the addition of heterogeneous nucleation sites ($Ca(OH)_2$[39,40,41,42], $CaCO_3$[43], (synthetic) C-S-H phases[44,45] (x-seed®)[46,47,48,], nano-sized SiO_2[49,50,51]) cause a substantial acceleration in the hydration of cement and C_3S, respectively. The initial consideration was that nucleation can be accelerated when crystallization surfaces are provided. Among other things Garrault-Gauffinet et.al[52] investigated the influence of the presence of calcite, C_2S and C_3S surfaces on C-S-H nucleation. They could evidence that C_3S is the most favored surface for heterogeneous C-S-H nucleation compared to surfaces of C_2S and calcite. Later Thomas et al.[48] described the accelerating effect of a well-dispersed form of C-S-H on the C_3S hydration for the first time. Based on the theory of autocatalytic C-S-H formation they show that seeding with C-S-H a) eliminates the induction period, b) increases the acceleration of early hydration rate and the maximum of hydration rate, and c) increases the total amount of hydration. Alizadeh et al.[44] could prove that dissolution of C_3S is significantly enhanced due to nucleation/ growth of C-S-H on supplied C-S-H seeds. However, seeding materials always influence material chemistry and in the case of synthetic C-S-H are still very expensive. Also handling might be difficult since especially synthetic C-S-H is offered as aqueous suspension.

2.2. Fluidity of cement suspensions

Workability of concrete includes mixing, placing, compacting and curing[53]. Hence, workability is used to refer to individual stages of the process of concrete production. In this content the fluidity (consistency) of fresh concrete is crucial since it influences mixing time, pumpability and required compaction work. "Rheology as the science of the deformation and flow of matter"[54] is used to estimate concretes/ mortars/ and cement suspensions workability (fluidity)[55]. The simplest rheological behavior (fluids) can be observed for ideal viscous materials (water) following the Newton´s law[53] ($\tau = \eta \dot{\gamma}$), were τ is the shear stress, η is the viscosity of the fluid and $\dot{\gamma}$ is the rate of shear.

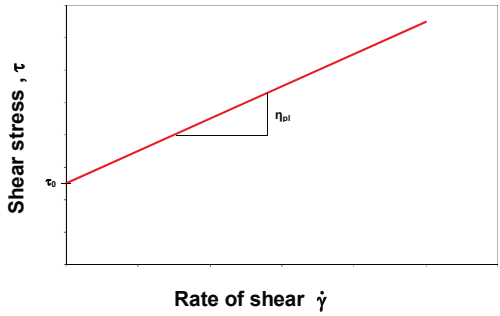

Figure 4: Bingham model.

However, for most suspensions (also for concrete) a minimum stress (the yield stress τ_0) is required for irreversible deformation and thus to initiate flow[56,65] (**Figure 4**). Thus, the mathematical description becomes

$$\tau = \tau_0 + \eta_{pl} \dot{\gamma} \qquad \textbf{Eq. 3}$$

that is known as the Bingham model. From **Eq. 3** it becomes obvious that fluidity of concrete is characterized by two rheological parameters that are the yield stress τ_0 and the plastic viscosity η_{pl}. The latter displays the slope of the straight line (**Figure 4**). In concentrated mineral suspensions (such as concrete/ mortar and cement suspension)[55] rheological parameters are governed by interparticle forces (van der Waals forces, electrical double layer forces, structural, hydrophobic, steric, bridging and depletion forces)[54,57,58,59] that are amongst others influenced by particle concentration[60,64,58], particle shape[65] and their size distribution[58,61], specific surface area[62], and the composition of solution[54]. To get information of these fundamental physical parameters (τ_0 & η_{pl}) several rheological measurements are available (e.g. stress rheometer, pulse shearometer, coaxial (double)-cylinder viscosimeter)[54,55,64]. However, the usage of this methods to determine rheological parameters for fresh concretes is often impracticable, expensive and requires much effort[54,56,64,63].
A more simple and cheap test method to estimate fluidity (yield stress and viscosity) of concrete was demonstrated to be the slump test[64] (mini cone test) and the V-funnel test[65,66] (Marsh cone test), respectively. It is generally accepted that the slump is mainly correlated with yield stress[63,64,67,68] and the V-funnel flow time is mostly influenced by viscosity[69,70].

Although there is much effort to relate e.g. determined slump to yield stress by mathematical models[55,71,72,56,63,67] there is still discrepancy between prediction and experimental results in many cases. Nevertheless the slump test as well as V-funnel flow time is an appropriate *in situ* test providing not absolute physical parameters (τ_0 & η_{pl}) but a classification of concrete/ mortar and cement paste[56,67].

Nowadays, to guaranty sufficient fluidity of concrete high efficient dispersing admixtures (superplasticizer, SP) based on polycarboxylates (PC) are added to the concrete mix. Although there are various products in the market, polycarboxylate based SPs are typically built of a backbone (commonly acrylic acid) and monomeric side chains of polyethyleneglycol (PEG). Linkage is performed via esterification, etherification, amids or imids. Every side chain ends up either with a methoxy group (termed methoxy polyethylenglycol: MPEG) or a hydroxyl group (termed hydroxyl polyethylenglycol: HPEG). To give a quick idea of the visual nature of these SPs it may be compared to a comb or bottle brush. When SPs are added to cement paste they adsorb at cement surfaces (via functional groups) and lead to repulsion and/ or steric hindrance. Thus particles are separated and consequently dispersion is increased. However, the drawback of superplasticizer addition is the retardation of cement hydration progress. Significant prolongation of the induction period leads to delayed compressive strength development. At the application side, e.g. in precast production, this in consequence increases formwork periods.[73]

2.3. Power ultrasound

In general sound is defined as waves of compression and expansion crossing gases, liquids or solids. Talking about ultrasound these sound waves possess frequencies above human hearing (approximately 20 kHz to 100 kHz[81,74,75]). To generate ultrasound most commonly a piezoelectric ceramic is exposed to a high altering electric current. In this electrical field the piezoelectric ceramic expands and contracts. Consequently occurring mechanical vibrations are transferred e.g. via an amplifying horn into the medium.
In 1894 fatal vibrations were noticed by Thornycroft and Barnaby for the first time. They observed significant erosions on the screw – propeller of British destroyers. Later (1917) Lord Rayleigh evolve a first mathematical model in order to calculate the pressure in a fluid during cavitation collapse[76]. The chemical effects of ultrasound were first investigated by a group around Alfred Lee Loomis in 1927[77]. Besides the description of discharging effects due to irradiation as well as "atomizing" effects they also call for attention to the fact that the temperature raises due to energy absorption. Among other things they could evidence the de-airing effect of PUS as well as the acceleration of certain chemical reactions.[77] In following years Patents on cleaning (1943, DE 733470C) and emulsification (Swiss Patent 394.390) were granted. Since the 1950´s research in the field of ultrasound and cavitation becomes intensified. The number of applications for ultrasound still increases.

2.3.1. General mode of action of power ultrasound in liquids

Because the velocity of sound in liquids is approximately 1500 m/s and related acoustic wavelengths of ultrasound (20 kHz to 100 kHz) ranges from 10 to 0.01 cm, effects on molecular dimensions as a result of ultrasonic irradiation is not expected[78]. Instead, several different physical and chemical mechanisms are responsible for observed effects induced by high frequency sound waves crossing through the medium. Most common physical mechanism is acoustic cavitation: the formation and subsequent dynamic life of bubbles in a liquid[79].

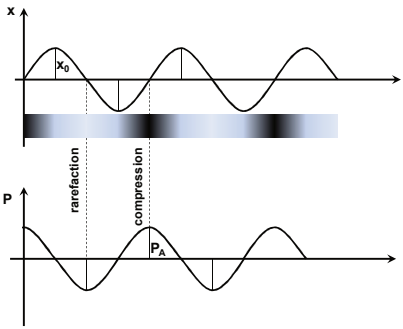

Figure 5: Molecule displacement and pressure in dependence of wave propagation.[81]

Every kind of sound wave consists of cycles of compression and rarefaction. When a (ultra)sound wave (intensity > 10 W/cm²)[80] travels through a liquid it causes the molecules to oscillate about their own position (**Figure 5**). This displacement can be expressed by **Eq. 4**

$$x = x_0 \sin 2\pi ft \qquad \textbf{Eq. 4}$$

Where x_0 is the maximum displacement and f is the frequency of sound. Corresponding acoustic pressure (P_a) is given by **Eq. 5**

$$P_a = P_A \cos 2\pi ft \qquad \textbf{Eq. 5}$$

where P_A is the pressure amplitude. Consequently, the total pressure (P_{tot}) in the liquid is given by the sum of the hydrostatic pressure (P_h) of the liquid and the acoustic pressure induces by sound wave propagation (**Eq. 6**)[81]

$$P_{tot} = P_h + P_a \qquad \textbf{Eq. 6}$$

With every expansion cycle molecules are drawn away from each other. If the resulting negative pressure is large enough to overcome attractive forces between the molecules (i.e. the “dynamic tensile strength” of the liquid) cavities will be formed.[81,82] Theoretically in really pure liquids the tensile strength (i.e. for water more than 1000 atmospheres)[82] is several orders of magnitude larger than the negative pressure produced by ultrasound generators. From this point of view, cavitation in liquids would not occur. Instead, some kind of “weak-

spots" reduces liquid´s tensile strength[79]. It is discussed if gas molecules trapped in crevices of very small particles may serve as such "weak-spots"[79,82,78].

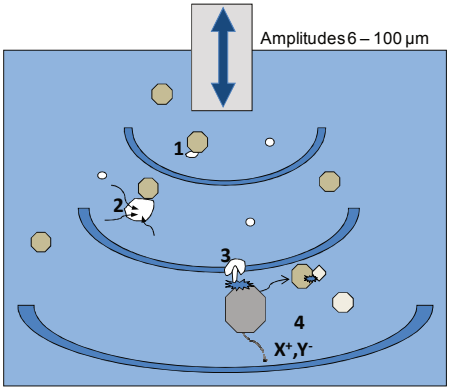

Figure 6: Principle life of cavitation bubbles in the presence of a high intensity sound wave field. 1: Bubble formation. 2: Bubble growth, energy adsorption. 3: Bubble collapse. 4: Formation of "jet streams" and shock waves.

Figure 6 illustrates the life of a cavity during sonication in an aqueous solution containing very small amount of particles. For the period of rarefaction cycle small bubbles of gas are released into solution out of crevices of particles due to gas expansion in the negative pressure field (no. 1, **Figure 6**). Subsequently altering compression and expansions cycles cause the cavity bubble to grow. Meanwhile the cavitation bubble absorbs energy from the system (no. 2, **Figure 6)**. However, the process of bubble growth depends on the intensity of sound. Hence, the intensity is another important criterion to identify a (sound) wave introduced here. As defined in **Eq. 7** the intensity (I) is the energy (E) per time (t) per unit area (A) carried by the sound wave[81]

$$I = \frac{E}{A \cdot t} \qquad \textbf{Eq. 7}$$

In acoustic fields of low intensity ultrasound (1-3 W/cm²)[81] cavities grow slowly over many cycles (stable cavitation). Otherwise for high intensity ultrasound (> 10 W/cm² = power ultrasound)[80] cavity bubbles grow rapidly in one or just a few acoustic cycles (transient cavitation).[81,82] Subsequently, if the bubble exceeds a critical radius (for 20 kHz between 150 µm[83] and 170 µm[78,82] in diameter) it collapses very impetuously (no. 3, **Figure 6**). This impetuous implosion generates localized high temperature and pressure areas[79,81,82,84,108,80] established in the so called "hot spot theory"[109,106,92,108]. Calculation of this extraordinary environment reveal that temperatures of more than thousands degree Celsius are possible[85]. Heating and cooling rates of less than a microsecond as well as pressures up to thousands of atmospheres are reported[82]. These "hot spots" are assumed to influence chemical reactions (nucleation and crystal growth)[108] by inducing radical formation in aqueous solutions (dissociation of water vapor into hydroxyl radicals ($^{\bullet}$OH) and hydrogen atoms ($^{\bullet}$H))[81]. As a result of radical formation not only decomposition (especially in organic systems)[93,80,86,117], but also changes in the chemical nature of reaction products by altering

reaction paths were observed ("sonochemical switching")[87,88]. Further phenomena linked to bubble implosion are the formation of "jet streams" and shock waves (no. 4, **Figure 6**). At the one hand, "jet streams" arise due to asymmetric implosion of cavity bubbles near a solid surface. Consequently, a jet of liquid flushes directed onto the solid surface. The speed of such "jets streams" can reach more than 400 km/h[82]. Hence, at the point and in the vicinity of jet impact surface erosions are produced[81]. As a consequence, not only particles may be ejected from the surface, but also the removal of passivating coatings is possible[89,90]. Furthermore, an increase in mass transfer to the particle surface is considered to be possible by disruption of the interfacial boundary layers[81]. However, generation of "jet streams" depends on particle size of solids present in the medium. In acoustic fields possessing a frequency of 20 kHz "jet streams" could not be observed in suspensions containing particles smaller than 200 µm[78] (150 µm[83]). In this case (suspensions of very fine powders < 150/ 200µm) only formation of shock waves, that cause physical events (turbulent mixing, microstreaming, particle acceleration), is observed[92]. Induced by accelerated particle motions, an increased number of particle collisions occur that in consequence also may cause surface abrasion.

A summary of the effects observed in suspensions (presence of small particles) induced by the high energy phenomena (hot spots, jet streams and shock waves) generated by bubble implosion (cavitation) including different physical effects[91] as:

- enhanced mass transfer[109,104,105,106,92,102,108]
- generation of surface damages[107,114,111]
- high velocity interparticle collisions[104,107,111,114,92]
- fragmentation of fracturable/ brittle solids, i.e. increase in surface area[107,114,116,117]

Chemical effects due to cavitation are reported to be

- radical formation[104,99,93,117,80,94]
- breakage of chemical bonds[117]
- chemically switching – change reaction paths[116,95]

2.3.2. Power ultrasound in industrial application

Conventional application of PUS in industry rages amongst others from surface cleaning[96], homogenizing and dispersing of suspensions[97,98], emulsification, deagglomeration[104], waste water treatment[99,100] and ultrasonic welding to the field of sonochemistry[79]. In the field of sonochemistry chemical and physico-chemical processes induced by acoustic vibrations in an aqueous medium are studied[101]. With regard to the present study the most interesting topic is the influence of PUS on chemical reactions of various organic[108,106,102] and inorganic[79,81,103,104,105,106,107,108] substances ($BaSO_4$[109,110], K_2SO_4[111], $CaCO_3$[112,113,114,115], $Al(OH)_3$[116,117]). The majority of these investigations deal with the effect of PUS on nucleation and crystal growth. Although most of the authors agreed that effects of PUS are observed, a controversial discussion regarding the origin of these effects is conducted.

Guo et al.[109,110] examined the influence of PUS on primary homogeneous nucleation of $BaSO_4$. They observed a decrease in induction time that is inversely related to the nucleation

rate. From diverse mathematical considerations they concluded that the main influence enhancing homogeneous nucleation of $BaSO_4$ is an accelerated diffusion process due to an increased diffusion coefficient. From obtained results they also conclude (employing the classical nucleation theory) that the nucleation coefficient but not the apparent nucleation order is significantly increased by PUS application[110]. Other influences e.g. changes of the interfacial tension were not assessed by the authors[109,110]. Lyczko et al. [111] also investigated the influence of ultrasound on primary nucleation. Their study deals with the cooling crystallization of potassium sulfate (K_2SO_4). Results demonstrate the reduction of induction time induced by sonication especially for low supersaturations. Since primary nucleation of K_2SO_4 was identified to be mainly heterogeneous the authors discussed that PUS changes the activation energy to act either on the surface energy crystal/solid interface or the contact angle and thus decrease the critical nuclei radius. Furthermore, obtained results indicated that the metastable zone width (MZW) can be reduced by sonication. Finally, Lyczko et al. [111] consider the capability that PUS modified the mechanism of nucleation itself. Likewise, Enomoto et al.[116] reported about altered reaction paths ("sonochemical switching") due to increasing PUS intensities: During the ripening of aluminum hydroxide the unusual/ metastable phase pseudo boehmite seems to be stabilized due to sonication. Moreover, the authors[116] notice an enhanced dissolution of aluminogels during hydration process of amorphous alumina powder caused by microscopic and macroscopic flow induced by PUS. Increased dissolution of sodium sulfide in acetonitrile was also observed by Thompson and Doraiswamy[92]. They ascribed the enhanced solubility to the formation of a supercritical fluid (SCF) as a result of cavitational events. In the region of SCF the solubility of a solute is increased compared to ambient conditions.

Nishida[112] and Li et al.[105] also found that PUS influences the streaming in solution. Whereas Nishida identify the macrostreaming (physically mixing) as dominant effect for increased precipitation rates of $CaCO_3$, Li et al.[105] are convinced that microscopic mixing promotes nucleation/ crystal growth of salts as a result of enhanced mass transfer. In a further study Li et al.[108] analyses the effects of PUS application to the acid-base reaction crystallization of 7-ACDA acid. In similarity, as shown for other substances, induction time and MZW were reduced. Hence, nucleation was possible even at lower supersaturation (compared to conventional reaction) because sonication reduces the critical potential barrier for nucleation in the regions of hot spots[108].

Other explanation for reduced induction periods and hence accelerated crystallization are given by Amara et al.[107], Boels et al.[114], Santos et al.[115], and Liu et al.[117]. They postulated that PUS produces more nucleation sites[107,115,117] and/or leads to greater surface area[114] (explained by surface damages) to serve as increased growth region for crystals. Furthermore, changes in crystal habits/morphology induces by sonication were reports by several authors[107,115].

3. Objectives

PUS is known in widespread industrial application fields. Benefits of high intensive sound waves are used for example in the process of (surface)cleaning, dispersion and emulsification, waste water treatment, and sonochemistry (altering chemical reactions). Up to know there are no experiences in using PUS for accelerating cement hydration. Thus the subject of this thesis is to gain a fundamental knowledge on the capability of the application to use this technology in concrete production. Therefore the study can be divided in five main parts.

The aim of the first part is to get an overview how cement pastes (OPC) are influenced by PUS application. Important properties of fresh and hardened cement suspensions are determined, optimum PUS parameter are identified. Furthermore, to highlight the effects of PUS application, in-depth investigations are performed in C_3S-water and C_3S-lime-systems.

In the second part, investigations focus on the influence of PUS on fluidity of cement suspensions. Besides the ascertainment of generally known effects due to PUS application (de-airing, homogenizing and dispersion) effects on fluidity (rheology) are determined. However, rheological examination is limited to providing a qualitative assessment (determination of slump flow and V-funnel flow times). In the third part the above investigations are repeated, only this time with slag cements. The focus is to evaluate if it is possible to improve the reaction yield of the glassy phase.

Finally, the last two parts address subjects which are more relevant to the practice. At the one hand the capability of the application of PUS in ready mixed mortars (part four) is evaluated. At the other hand, in the last part of this thesis, the PUS technique is applied to optimize production (especially reduction of required heat treatment) of a commercial self compacting concrete mix used in precast production. Obtained economic benefits are discussed.

4. Materials and methods

4.1. Materials

Two batches of Ordinary Portland Cement (OPC) of type CEM I 42.5 R and CEM II/B-S 32.5 R according to DIN EN 197-1 were used for investigations. Furthermore synthesized triclinic tricalcium silicate (C_3S) and granulated grounded blast-furnace slag (GGBFS) were used for in-depth investigations. Two batches of C_3S were purchased from VUSTAH (Brno, Czech Republic).
The chemical compositions of the raw materials (m.-% oxide content) were determined by Inductively Coupled Plasma – Optical Emission Spectroscopy (ICP-OES, Optima 3000, Perkin-Elmer and ACTIVA-M, HORIBA, Germany) after dissolving solids in hydrofluoric acid as given in **Table 1**. The free lime content was determined by the Franke method.

Table 1: Chemical composition (oxide content) of raw materials (OPC and C_3S) determined by ICP-OES given in m.-%.

composition	SiO_2	Al_2O_3	Fe_2O_3	CaO	MgO	MnO	K_2O	Na_2O	TiO_2	SO_3	S	free lime	loI
CEM I 42.5 R (06/09)	20.4	4.7	2.4	63.1	1.2	0.03	1.22	0.24	0.18	n.d.	n.d.	1.8	2.3
CEM I 42.5 R (3/10)	20.0	4.4	2.4	63.5	1.5	0.03	1.26	0.32	0.18	3.7	n.d.	1.2	3.0
CEM II/B-S 32.5 R	24.1	8.0	1.5	57.0	2.6	0.18	0.92	0.56	0.33	2.0	0.39	n.d.	2.9
C_3S (08/09)	26.7	0.5	0.1	71.8	0.2	0.01	0.04	0.1	0.07	n.d.	n.d.	0.2	0.1
C_3S (09/13)	26.3	0.2	0.1	72.3	0.3	0	0.02	0.02	n.d.	n.d.	n.d.	0.1	0.2
GGBFS	36.5	12.8	0.8	39.5	6.2	0.25	0.59	0.48	0.98	0.1	1.25	n.d.	0.7

n.d.= not determined

Particle densities of the raw materials were determined using a helium pycnometer (AccuPyc 1330, micromeritics, Germany). Particle densities were determined to be 3.12 g/cm³ (OPC delivery batch 06/2009) and 3.10 g/cm³ (OPC delivery batch 03/2010); 3.09 g/cm³ (CEM II/B-S 32.5 R); 3.15 g/cm³ (08/2009) and 3.14 g/cm³ (09/2013) for two synthetic C_3S batches and 2.20 g/cm³ for GGBFS.
Specific surface areas of powders were measured by Blaine method. For OPC specific surface areas of 4500 cm²/g (06/2009) and 4620 cm²/g (03/2010) were determined. CEM II/B-S 32.5 R possesses a specific surface area of 3675 cm²/g. After grinding (< 63 µm) the specific surface areas of the C_3S batches were about 3500 cm²/g (08/2009) and 3100 cm²/g (09/2013), respectively. The specific surface area of GGBFS was 3805 cm²/g.

In order to address certain issues during experimental work the usage of polycarboxylate type SP was necessary (sufficient workability). For the majority of investigations a SP synthesized by radical polymerization of methacrylic acid and subsequent esterification of PEG side chains (supplied by Bozzetto S.P.A., Italy) was applied. The side chain density (acid/ copolymer) of the SP is 2.9 and the side chain length exhibits 1000 g/mol PEG. The solid dry mass (SP) in aqueous solution was about 40 m.-% and the density of solution was 1.11 g/cm³. Throughout the investigations SP was added in varying dosages (always given as SP dry mass referred to cement/ C_3S /binder mass).
Mortars were produced using CEN standard sand (DIN EN 196-1).

4.2. Methods

4.2.1. Power ultrasound

PUS was generated with a laboratory device (UIP 1000hd, Hielscher, Germany) working with a constant frequency of 20 kHz. Different ultrasonic horns (sound transmitter) and booster (reducer or amplifier) are available. In combination of both tools (ultrasonic horn and booster) a spread of varying amplitudes are possible, marked in green (**Table 2**). The red circles highlighted the amplitudes used for investigations described in **section 5.1.1**.

Table 2: Adjustable PUS amplitudes in dependence of ultrasonic horn/booster combination.

UIP 1000hd	Maximum amplitude** [µm]								
	Booster as reducer				Without booster	Booster as amplifier			
Ultrasonic horns/ front face diameter [cm²]	B2-2.2	B2-1.8	B2-1.4	B2-1.2		B2-1.2	B2-1.4	B2-1.8	B2-2.2
BS2d18/ 2.5	41	43	65	70	85	102*	123*	154*	177*
BS2d22/ 3.8	25	26	40	44	57	69	81	106*	125*
BS2d34/ 9.0	11	12	18	20	24	30	35	43	53
BS2d40/ 12.5	8	9	14	15	17	22	26	31	39
BS2d50/ 19.6	6	7	9	10	12	15	17	22	27

** determined in water at 100 % power
* significantly reduced lifetime of ultrasonic horn due to massive erosion effects

In assumption that most effective sonication (i.e. generation of cavitation) is achieved in aqueous phase only cement suspension is treated with PUS. Hence, the cement suspension was produced before it was treated with PUS. This termed “suspension mix design” was applied as follows: cement and water (in different mass ratios) were mixed in a Hobart mixer (140 ± 5 rpm) for one minute and 30 seconds. If necessary, SP was added after first

30 seconds of mixing. After a rest time of one minute and 30 seconds the suspension was mixed another minute at 285 ± 10 rpm.

Huge amounts of media (cement suspensions up to maximum 1.5 l) are sonicated using a flow-through cell (**Figure 7a**). The advantage of this experimental set-up is to guarantee an all-over continuous sonication of media: external mixed cement suspension was introduced in the storage container (no. 2, **Figure 7a**). The rotary pump (no.1, **Figure 7a**) hauls the material to flow through the cell (no.3, **Figure 7a**). At this point the PUS energy is transmitted to the media via the ultrasonic horn (no.4, **Figure 7**). A flexible tube connected to the flow-through cell returns the media back to the storage container. So the circular flow is closed and the media can pass it again if necessary. Thus a uniformly continuous sonication is guaranteed until the required specific energy input is achieved.

Smaller amounts of media (100 ml – max. 500 ml) were sonicated by introducing the ultrasonic horn in the suspensions stored in a beaker (**Figure 7b**). To ensure an uniformly sonication the media is stirred by hand during the PUS treatment. With the help of a power meter (no.8, **Figure 7**) the total energy input applied by the PUS setup was monitored for all experiments.

a) Flow-though cell for sonication if huge amounts of media

b) Sonication of small amounts of media

Figure 7: Experimental set-up of PUS device.

4.2.2. Initial setting of cement suspensions and strength development of mortars

The setting of cement pastes was determined by the Vicat needle test method (VICATRONIC MA-E044, ATH, Austria) according to DIN EN 196-3.

The mixing procedure for all suspension was similar to that described in **section 4.2.1.**, p. 36. Subsequently, if required, PUS was applied after mixing, generally after approximately 5 minutes after water addition.

The early strength development of mortars (with varying ratio of cement to aggregates) was tested according to DIN EN 196-1. Since PUS was applied to the cement suspension, mixing process for mortar has to be changed, i.e. “suspension mixing design” was applied. Therefore first water, cement, and SP were mixed as mentioned before (**section 4.2.1.**, p. 36). Afterward PUS is applied to the cement suspension (similar to setting time determination). Then successively aggregates are added (30 s at 140 rpm ± 5 rpm) in the Hobart mixer before the final mixing (60 s at 285 rpm ± 10 rpm) is applied. The mortar bars were stored at 20 °C and 95 % relative humidity until their examination (< 24 h).

4.2.3. Sample temperature evolution

The measurements of the sample temperature evolution were recorded to get an idea of how PUS application influences the hydration process of the cement suspensions and mortars. With this method 500 g of cement suspension (850 g of mortar) were placed in a semi adiabatic sample container. A temperature sensor (NiCr-Ni thermo wire) connected to a data logger (Almemo 2590-4S, Ahlborn, Germany) was added to determine the sample temperature continuously. The temperature development was determined until 48 h of hydration.

4.2.4. Isothermal heat conduction calorimetry

A current method to characterize the cement hydration progress is the isothermal heat conduction calorimetry. The measuring principle is based on the measurement of the differences of reaction heat (exothermic/ endothermic) between a sample and an inert reference. The measurement signal in this case is the thermoelectric voltage which is proportional to the heat flow of the reacting sample.
The measurements in current study were carried out with an isothermal heat conduction calorimeter (TrioCAL 7339, ToniTechnik, Germany). The experimental procedure differs from the standard method due to PUS application: The samples of cement suspensions (w/c < 1.0) were mixed outside the calorimeter, if necessary treated with PUS, and then placed in the measuring cell of the device. The heat flow was recorded during first 48 h of hydration at constant temperature (25 °C). For analyses of the heat release rate and total heat only data obtained after one hour after the measurements started were considered.

4.2.5. Non-destructive measurement of ultrasonic P-wave velocity

The measurement of the ultrasonic P-wave velocity (wave transmission or reflection method) provided a non-destructive method to get structural information of cement pastes (setting and hardening behavior)[118,119,120,121,122]. In the case of wave transmission method, the ultrasonic P-wave velocity (v_p) is given by

$$v_p = l / \Delta t \qquad \textbf{Eq. 8}$$

where Δt is the time that v_p needs to travel through the width of the sample (l).
In general, for determination in cement pastes, the P-wave velocity curve exhibits a region of constant P-wave velocity followed by an acceleration that indicated the beginning of structure formation[123,124].

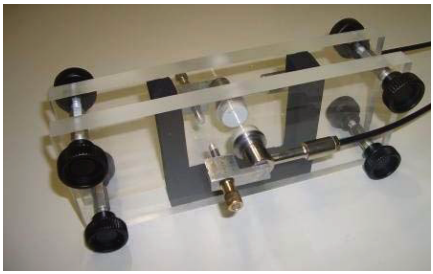

Figure 8: Testing device for non-destructive P-wave velocity examination.

For the current investigation the principle of direct transmission was applied (**Figure 8**). The measurement setup developed at the F.A. Finger Institute for building materials and science, Bauhaus-Universität Weimar, uses an ultrasonic measuring system CELplus (GEOTRON Elektronic, Germany).

4.2.6. Electrical conductivity of aqueous solutions/ diluted suspensions

A good method to follow chemical dissolution/precipitation processes in aqueous solution/ diluted suspensions is to measure its electrical (el.) conductivity. The method is based on electric-chemical resistivity survey. The el. conductivity is calculated from the current flow (depend on the ion concentration, the ion mobility and the ion valence)[125] using Ohm´s law. Thus the value of the el. conductivity (S/cm) mirrors the ion composition in aqueous solutions.
Using continuous measurement of the el. conductivity it is possible to draw conclusions concerning crystallization progresses due to the development of the el. conductivity with time. If fine solids are dispersed in solution, dissolution/precipitation will proceed. In this context a consumption of ions from the bulk solution due to nucleation/crystal growth can be determined as a decrease in the el. conductivity. A rise in the el. conductivity is equivalent to

the release of ions into solution due to dissolution, and a constant value of the el. conductivity indicates equilibrium of dissolution and precipitation processes.
The measurements of the el. conductivity of aqueous solutions and diluted suspensions in this thesis were conducted with a conductivity electrode (TetraCon® 325 WTW, Germany).

4.2.7. Inductively Coupled Plasma-Optical Emissions Spectroscopy

To determine chemical composition of solids and ion concentrations of solutions Inductively Coupled Plasma-Optical Emissions Spectroscopy (ICP – OES; Perking Elmer Optima 3000, Germany and ACTIVA-M, HORIBA, Germany) was used. With this method aqueous solution is injected in an inductively coupled argon plasma by means of pneumatic nozzles. Temperatures more than 6000 °C cause the elements to atomize/ionize and thus emit specific lights (wave length). The intensity of emitted light is equivalent to the concentration of corresponding element (requires calibration).
The chemical composition of solid raw materials (e.g. cement, C_3S, GGBFS) was analyzed after dissolving solids in hydrofluoric acid. To determine the ion concentration in solution/diluted suspension at least 10 ml solution was taken from the bulk/ batch filtered through a 0.2 µm syringe filter at given times. To avoid precipitation from aqueous solution approximately 0.2 g of 0.5 mol HNO_3 was added to the analyzed solution.

4.2.8. High resolution scanning electron microscopy

A high resolution Scanning Electron Microscope (Nova NanoSEM 230, FEI, Netherlands) equipped with a field emissions gun (FEG) was used to characterize microstructure of solids. In the majority of investigations secondary electron images were recorded with a Through the Length Detector (TLD) at high vacuum (approximately 10^{-6} mbar) at very low acceleration voltages (2 kV). Additionally cryo- SEM investigation on the dispersion constitution of cement suspension was performed after high pressure freezing (HPM 100, BalTec/ Leica) and partial sublimation.
The sample preparation for SEM examination varies with the aim of investigation and will be described in the corresponding sections of this thesis.

4.2.9. X-ray powder diffraction

X-ray diffraction is a current method to determine the phase content of crystalline powder substances. In 1969 Rietveld[126] introduce a method that enables the quantitative crystalline phase analysis (even for powder mixtures[127]). However, a challenging task for quantitative phase analysis in (hydrated) OPC systems by X-ray diffraction is the presence of amorphous phases causing discrepancy between the calculated and the actual crystalline phase content.

Therefore, several methods were applied to determine amorphous phase content that are the internal standard method and the external standard method as referred by Jansen[128].
For the current investigations sample preparation was performed by adding 2-propanol to the concentrated suspension to stop the hydration process. Subsequently samples were dried at 35 °C and ground by micronizing mill (McCrone) to a particle size < 5 µm (according to laser diffraction analysis, Coulter LS 230). X-ray measurements were performed with an X-ray powder diffractometer (D-5000, Siemens, Germany). The CuKα (λ = 1.5418 Å) radiation was generated at 40 mA and 40 kV. Data have been collected over a Bragg angle range of 6-70° 2 θ using an angular step with of 0.05° and 5 s counting time. Quantification was done by Rietveld analysis (Autoquan, BGMN, Germany) applying the external standard method (zincite) according to Jansen[128].

4.2.10. Fluidity and rheological characterization

The influence of PUS on the fluidity of cement suspensions and mortars was estimated by the mini cone test (slump flow measurement according to DIN EN 12 350-5 and DIN EN 12 350-8) and the V-funnel test (flow time measurement according to DAfStb SCC guideline 2003-11). Dimensions of the mini cone and V-funnel are displayed in **Figure 9** & **Figure 10**, respectively. The mortar V-funnel was used because of limited aggregate size in mortars (< 4 mm). All measurements were carried out 15 minutes after water addition.

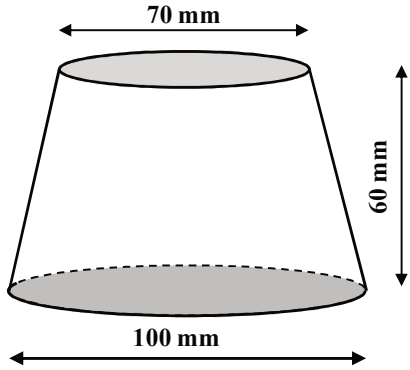

Figure 9: Dimension of mini cone (Hägermann cone) for slump flow determination.

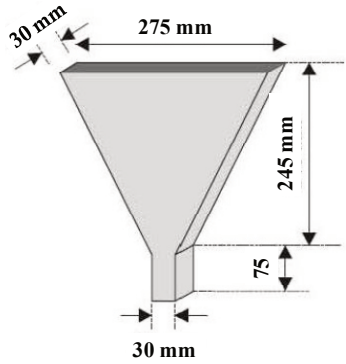

Figure 10: Dimension of mortar V-funnel for flow time determination.

5. Results

5.1. Influence of power ultrasound on setting and hardening of OPC suspensions

5.1.1. Identification of optimized PUS parameter

To gain basic knowledge to the influence of PUS on the setting and hardening of OPC suitable PUS parameter have to be identified. Thus, different PUS amplitudes and specific energy inputs were defined for investigation. For applicational reasons certain criteria of PUS treatment for concrete production are set:

- The initial set of cement suspension should be accelerated significantly.
- The increase of cement suspension temperature due to PUS application has to be limited to 45 °C.
- The period of PUS treatment to reach required energy input should be as short as possible.

Manufactures suggestion to use the specific energy input of $E_v \approx 1000$ Ws/ml (= J/ml) emerged as not practicable. The reason was that, induced by the high energy input (0.278 kWh for 1 l cement suspension to ensure 1000 J/ml), the temperature of cement suspension exceeds given limits (80 °C >> 45 °C). Consequently, E_v was set to be 75, 150, and 300 J/ml.
With the provided PUS equipment, generation of several PUS amplitudes was possible (colored in green, see **Table 2**). To cover a wide range of working area of PUS a small (12 µm), a medium (43 µm), and a large (85 µm) amplitude were selected (red circles, see **Table 2**). Amplitudes of 12 µm and 43 µm were generated with the same ultrasonic horn (BS2d34, front face diameter = 9 cm²) whereas the PUS amplitude of 85 µm was generated by an ultrasonic horn (BS2d18) possessing a front face diameter of 2.5 cm².

Cement pastes were mixed applying the “suspension mix design” as described in **section 4.2.1**. To obtain sufficient fluidity of cement suspension for pumping through the PUS circuit (**Figure 7**) SP was added to the mix. The water to cement ratio (w/c) of the suspension was 0.37 and the SP content was 0.1 m.-% (dry SP mass referred to cement mass).

The sonication duration was controlled using a microchronometer. Initial setting times and the development of sample temperatures during first 24 h of hydration were determined for quick overview measurements.

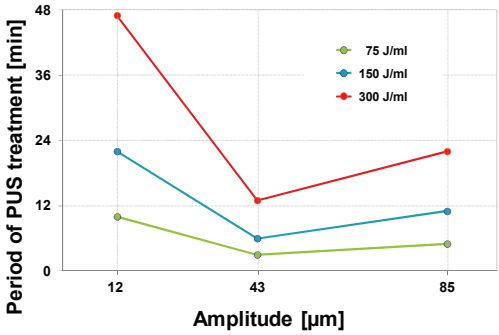

Figure 11: Period of PUS treatment (1500 ml cement suspension) in dependence of amplitude and specific energy input.

The period of PUS treatment (approximately 1500 ml cement suspension) to achieve required specific energy input is presented in **Figure 11**. From this figure it becomes obvious that at constant PUS amplitude (e.g. 12 µm) increasing specific energy input requires longer sonication times. In contrast, if one compares required sonication times at varying PUS amplitudes and constant specific energy input (e.g. 300 J/ml) a non-linear dependence of the duration of PUS treatment is observed (**Figure 11**). In detail this means that using the same front face diameter of ultrasonic horn to generate different PUS amplitudes, i.e. 12 and 43 µm, a lager amplitude reduces the sonication time. But, for generating the PUS amplitude of 85 µm a smaller front face diameter of ultrasonic horn is used and longer sonication times are required to achieve a similar specific energy input. This can be explained by the fact that the emitted acoustic power (P_{ac}) depends on both, the sound intensity (that is proportional to the square of acoustic amplitude)[81] and the front face diameter of used ultrasonic horn (c.f. **Eq. 7**; **Figure 12**).

$$P_{ac} = \frac{\Delta E}{\Delta t} = I \cdot A$$

$P_{ac.}$ … acoustic power [W] **Eq. 9**

I … acoustic intensity [W/cm²]

A … surface area of ultrasonic horn [cm²]

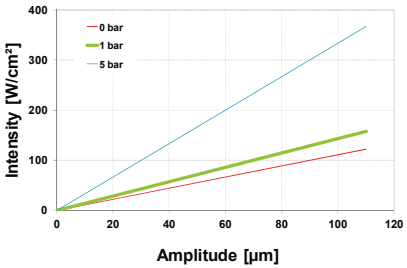

Figure 12: Relationship between PUS amplitude, intensity and pressure in water (20 °C, 1 bar)[129].

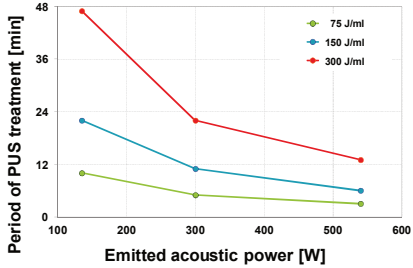

Figure 13: Period of PUS treatment in dependence of emitted power and specific energy input.

For the used PUS device (UIP 1000hd, Hielscher, Germany) PUS intensities in dependence of the amplitude and the ambient pressure (in the medium) are provided by the manufacturer (**Figure 12**). From **Figure 12** it can be calculated (**Eq. 9**) that at assumed ambient pressure in the cement suspension during sonication (1 bar) the emitted acoustic power of the ultrasonic horn BS2d34 (front face diameter 9 cm², **Table 2**) generating the PUS amplitude of 43 µm (12 µm) is about ≈ 540 W (≈ 140 W). Compared to that, the PUS amplitude of 85 µm is generated by the ultrasonic horn possessing a smaller front face diameter (BS2d18/ 2.5 cm², **Table 2**). Thus, although the intensity is much higher with the 85 µm amplitude (≈ 120 W/cm² vs. ≈ 60 W/cm² for the 43 µm amplitude) the emitted power is about 300 W. Consequently, considering emitted power a nearly linear dependence of the duration of sonication times is observed in **Figure 13**: the higher the emitted power the shorter the required period of PUS treatment. In other words, the sonication time is directly correlated to the emitted power (governed by amplitude and front face diameter of ultrasonic horn). Consequently, high amplitudes transmitted via large front face diameter of the ultrasonic horn are advantageous to ensure short sonication times for given specific energy inputs.

Additionally, **Figure 14** displays the corresponding temperature increase of the cement suspension induced by sonication.

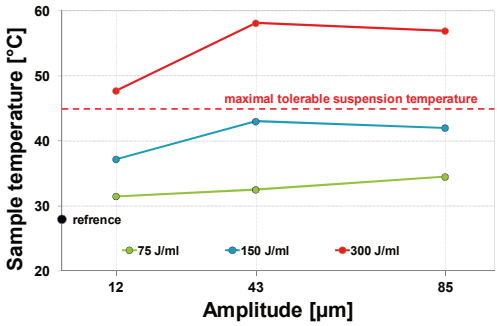

Figure 14: Resulting temperature of cement suspension (w/c = 0.37 + 0.1 m.-% SP dry mass refers to cement mass) due to PUS application in dependence of amplitude and specific energy input.

As expected, results in **Figure 14** demonstrate that the temperature rise induced by sonication is governed by specific energy input. The higher the introduced energy the higher the resulting sample temperatures after PUS application. Furthermore results shown in **Figure 14** reveal that the highest applied specific energy input (300 J/ml) always causes a temperature rise up to more than 45 °C which is not desired.

At this point of investigation, subsequent to the ascertainment of the general handling of PUS treatment, the overall effects on cement hydration were estimated. Therefore initial setting times and the development of sample temperature during first 24 h of hydration were determined. Results of the initial setting time in dependence of PUS amplitude and specific energy are shown in **Figure 15**.

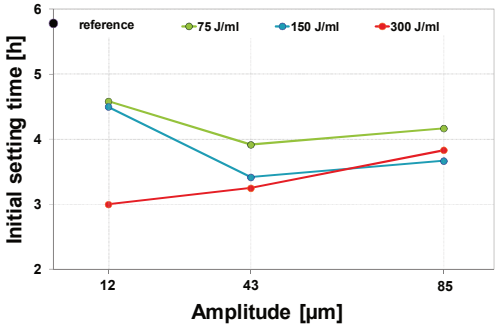

Figure 15: Initial setting time of cement suspension (w/ = 0.37 + 0.1 m.-% SP dry mass referred to cement mass) in dependence of PUS application (varying amplitude and specific energy input)

From this figure (**Figure 15**) it becomes obvious that independently on used PUS parameters, sonication always shifts the initial setting of cement pastes to earlier times. An average acceleration of two hours could be observed (e.g. reference: 5 h 47 min vs. PUS: 3 h 55 min). An above-average acceleration of the initial set was determined with the PUS amplitude of 12 µm and a specific energy input of 300 J/ml. Although the superior acceleration caused by this high energy input of 300 J/ml this PUS treatment is not applicable due to extended sonication duration (47 min) and sample heating (48 °C; + 20 K compared to the reference). Apart from that, the use of the 43 µm amplitude yields the best gain in initial setting times of the tested cement suspensions.

Additionally, the accelerating effect of PUS is evaluated by comparing the time of maximum temperature during acceleration period (marked by asterisk, see **Figure 16)**. Consequently, **Figure 17** shows the occurrence of the maximum temperature of cement suspension in dependence of PUS amplitudes and specific energy inputs. Results clearly reveal that due to the PUS treatment an accelerated heat development is generally achieved. To exclude that the temporary rising temperature (induced by PUS application at the beginning of hydration) is responsible for accelerated hydration progress, the reference suspension is heated up to comparable temperatures (max. 60 °C in accordance with max. temperature increase due to PUS application) in a comparable period of time. As expected this temporary heating at the beginning of hydration also shifts the occurrence of the maximum sample temperature to earlier times. But compared to the corresponding sonicated sample (e.g. PUS 43 µm & 300 J/ml) the acceleration gain is less important. From the results presented in **Figure 17** it is also recognizable that increasing PUS amplitudes at similar front face diameter (43 µm vs. 12 µm amplitudes) accelerate the main hydration (indicated by maximum temperature at earlier periods of time). However, the variation of PUS amplitudes from 43 µm to 85 µm does not significantly influence the occurrence of maximal sample temperature. Moreover, considering these amplitudes (43 µm and 85 µm) a linear correlation for increasing energy inputs was determined, i.e. increasing specific energy inputs cause acceleration of the occurrence of maximal sample temperature.

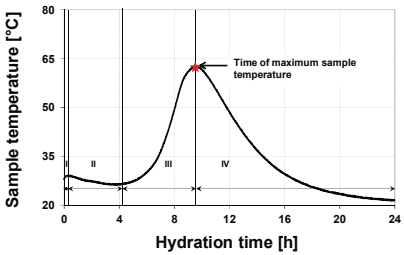

Figure 16: Temperature development of cement suspension during hydration (I: induction period, II: dormant period, III: acceleration period, IV: deceleration period).

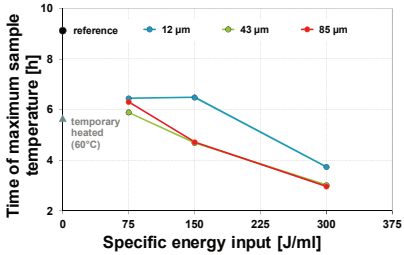

Figure 17: Time of maximum temperature in dependence of PUS amplitude [µm] and specific energy input. Reference = without PUS application and temp. 60 °C = reference with initial temperature pulse of 60 °C.

As a result from the investigations presented previously, appropriate PUS parameters that meet all demands concerning accelerated hydration, minimal temperature increase of cement suspension, and minimal period of PUS treatment emerge to be the PUS amplitude of 43 µm and a specific energy input of 75 J/ml. **Table 3** displays the changes of relevant properties of tested cement suspension (w/c = 0.37 + 0.1 m.-% SP dry mass referred to cement mass) induced by sonication using these optimal PUS parameters. A sufficient acceleration of the initial set of about approximately two hours was achieved by a PUS treatment of three minutes (UIP 1000hd, Hielscher, Germany; 1500 ml cement suspension). The maximal sample temperature after sonication was determined to be 35 °C and thus less than the crucial value of 45 °C given by initial considerations. Hence, during subsequent investigations the influence of PUS on properties of fresh and hardened cement suspensions (OPC) is employed with these optimal PUS parameters (43 µm and 75 J/ml).

Table 3: Change in relevant properties of cement suspension induced by sonication using optimal PUS parameters

Sample	sample temperature [°C]	Sonication duration [min]	Initial setting time [h:min]	Time of max. sample temperature [h]
Reference	27.2 ± 1.2	0	05:47 ± 00:14	9.1 ± 0.7
PUS 43/75	33.5 ± 1.8	3	03:55 ± 00:05	5.9 ± 0.1
Differences	+ 6.3	+ 3	- 01:52	- 3.2

5.1.2. Influence of PUS application on hardening of cement suspension and strength development of mortar

In addition to the determination of the initial set and the development of sample temperature (**section 5.1.1**), the influence of PUS application on hydration progress was assessed by measuring the isothermal hydration heat release (isothermal heat conduction calorimetry, TrioCAL 7339, ToniTechnik, Germany), the non-destructive ultrasonic P-wave velocity (ultrasonic probe CELplus, GEOTRON Elektronic, Germany) and the compressive strength development of mortars (cement : aggregates = 1:3; DIN EN 196-1). To produce the mortars "suspension mix design" was performed as described in **section 4.2.2**. Furthermore microstructural characterization of hydration progress is performed by SEM imaging (Nova NanoSEM 230, FEI, Netherlands).

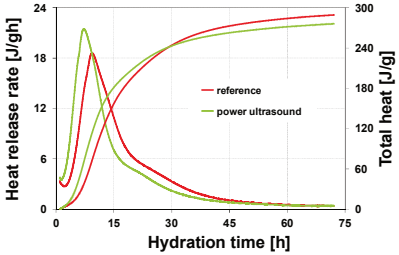

Figure 18: Heat release rate and total heat during first 72 h of cement hydration (CEM I 42.5 R, w/z = 0.37 + 0.1 m.-% SP dry mass referred to cement mass) in dependence of PUS application.

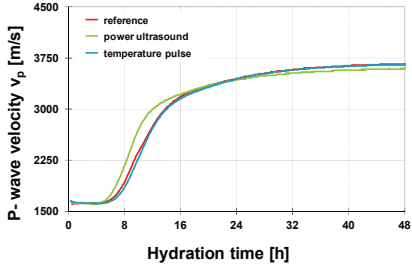

Figure 19: P- wave velocity (v_p) in dependence of hydration time, temperature pulse and PUS application.

The heat release rate and the total heat during first 72 h of cement hydration in dependence of PUS application are presented in **Figure 18**. The initial heat release rate (< 1h) was not considered because suspensions were mixed outside the calorimeter. The accelerating effect of PUS application on the heat release rate during cement hydration is clearly demonstrated by the results shown in **Figure 18**. However, the accelerating effect of PUS was limited to the duration of the induction period and acceleration period. The total heat release after 72 h of hydration is unaffected by PUS application.

To back up results of isothermal heat conduction calorimetry, non-destructive ultrasonic P-wave velocity was determined continuously during first 48 h of cement hydration. Results are presented in **Figure 19**. Obviously, in PUS treated sample an accelerated increase of P-wave velocity is detected. Based on previous findings the accelerated increase in P-wave velocity can be correlated with the increased compressive strength[119,120]. Therefore an improved strength development due to the acceleration of cement hydration is demonstrated.

Finally, these results are in good agreement with the results of isothermal heat calorimetry and thus confirm the accelerated hydration due to PUS application.

The development of microstructure in dependence of hydration time and PUS application was examined by high resolution SEM imaging (Nova NanoSEM 230, FEI, Netherlands). Images were recorded at the time of initial setting of sonicated and unsonicated cement suspensions (3 h 30 min and 5 h, respectively) and additionally after 6 h 30 min (**Figure 20**). Therefore the hydration was stopped by adding 2-propanol with its subsequent removal.
From **Figure 20a** it becomes visible that only ettringite can be observed in the reference sample after 3 h 30 min of hydration. At the same time typical etch pits (dissolution voids) on C_3S surfaces as well as first C-S-H phases are already to be seen in the sample treated with PUS (**Figure 20b**). These observations are in good correlation with the accelerated heat release (**Figure 18**) and the documented set time (3 h 55 min) of the sonicated sample. After 5 h of hydration in the reference first C-S-H phases can be observed (**Figure 20c**). This is also in a good agreement with documented initial set time (5 h 40 min) and the start of acceleration period in the heat development determination (**Figure 18**). C-S-H phases in the sonicated sample have grown up to a length of 250 nm in comparable period of time (**Figure 20d**). Comparing reference and sonicated sample, the observed C-S-H growth (PUS treated sample after 5 h of hydration) is similar in the reference after 6 h 30 min of hydration (**Figure 20e**). In the sample treated with PUS typical tapered, interlocked C-S-H phases can be observed after 6 h 30 min of hydration. Consequently, microstructural investigations show that PUS enhances the dissolution of C_3S and accelerates the growth of C-S-H phases. On the basis of the characterization of microstructural development it is evidenced that accelerated initial setting times (**Figure 15**), enhanced heat release (**Figure 18**), and increased P-wave velocity (**Figure 19**) of cement paste due to PUS application are caused by accelerated alite hydration.

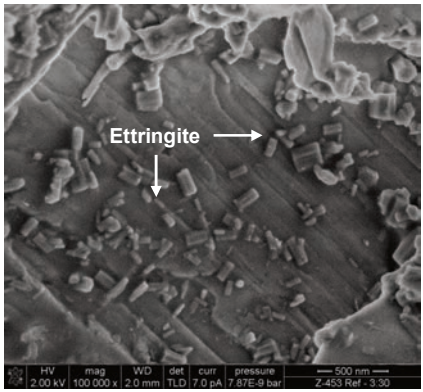

a) Reference 3 h 30 min hydration

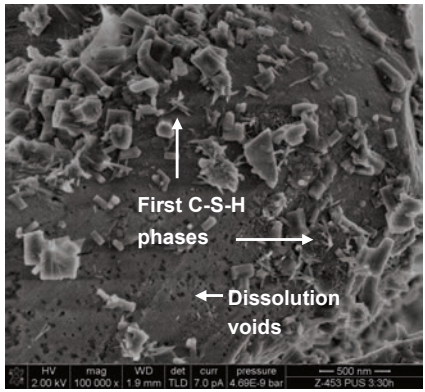

b) Power ultrasound 3 h 30 min hydration (initial set)

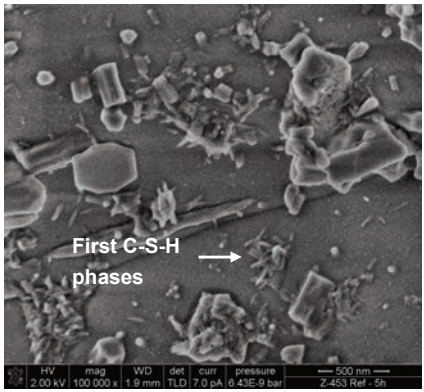

c) Reference 5 h hydration (initial set)

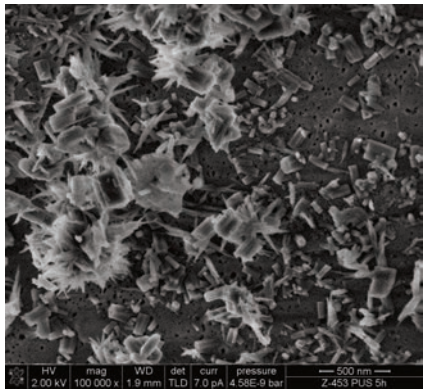

d) Power ultrasound 5 h hydration

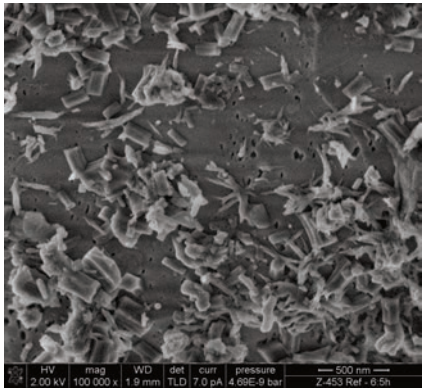

e) Reference 6 h 30 min hydration

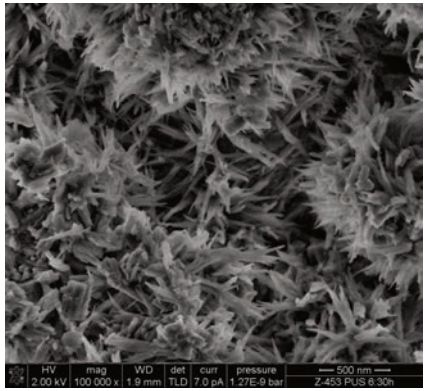

f) Power ultrasound 6 h 30 min hydration

Figure 20: Microstructure of cement suspension (CEM I 42.5 R, w/c = 0.37 + 0.1 m.-% SP dry mass referred to cement mass) with and without PUS application recorded in a SEM equipped with a Trough the Lens Detector (TLD) at approx. 10^{-6} mbar (high vacuum) at 2 kV acceleration voltages.

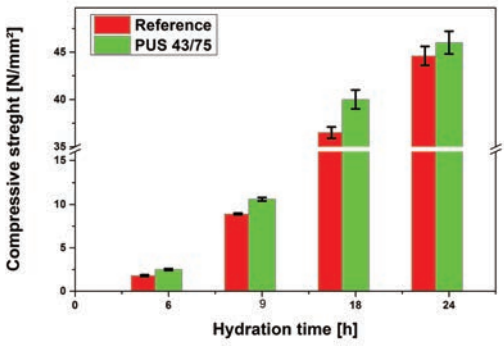

Figure 21: Compressive strength development of mortars (cement : aggregates = 1:3) in dependence of hydration time and PUS application.

The positive effect of the PUS treatment on the early strength development is also proven by means of compressive strength of mortars (**Figure 21**). During the first 24 h of hydration statistically significant increase of very early compressive strength (Student´s t-test) of about up to 25 % is determined.

In summary, the results of in-depth investigations on the influence of PUS application on initial setting, heat release, continuous ultrasonic P- wave velocity of cement pastes (w/c = 0.37 + 0.1 m.-% SP dry mass referred to cement mass) and strength development of mortars (cement : aggregate = 1:3) underscore the accelerating effect of PUS. The characterization of microstructural development indicates an enhanced dissolution of the main clinker phase alite and thus accelerated C-S-H formation. Results of isothermal heat conduction calorimetry show a shortened induction period and accelerated main hydration. Similar results are reported by Thomas[48] and Alizadeh[44] for the influence of C-S-H seeds on hydration of C_3S. They observed that seeding with C-S-H reduces the induction period, accelerates the early hydration rate, and increases the maximum peaks during isothermal conduction calorimetry measurements. From their results they conclude that more nuclei are provided and thus leading to more regions of growing hydration products at the same time. However, PUS is also known to enhance the nucleation by providing/generating nucleation sites[107,115,117]. Hence, to evaluate if this mechanism is responsible for accelerated OPC (alit) hydration, more detailed investigations are required. Therefore the next part of investigation puts some light in the influence of PUS on the hydration of the model substance C_3S and on the precipitation (nucleation and growth) of C-S-H phases.

5.1.3. Influence of power ultrasound on the nucleation of C-S-H

Nucleation from clear to the eye solutions (primary nucleation)

Primary nucleation occurs during the crystallization from clear to the eye solution i.e. in a solution containing no pre-existing crystals[104,111]. Primary nucleation may appear as homogeneous (in the bulk of a liquid in the absence of solid surfaces[104]) or heterogeneous (in the presence of any solid interfaces) nucleation. To obtain a primary nucleation of C-S-H a solution statured with Ca and Si ions is required. Therefore 2.00 g of C_3S were dissolved in

100 ml of bi-deionised water (25 °C ± 1°C) for two minutes with a magnetic stirrer (300 rpm). After this time the solution was filtered (pore size 0.1 µm) in nitrogen atmosphere to remove solid particles. The chemical characterisation of solution by ICP-OES (ACTIVA-M, HORIBA, Germany) reveals a Ca ion concentration of 4.33 mmol/l (± 0.08 mmol/l) and a Si ion concentration of 1.38 mmol/l (± 0.01 mmol/l).

PUS was applied immediately after the filtration process. The energy input was about 75 J/ml using the PUS amplitude of 43 µm (ultrasonic horn with front face diameter of 9.0 cm²)

To estimate the crystallization progress the el. conductivity of aqueous solution was determined. The measurements started immediately after the filtration process and PUS treatment. Solutions were stored in a thermostatic bath to keep a constant temperature (25°C ± 1°C) during measuring time for all experiments.

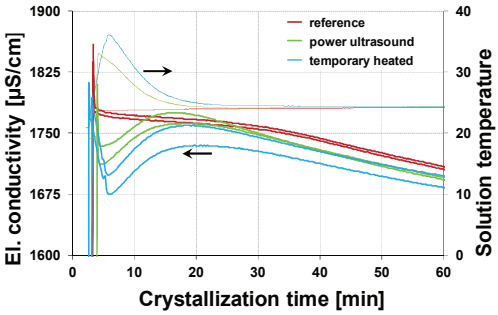

Figure 22: Development of the el. conductivity and temperature in a Ca-Si-solution in dependence of PUS application and initial temperature pulse.

The development of the el. conductivity and the solution temperature in a clear to the eye aqueous Ca-Si-solution in dependence of time, PUS application and initial temperature increase (temporary heated) is shown in **Figure 22**. Obviously during the first 30 minutes only a slight decrease in the el. conductivity is detected for the reference sample indicating a constrained precipitation of C-S-H phases. After this period (at approx. 30 min) the el. conductivity decreases rapidly due to proceeding phase precipitation that is expected to be C-S-H. Furthermore, during the first five minutes of crystallization in the sample treated with PUS a minimum in the el. conductivity is observed. A similar minimum is observed in the sample temporarily heated to 35 °C, but the absolute value at the minimum is at a lower level in latter one. The following maximum in the el. conductivity curve in the PUS treated sample and the “plateau” in the reference sample are at similar value (i.e. within standard deviation). Again the maximum in the temporary heated sample does not reach these values. This observation is ascribed to the slightly higher sample temperature of the temporary heated solution at considered time (**Figure 22**). Nevertheless the minimum in the el. conductivity is detected at same period for sonicated and temporary heated sample. This indicates that the development of the el. conductivity is significantly modified by temperature. A modification of the crystallization process that can be ascribed purely to PUS application could not be observed. This

conclusion is confirmed by measurements of ion composition in aqueous solutions at given times (**Figure 23**).

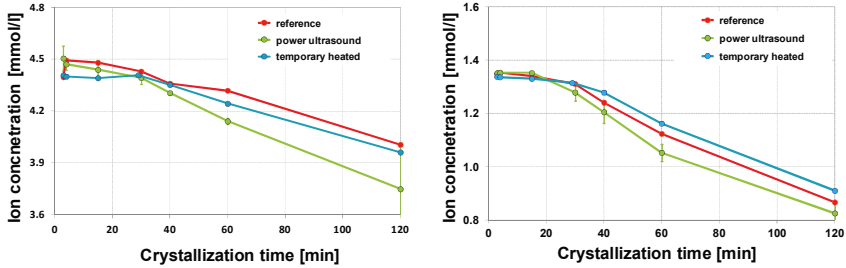

Figure 23: Development of ion composition of Ca-Si- solution in dependence of crystallization time, temperature and PUS application.

Figure 23 displays the development of Ca and Si ion concentration in aqueous solution during the first 120 minutes of crystallization. At the beginning of the crystallization process (during the first 30 minutes) only a slight decrease of both ion species (Ca and Si ions) was detected. Nevertheless, a temporary decrease in the el. conductivity in sonicated and temporary heated sample indicates precipitation (i.e. ion consumption) as deduced from **Figure 22**. However, in this case, the precipitates are probably smaller than 0.2 µm (pore size of syringe filter). Therefore, these particles are not separated by the syringe filter and can dissolve in aqueous HNO_3 solution. As a result Ca and Si ion concentration is artificially increased. Consequently, a decrease in the ion concentration as proposed by results of the el. conductivity measurement could not be detected. After approximately 30 minutes of crystallization time accelerated ion consumption proceeds. The calculation of ion consumption in the period from 30 min to 2 h of crystallization (slopes of the curves in **Figure 23**) indicated that a C-S-H phase possessing a Ca/Si ratio of approximately 1.4 – 1.6 precipitates (**Table 4**).

Table 4: Ion consumption in the period of rapidly decreasing the el. conductivity expects to be ascribed to C-S-H precipitation/ growth (30 – 120 minutes of crystallization).

Ion species	Reference		PUS		Temporary heated	
	mmol/l	g	mmol/l	g	mmol/l	g
Δ Ca [g]	0.42	0.00168	0.45	0.00180	0.45	0.00180
Δ Si [g]	0.44	0.00124	0.44	0,00124	0.40	0.00112
Δ Ca/Si [-]	0.95	1.35	1.02	1.45	1.12	1.61

To examine the precipitates that are expected to be C-S-H phases microstructural investigations were conducted by high resolution SEM (Nova NanoSEM, FEI, Netherlands). In a first step a sample of 10 µl was taken directly from the aqueous Ca-Si-solution (reference, without PUS application) after 30 and 60 minutes. One droplet of solution was placed on a SEM carbon foil sample holder on a support grid (Quantifoil® Micro Tools, Germany). The aqueous phase was removed immediately by applying the sample holder on filter paper. Subsequently, the residue was imaged by SEM. However, up to 60 minutes of the crystallization process precipitates could not be found by SEM investigation. This result was unexpected because the development of the el. conductivity indicated precipitation already after 30 minutes. Consequently further samples were collected by fixing the support grid inside of the reaction vessel before aqueous solution was filled in. Then, at given times support grids were taken out of solution and sample was blotted on filter paper as described earlier. With this preparation method already after 15 min of the crystallisation process first C-S-H phases were visible (**Figure 24a**). This observation correlates well with the slight decrease in the el. conductivity indicating precipitation (reference **Figure 25**). Since C-S-H phases were only found at the support grid (reaction vessel and conductivity electrode), this indicates that at the given constitution of the aqueous Ca-Si- solution (supersaturation, temperature) nucleation takes place preferentially on surfaces. This observation suggests that heterogeneous nucleation predominates. The el. conductivity decreases rapidly after 30 minutes of crystallization (**Figure 22**). At this period of time foil like C-S-H phases are observed by SEM (**Figure 24c**). After 2 h the whole sample holder is covered with C-S-H phases (**Figure 24d**). The decrease in the el. conductivity becomes less rapid since Ca and Si ions are depleted from solution until equilibrium is reached. Therefore no further significant changes in growth of C-S-H could be detected by SEM up to 24 h of crystallization.

Figure 24b displays the first C-S-H phases obtained from sonicated solution after 15 minutes of crystallization. Compared to the reference, the growth of C-S-H phases in a sonicated solution proceeds in a similar manner during the observed crystallization process (i.e. up to 24 h) by SEM imaging. Thus it is concluded that PUS application neither influences the el. conductivity (except temporary decrease due to increased solution temperature) nor changes the growth of C-S-H phases from solution.

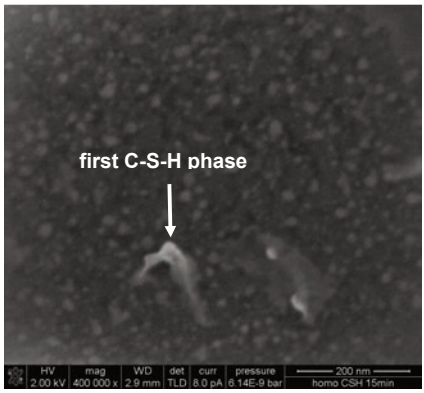

a) First C-S-H phase after 15 minutes of crystallization without PUS

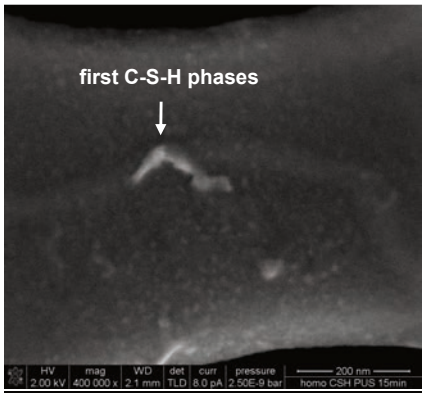

b) First C-S-H phases after 15 minutes of crystallization with PUS application

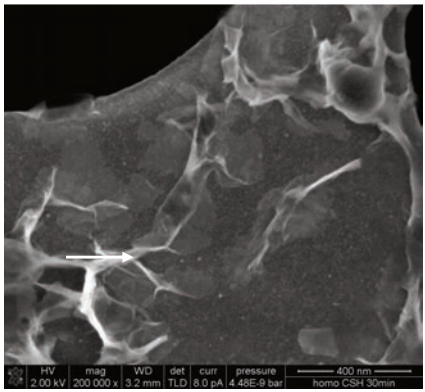

c) C-S-H phase after 30 minutes of crystallization

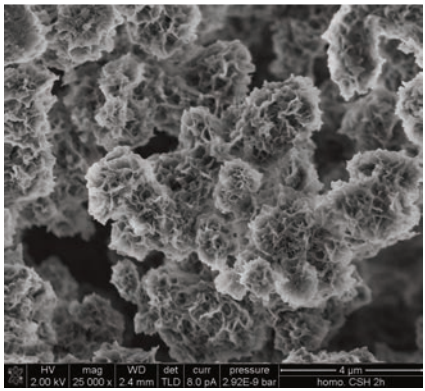

d) C-S-H phases after 2 h of crystallization

Figure 24: Microstructural development of C-S-H phases precipitating from clear to the eye solution (without PUS application) recorded with a Through the Length Detector (TLD) at approximately 10^{-6}mbar (high vacuum) at 2 kV acceleration voltages.

In conclusion the investigations on the influence of PUS on precipitation (nucleation and crystal growth) of C-S-H from clear to the eye aqueous Ca-Si-solutions reveal that sonication does not alter the crystallization process. Documented significant variation in the development of the el. conductivity was identified to be caused by temperature changes. The determination of the relevant ion concentration (Ca, Si ions) in solution evidenced similar concentrations for all samples. Hence, an acceleration of homogeneous reaction due to sonication as described by Suslick ("hot spots" and radical formation)[79] and Guo et.al.

(accelerated diffusion and increased nucleation coefficient)[109,110] could not be determined to be significant for C-S-H precipitation under current experimental conditions.
From microstructural investigation it is deduced that even in the case of nucleation from clear to the eye aqueous Ca-Si- solution, C-S-H preferentially precipitates heterogeneously. Changes in crystal morphology as described by Amara[107], Li[108], and Gou[130] due to PUS application cannot be observed.

Hydration of C_3S in H_2O at w/s = 50 (diluted suspension)

The development of the el. conductivity of stirred and highly diluted (C_3S-) suspensions is often monitored to investigate dissolution and precipitation processes (heterogeneous nucleation in terms of classical nucleation theory)[132,132,134,135,137]. Thus, this method is also used to investigate the influence of PUS on heterogeneous nucleation of C-S-H. Therefore 2.00 g of C_3S (particle size < 63 µm) were introduced into 100 ml bi-deionized water (l/s = 50). All suspensions were stirred at 300 rpm using a magnetic stirrer during whole measurement period. In the case of PUS application, suspension was sonicated after one minute of pre-homogenizing (300 rpm). The temporary temperature increase was achieved by placing the reaction vessel into a heated water bath (temperature = 95 °C). To guarantee similar temperatures during measurements (25 °C ± 1 °C) for all experiments, suspensions were stored in a thermostat-controlled water bath.

Figure 25 displays the development of the el. conductivity in 100 ml water containing 2.00 g of C_3S (particle size < 63 µm) during the first 20 minutes of hydration. As shown in **Figure 3** (page 23) period of quasi-pure C_3S dissolution (period I) can be detected during the first minute of hydration (**Figure 25a**). Subsequently, when the suspension becomes supersaturated with respect to C-S-H initial precipitation occurs simultaneously to C_3S dissolution (period II, **Figure 3 & Figure 25a**). Since the precipitation rate of C-S-H is higher than the dissolution rate of C_3S the el. conductivity remains constant[134]. From **Figure 25a** it becomes obvious that a PUS treatment as well as a temporary heating results in a slightly lower level of the el. conductivity during the induction period (II). Whereas in the reference the el. conductivity starts to increase after 12 minutes, it rises after 8 minutes in the sonicated and temporary heated samples. However, within the next two hours the evolution of the el. conductivity curve of the temporary heated sample becomes close to the reference (**Figure 25b**). In contrast an accelerated increase of the el. conductivity is detectable in the sonicated sample. According to **Figure 3** (page 23) the dissolution rate of C_3S and the precipitation rate of C-S-H are similar during period (III)[134]. Thus, an accelerated dissolution of C_3S and an enhanced C-S-H growth(-velocity) due to PUS application is deduced. As a result of the accelerated dissolution of C_3S the accumulation of Ca ions in aqueous suspension is also accelerated. Consequently, in PUS treated sample the typical portlandite peak is observed after approximately 18 h of hydration. Compared to the reference and the temporary heated sample this is an acceleration of about 5 h. Furthermore, results in **Figure 25b** reveal that the portlandite precipitation in sonicated samples occurs at the same total el. conductivity value as for the reference and temporary heated sample. Thus it is

concluded that not the portlandite precipitation mechanism, rate or supersaturation, but only the time of incidence is influenced by PUS application.

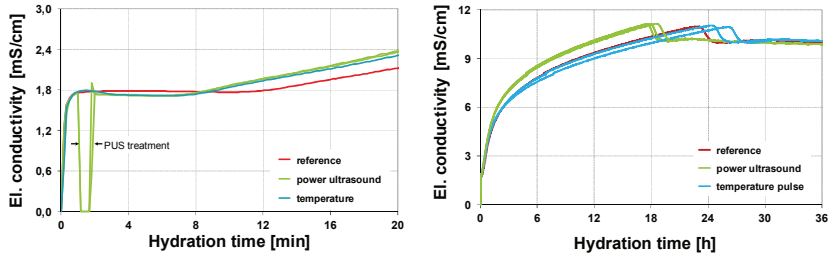

a) First 20 minutes of hydration **b) 36 h of hydration**

Figure 25: Development of the el. conductivity in a diluted C_3S suspension (water) in dependence of PUS application and temperature pulse.

In addition to the measurements of the el. conductivity of stirred and diluted suspension, relevant ion concentrations (Ca and Si ions) in the aqueous phase were determined by ICP-OES (ACTIVA M; HORIBA, Germany) during first 4 h of hydration. The results are presented in **Figure 26**. In accordance to the report by Garrault[52,131], the development of the el. conductivity is dictated by the Ca ion concentration (**Figure 26a**). During the observed plateau of the el. conductivity (induction period) related Ca ion concentration in the aqueous solution is also nearly constant (**Figure 26a**: 0-12 min). Significant differences in the Ca ion concentration between PUS treated sample, reference and temporary heated sample could not be determined for this period. At the same time (induction period) the Si ion concentration decreases. A consumption of the Si ions indicates initial precipitation of C-S-H phases[52]. This is in line with the results observed by Damidot[134] confirming a faster C-S-H precipitation rate compared to C_3S dissolution rate. Once again, the rise in the el. conductivity after induction period coincides with an increasing Ca ion concentration and thus confirms proceeding C_3S dissolution. Simultaneous decrease in the Si ion concentration goes along with the nucleation and growth of C-S-H phases.

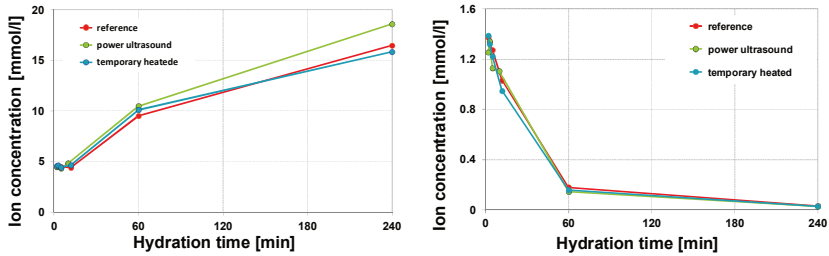

a) Ca ion concentration

b) Si ion concentration

Figure 26: Ion concentration (Ca and Si ions) in aqueous phase of diluted C_3S suspension (l/s = 50) in dependence of hydration time, PUS application and temporary heat treatment.

In summary latest investigation focuses on the (heterogeneous) dissolution-precipitation process of C_3S and C-S-H in stirred and diluted suspensions (water, l/s = 50) in dependence of PUS application. Also the influence of a temporary temperature increase was investigated. From the el. conductivity measurements (**Figure 25**) it was observed that a temporary increased suspension temperature at the beginning of hydration (sonicated and temporary heated suspension) reduces the induction time (period of constant el. conductivity characterized by greater C-S-H precipitation rate compared to C_3S dissolution rate[134], **Figure 3**). Since the duration of the induction period only depends on the number of C-S-H nuclei as proposed by Garrault et al.[131,52] and Damidot et al. [132], this implies that an increased suspension temperature causes the formation of an increased amount of smaller nuclei (Ca and Si ion concentration is similar for all samples). In the following hydration process, more C-S-H nuclei should lead to an accelerated C_3S hydration during period III (providing higher amount of growth regions for C-S-H) as shown by Alizadeh et al.[44]. However, the development of the el. conductivity measured in the temporary heated sample becomes close to the reference after approximately two hours during period III. Thus, an accelerated hydration was not observed. Therefore it is concluded that in the case of increasing suspension temperature a similar number of nuclei are formed only in a shorter period of time. This is supported by identical ion composition (**Figure 26)** and similar el. conductivity during period III of reference and temporary heated sample. Indeed, an accelerated C_3S hydration was observed for the sonicated samples (**Figure 25**). Provided that the number of C-S-H nuclei is not increased even in the case of PUS (as concluded from identical induction time and ion concentration of sonicated and temporary heated sample) the acceleration induced by PUS application is considered to be based on another principle: As known from the literature PUS generates its effects from cavitation[79,81]. Cavitational phenomena include hot spots, shock waves and jet streams. In acoustic fields (20 kHz for UIP 1000hd) jet streams are generated in the neighborhood of particles larger than 200 µm[78] (150 µm)[83] particle size. Depending on the constitution of C_3S suspension (particles size < 63 µm) the generation of destructive “jet streams” can be excluded due to the small particle size.

Consequently, the occurrence of hot spots (influence on nucleation and crystal growth)[108] and shock waves (microstreaming and particle acceleration)[92] is most probable. However, during primary nucleation, where the generation of hot spots is expected to have major influence on crystallization process (reduction of induction time as reported by Suslick[79] and Guo[109,110]), significant changes induced by PUS treatment could not be evidenced (**section 5.1.3** – Nucleation from clear to the eye solutions). Also in the case of heterogeneous nucleation the variation of the induction period was ascribed to temperature effects. Thus it is concluded, that the formation of shock wave appears to have major influence on the hydration process. Shock waves lead to particle acceleration and increased particle collisions[91,83]. As a result localized erosion on particle surfaces can be observed as shown elsewere[78,114,107]. Consequently, since C-S-H phases have been shown to nucleate (immediately) merely heterogeneously on C_3S surfaces[52] the effect of PUS (in narrower sense shock waves and particle collisions) on these primary precipitates may be a removal from the particle surfaces. Thereby, C_3S surfaces will not be covered by reaction products and thus remain still available for the dissolution process. Additionally the C-S-H nuclei that are now resided in solution provide further new growth regions for C-S-H. Comparable acceleration mechanism was observed during C_3S hydration in the presence of different types of $CaCO_3$[43] (**Figure 27**) and synthetic C-S-H[44,46].

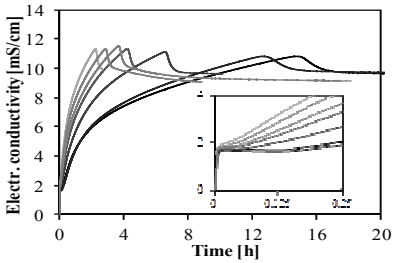

Figure 27: Evolution of the el. conductivity in C_3S suspension in dependence of time and calcite dosage.[43] (Inset show the first minutes in more detail).

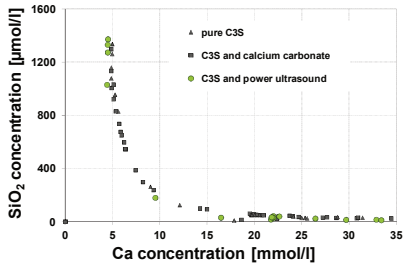

Figure 28: Ca- SiO_2 diagram of aqueous solution during C_3S hydration (kinetic path) with and without calcium carbonate addition[136] and PUS application.

Results of the previous investigations reveal that an increased calcite/synthetic C-S-H addition significantly reduces induction times and accelerates portlandite precipitation[44,43]. Consequently, it was shown[43] that C_3S hydration is significantly controlled by surfaces. In the presence of additional surfaces affine for nucleation and growth of C-S-H (as provided by calcite and/ or synthetic C-S-H), precipitation is not delimited solely to C_3S surfaces[43]. Hence, improved dissolution of C_3S and crystal growth (C-S-H) is observed if suitable nucleation sites are provided[52].

Furthermore the results of the el. conductivity measurements reveal that the maximum values at the end of pure dissolution period (period I) and at the end of period III (**Figure 3**)

are on the same level for all samples (**Figure 25**). Since the maximum value corresponds to the maximum supersaturation with respect to C-S-H (period I) and portlandite (period III), this suggests that PUS (and a temporary heat treatment) does not alter the maximum of supersaturation with respect to C-S-H and portlandite. Thus, a divergence from the kinetic path[3,135,133] due to PUS application is not observed (**Figure 28**), but rather a pure acceleration of the crystallization process was observed due to sonication. This is comparable to results found for C_3S hydration in the presence of $CaCO_3$ and synthetic C-S-H.

Whereas the effect of PUS on the dissolution of C_3S and the precipitation of C-S-H in water (diluted suspension, l/s = 50) is now obvious, the next part of investigation focuses on the influence of PUS on C_3S hydration close to cementitious conditions (increased Ca ion concentration, pH- value).

Hydration of C_3S in $Ca(OH)_2$ at l/s = 50 (diluted suspension)

In cement pastes, alite hydration proceeds under specific aqueous conditions, i.e. the Ca ion concentration and the pH- value increase immediately after water addition. Consequently, compared to the hydration of C_3S at high l/s in pure water, hydration in a calcium hydroxide (CH) solution is more close to cementitious environment. Therefore, to obtain comparable conditions found in cement pastes, C_3S is added to a saturated CH solution. A Ca ion concentration of 21.0 mmol/l (ICP-OES, ACTIVA M, HORIBA, Germany) and a pH- value of 12.59 (pH/ ION Meter pMX 3000, WTW, Germany) were determined for saturated CH solution.

In analogy to the experiments performed in pure water at l/s = 50, the influence of PUS on C_3S hydration in stirred diluted lime suspensions (l/s = 50) was estimated by means of the development of the el. conductivity (TetraCon® 325, WTW, Germany), the ion concentration of aqueous phase (ICP-OES, ACTIVA-M, HORIBA, Germany), and additionally microstructural high resolution SEM examinations (Nova NanoSEM 230, FEI, Netherlands).

Results of the development of the el. conductivity are shown in **Figure 29**. After the addition of C_3S to saturated CH solution a constant value of el. conductivity was detected for the reference sample. This plateau (induction period) lasted for approximately one hour. Hence, during this period of time either no significant dissolution of C_3S occurs or dissolution of C_3S and precipitation of C-S-H are balanced (C_3S dissolution rate is less compared to C-S-H precipitation rate, c.f. **Figure 3**). At the end of the induction period in the reference sample (after approximately one hour) a rapid increase of the el. conductivity indicates an increase in dissolution rate of C_3S. As a result the solution becomes enriched with Ca ions until it becomes supersaturated with respect to portlandite. Subsequent portlandite precipitation is indicated by the sudden drop in the el. conductivity after approximately 6 h of hydration in the reference sample. In the case of PUS, applied immediately after adding C_3S to CH solution, a minimum in the el. conductivity is observed (**Figure 29**).

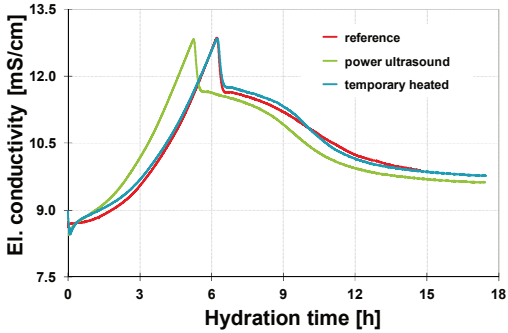

Figure 29: The el. conductivity of C_3S hydrated in a saturated CH solution (l/s = 50) in dependence of time, temperature and PUS application

A similar minimum is determined for the sample that was temporary heated by a short heat treatment to obtain equivalent temperature rise as induced by PUS application. Therefore the results demonstrate that the decrease in the el. conductivity is a temperature effect. Nevertheless, a rapid rise in the el. conductivity follows without the appearance of a plateau in both samples (PUS and temporary heated), that means a distinction of a "real" induction period is ambiguous. Whereas the el. conductivity curve of the temporary heated sample follows closely that of the reference after approximately 4 h of hydration, a sharper increase is documented for the sonicated sample. Thus, it is evidenced that the hydration of C_3S is accelerated due to PUS application. This observation is confirmed by the earlier appearance of the typical portlandite peak that is portlandite precipitation.

To investigate the contribution of the Ca and Si ion concentration on the el. conductivity, the ion composition of the aqueous phase was determined simultaneously. In **section 5.1.3** (*Nucleation from clear to the eye solutions (primary nucleation)*) results revealed that a temporary temperature increase does not influence the development of ion composition compared to the reference (**Figure 23** and **Figure 26**). Thus, only the ion composition of aqueous phase of the reference and the sonicated sample were considered here. Results are shown in **Figure 30**.

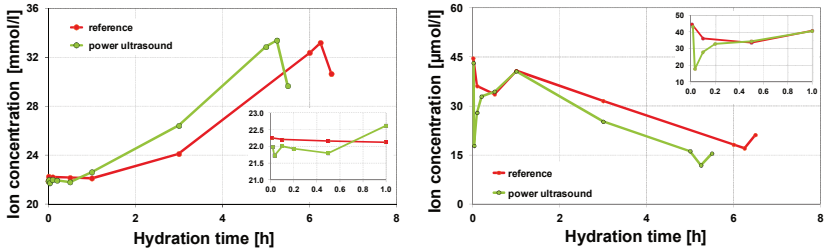

a) Ca ion concentration **b) Si ion concentration**

Figure 30: Ca and Si ion concentration in C_3S suspension (l/s = 50) hydrated in saturated CH solution in dependence of PUS application (Inset show the first hour in more detail).

Once more the results in **Figure 30a** confirm that the el. conductivity is dictated by Ca ion concentration[52]. But whereas an initial decrease in the el. conductivity (PUS and temporary heated sample) was documented (**Figure 29**) corresponding Ca ion composition remains unaffected. This is attributed to sample preparation. Thereby if C_3S particles and/or very first precipitates (assumed to be portlandite due to temperature depend solubility of $Ca(OH)_2$) possess a particle size smaller than 200 nm these precipitates can pass the syringe filter (0.2 µm). In the acidic environment (addition of approx. 0.2 g of 0.5 mol HNO_3 to 10 – 14 ml sample solution) of analyzed aqueous solution these small particles dissolve and then are detected by the ICP-OES measurement. Nevertheless, in the sonicated suspension a decrease of the Ca and Si ion concentration was determined immediately after the addition of C_3S to the saturated CH solution (Insets **Figure 30**). Previous investigations showed that first reaction products (C-S-H) precipitate promptly when C_3S is suspended in lime solutions (Ca in concentration > 8 mmol/l[52])[134,135]. If the C-S-H precipitation rate is increased compared to the C_3S dissolution rate a decrease in Si ions concentration can be determined. Whereas in the sonicated sample a minimum in the Si ion concentration is reached after several minutes, a continuous slow consumption of Si ions up to 30 minutes could be detected in the reference (**Figure 30b**). The insets in **Figure 30** that show the first hour of hydration in more detail reveal a time period where the Ca and Si ion concentrations in the sonicated sample are lower than the reference sample. This is a fairly good indication that at least in this early hydration time precipitation in the PUS sample was increased compared to reference. The renewed increase in Si ion concentration up to 60 minutes of hydration might be attributed to three different phenomena: On the one hand increasing Si ion concentrations indicate that the dissolution of C_3S exceeds precipitation/growth of C-S-H. Also the dissolution of previously formed hydrates is possible. In both cases the absolute increase in the Si ion concentration (max. Δ Si = 23 µmol/l for sonicated sample) only accounts for an increase of max. 69 µmol/l Ca. This value lies within the Ca ion detection limit (± 0.06 mmol/l). Therefore a significant change in the Ca ion concentration is not expected (**Figure 30**). However, also another explanation for the minimum and subsequent increase of the Si ion concentration during induction time is possible: At the beginning a Si-rich C-S-H phase precipitates which later converts into a Ca-rich C-S-H phase. This proceeds until a maximum in the Si concentration (similar for reference and PUS treated sample) is reached again. At the end of the induction period a continuous increase of the Ca ion concentration linked with the simultaneous decrease of the Si ion concentration indicates a proceeding dissolution of C_3S (release of Ca ions) and growth of C-S-H phases (consuming Si ions).

The occurrence of the maximum Ca ion concentration is associated with the time when the solution becomes supersaturated with respect to portlandite[134,135]. From **Figure 30a** it becomes obvious, that sonication influences the time of incidence of the maximum Ca ion concentration but does not affect its absolute value. In the reference sample the maximum of Ca ion concentration is reached after six hours and after five hours in the PUS treated sample. Because the absolute value of the Ca ion concentration of sonicated sample is similar to that measured for the reference, it is concluded that PUS treatment has no influence on saturation degree to initiate portlandite precipitation. Simultaneously to the portlandite precipitation C_3S dissolution is increased again as indicated by the renewed

increase of the Si ion concentration after five hours for sonicated sample and six hours for reference (**Figure 30**).

Additional to the measurements of the el. conductivity and the determination of the ion composition of aqueous phase, microstructural investigations by high resolution SEM (Nova NanoSEM 230, FEI, Netherlands) were performed to characterize the structural development, i.e. C_3S dissolution and growth of hydrate phases (C-S-H and portlandite) during hydration process (**Figure 31**).
After 12 minutes of hydration SEM images reveal that in the reference sample indication of proceeding C_3S hydration could not be found. C_3S particles posses a smooth surface without any dissolution voids (**Figure 31a**). In contrast, in the PUS treated sample first regions of C_3S dissolution were detected (**Figure 31b**), clearly showing advanced initial dissolution of C_3S. Also first C-S-H phases are visible in the sonicated sample. After a hydration time of 3 h dissolution voids all over C_3S surfaces are visible in the reference sample. Also locally, very small C-S-H phases can be observed (**Figure 31c**). In comparison in the sonicated sample dissolution of C_3S seems to be more advanced. Additionally, a significantly accelerated C-S-H growth in the sonicated sample becomes obvious from **Figure 31d**. Smaller C_3S particles are already fully covered with C-S-H phases. After a hydration time of 5 h 30 min besides C-S-H also portlandite can be observed in the sonicated sample (**Figure 31f**). This observation time correlates well with timely process of the el. conductivity curve (**Figure 27**). After this time (5 h 30 min) a drop in the el. conductivity was detected in the sonicated sample that is associated with portlandite precipitation[134,135]. In contrast only C-S-H phases are visible in the reference sample at the same time (**Figure 31e**). Here (in the reference) all C_3S particles are fully covered with C-S-H phases. Finally, microstructural investigations show that an accelerated C_3S dissolution is achieved and the precipitation of C-S-H phases and portlandite is accelerated by PUS application.

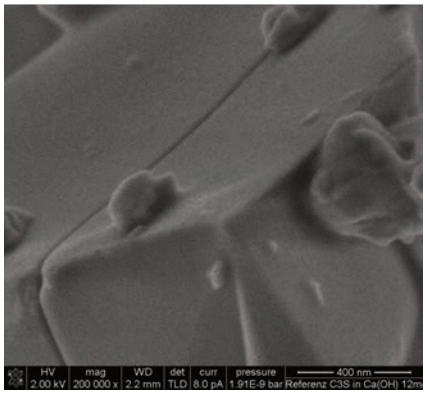

a) Reference after 12 minutes of hydration: smooth C_3S particle surfaces.

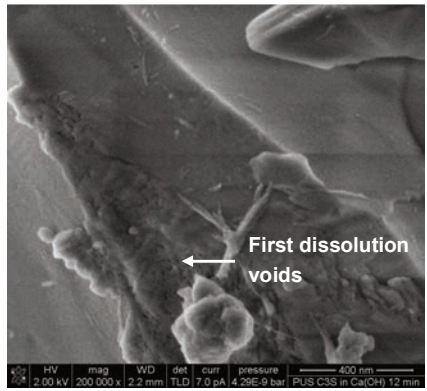

b) Power ultrasound after 12 minutes of hydration: first dissolution voids on C_3S surfaces.

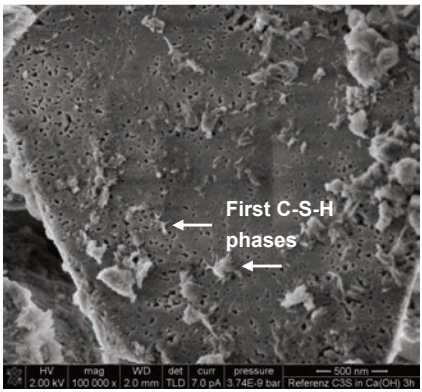

c) **Reference after 3 h of hydration: dissolution voids on C_3S surfaces and first C-S-H phases.**

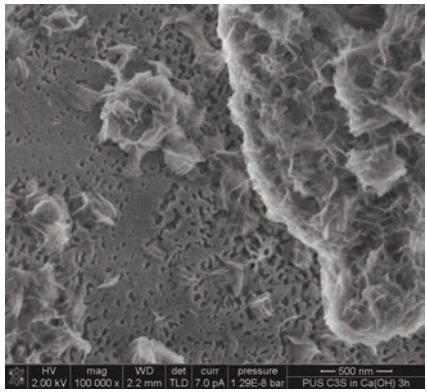

d) **Power ultrasound after 3 h of hydration: smaller C_3S particles are fully covered with large C-S-H aggregates.**

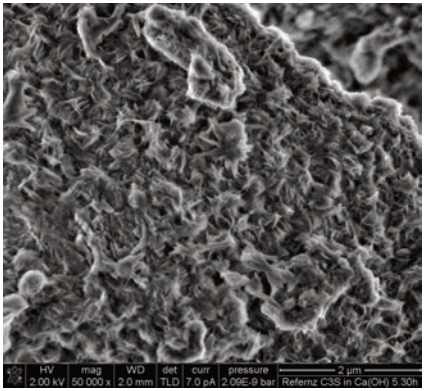

e) **Reference after 5 h 30 minutes of hydration: C_3S surfaces are covered with C-S-H.**

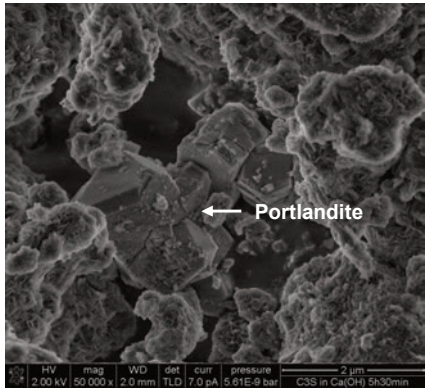

f) **Power ultrasound after 5 h 30 minutes of hydration: portlandite crystals**

Figure 31: Microstructure of C_3S hydrated in calcium hydroxide solution with and without PUS application in dependence of hydration time recorded with a Through the Length Detector (TLD) at approximately 10-6 mbar (high vacuum) at 2 kV acceleration voltages.

In summary, the influence of PUS on the C_3S dissolution and C-S-H as well as portlandite precipitation at chemical conditions similar to cement hydration (high Ca ion concentration and high pH- value) is comparable to effects found for the diluted C_3S-H_2O system (l/s = 50): The variation of the el. conductivity during the induction period in sonicated sample can be attributed to temperature changes. It was demonstrated that immediately after C_3S is added to the saturated (lime)-solution precipitation of C-S-H is initiated as indicated by Si ion

consumption. It is deduced that the increased very early C-S-H precipitation determined in the sonicated samples paves the way for acceleration during the main stage of C_3S hydration. The increase of Si ion concentration up to 60 minutes of hydration may be induced by three different processes:

1. The dissolution of C_3S is more pronounced than C-S-H precipitation (C_3S dissolution rate >> C-S-H precipitation rate).
2. Preliminarily formed C-S-H dissolves again.
3. A Si- rich C-S-H converts into a Ca- rich C-S-H phase until the maximal Si concentration is reached again. Furthermore similar maximum values in the reference and sonicated sample of the el. conductivity and Ca ion concentration indicated that maximum supersaturation with respect to portlandite is not influenced by PUS. Finally, similarity of mechanism induced by PUS application leading to accelerated C_3S hydration in pure water is assert for saturated lime solution. Effects due to the formation of hot spots (increased diffusion coefficient, radical formation), if there are any, are less important. Jet streams are excluded because the particle size of C_3S is smaller than 63 µm. Consequently, significant acceleration of C_3S hydration process in saturated lime suspension is also ascribed to the formation of shock waves leading to particle acceleration, increased particle collisions and thus locally erosion effects producing free C_3S surfaces and increased regions for C-S-H growth.

Hydration of C_3S in presence of superplasticizer

In view of the aim of this thesis (application of PUS in precast production) it has to be considered that in modern precast production mostly SP is added to the concrete mix. Consequently, the influence of PUS on the nucleation of C-S-H in the presence of SP is the focus of this section.

Analogous to the investigations without SP addition, primary (in the absence of particles) and heterogeneous C-S-H precipitation and growth were examined in the presence of SP and PUS. In the case of primary C-S-H nucleation 20 µl (0.08 m.-% SP dry mass) of polycarboxylate type SP were added to 100 ml of aqueous Ca-Si-solution (prepared as described in **section 5.1.3**, pp. 51). In the case of heterogeneous nucleation (stirred, diluted C_3S suspension, l/s = 50) a very small amount of SP dosage (0.007 m.-% SP dry mass referred to C_3S mass) was added to the suspension. The measurements of the el. conductivity were performed during first 18 h of the crystallization process. Solutions and suspensions were stored at constant temperature (25 °C ± 1 °C) during the whole measuring period. In Addition to the determination of the el. conductivity microstructural investigations (Nova NanoSEM 230, FEI, Netherlands) were performed (heterogeneous nucleation) to characterize microstructural development of solids in dependence of hydration time, SP addition and PUS application.

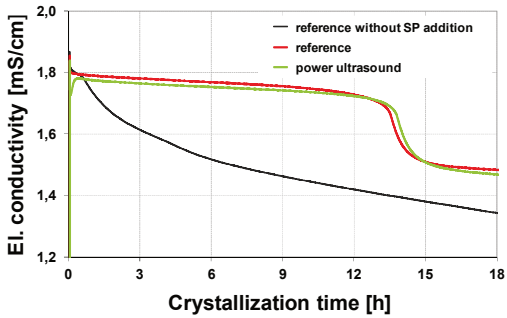

Figure 32: Development of the el. conductivity of a clear to the eye Ca-Si-solution in dependence of SP addition and PUS application.

The development of the el. conductivity during primary nucleation of C-S-H is presented in **Figure 32**. Obviously, adding a very small amount of SP (20 µl, 0.08 m.-% SP dry mass) to a clear to the eye aqueous solution of Ca and Si ions leads to a significant increase of the period with nearly constant el. conductivity (induction time). Without SP addition a rapid decrease of the el. conductivity after approximately 30 minutes indicates proceeding C-S-H precipitation (cf. **section 5.1.3** *Nucleation from clear to the eye solution (primary nucleation)*). In solution containing a very small amount of SP, the rapid slope is detected only after 13 h of crystallization. Thus, SP addition definitively affects (hinders) C-S-H precipitation (nucleation and growth) as described by Sowoidnich[136]. A more rapidly decrease of the el. conductivity in the SP containing solution (**Figure 32**: 13 h of crystallization time) indicates an increased growth rate of C-S-H compared to the reference without SP addition. However, an additional PUS treatment immediately after the filtration process does not significantly change the crystallization process (nucleation and growth) of C-S-H phases from clear to the eye solutions in the present of SP (except initial reduction of the el. conductivity induced by temperature increase). This is in line with investigation of primary nucleation without SP addition. Consequently, results verify that PUS does not alter precipitation process in the absence of solid particles.

On the other hand, a significantly accelerated dissolution/precipitation process during hydration of stirred diluted C_3S suspensions (l/s = 50) without SP addition was documented. Thus following section discusses if comparable influence of PUS on nucleation process of C-S-H can observed in the presence of SP.

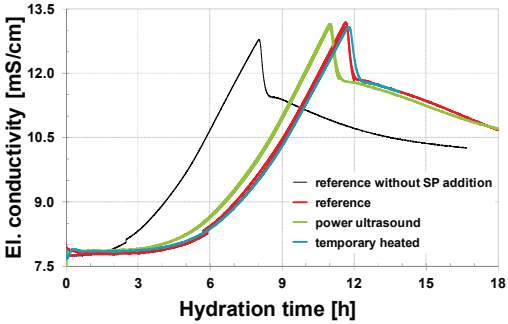

Figure 33: Development of the el. conductivity of C_3S hydration in CH solution in dependence of SP addition, temperature, and PUS application.

Results in **Figure 33** display the development of the el. conductivity in dependence of time, SP addition, and PUS application in stirred diluted C_3S-CH suspensions (l/s = 50). Clearly it is demonstrated that even a very small amount of SP (0.007 m.-% SP dry mass referred to C_3S mass) causes a significant prolongation of the induction period. In comparison to the reference without SP addition (induction time t_{ind} = 1 h; **Figure 33**) the plateau of the el. conductivity with SP addition lasts for approximately 4 h. Additionally, it can be seen from **Figure 33** that also the absolute value of the el. conductivity during the plateau is unaffected by SP. These observations coincide with results found by Sowoidnich[136] on the influence of polycarboxylate based SP on C_3S hydration.

In view of the influence of PUS application on C_3S hydration in diluted and stirred (lime-) suspension containing SP the effects emerge to be:

1. The induction time (indicated by the plateau) is shortened, i.e. the el. conductivity increases earlier compared to the reference and temporary heated sample (both with SP addition).

2. Also portlandite precipitation occurs earlier in sonicated sample. Whereas in diluted C_3S suspensions in the absence of SP induction time was also shortened by temporary heat treatment (**Figure 25** and **Figure 27**) this is not observed when SP is added to the mix. This indicates that shortening of nucleation time by increased suspension temperature is less significant compared to the retarding effect induced by SP. Nevertheless, sonication effects are similar to those observed in diluted C_3S suspensions (l/s = 50, water and saturated CH solution) in the absence of SP. But when SP is added, the acceleration of C_3S hydration due to PUS treatment is less effective. Without SP addition the acceleration of portlandite precipitation in sonicated sample was about one hour (**Figure 29**). In the solution containing SP only an acceleration of half an hour could be detected. Additionally it is observed that PUS application does not chance the absolute values of the el. conductivity, but SP addition does. Whereas in the reference without SP addition the el. conductivity maximum is about 12.7 mS/cm it is at 13.2 mS/cm when SP is added to the saturated lime suspension. In accordance with observations reported by Sowoidnich[137] this indicates that SP influences solubility of C_3S and/or supersaturation with respect to portlandite.

Microstructural investigations confirm changes in the crystallization progress (**Figure 34)** as determined by the el. conductivity measurements (**Figure 33**). As seen in **Figure 33,** the el. conductivity still exhibits a plateau in the reference sample after 3 h of crystallization process. At this time SEM-SE images reveal smooth surfaces of the C_3S particles (**Figure 34a**) in the reference. Compared to that, an initial dissolution of C_3S is indicated by a slightly increase in the el. conductivity in the sonicated sample (**Figure 33**). SEM images verify the initial dissolution by showing etch pits on the C_3S surface (arrow, **Figure 34b**). Also first C-S-H clusters are visible. **Figure 34c** displays the microstructure after 5 h of crystallization in the reference sample. Here (**Figure 34c**), etch pits (arrow) and first C-S-H phases confirm proceeding C_3S dissolution with simultaneous C-S-H precipitation. At the same time also in PUS treated sample propagated etch pit and C-S-H cluster formation can be observed (**Figure 34d**).

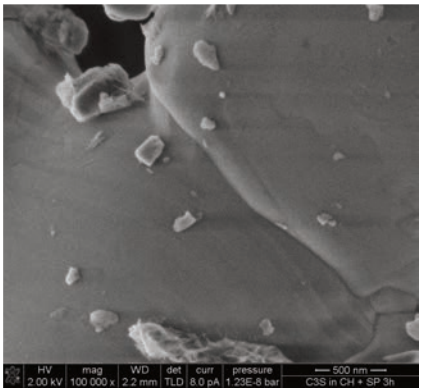

a) Reference 3 h: smooth surfaces of C_3S particles

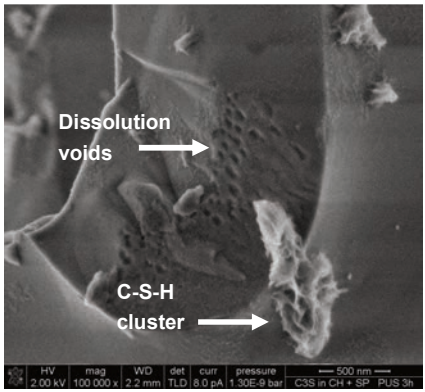

b) Power ultrasound 3 h: first dissolution voids and C-S-H

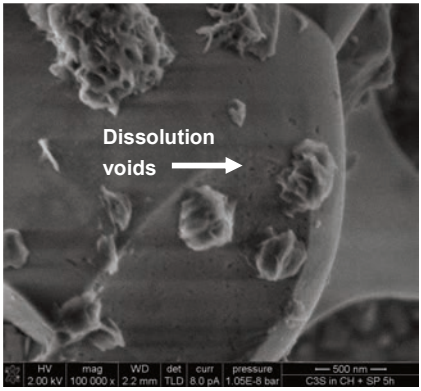

c) Reference 5 h: first dissolution voids and C-S-H

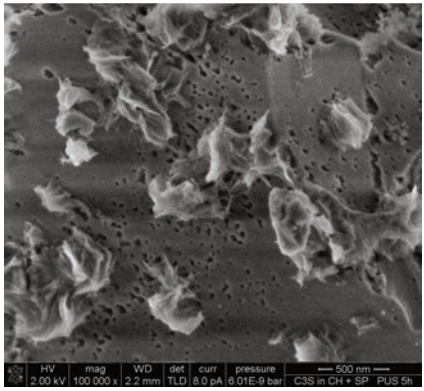

d) Power ultrasound 5 h: advanced dissolution and C-S-H cluster

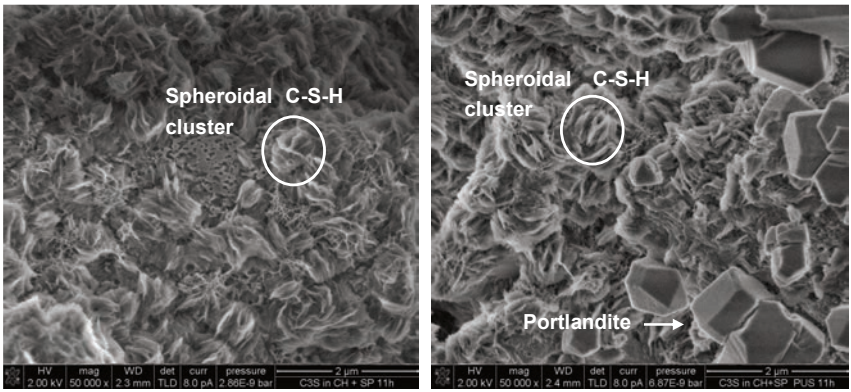

e) Reference 11 h: spheroidal C-S-H clusters

f) Power ultrasound 11 h: spheroidal C-S-H clusters and portlandite

Figure 34: Microstructure of C_3S (hydrated in $Ca(OH)_2$ solution with SP addition) in dependence of crystallization time and PUS application. Images were recorded in a SEM equipped with a Trough the Lens Detector (TLD) at approx. 10^{-6}mbar (high vacuum) at 2 kV acceleration voltages.

After 11 h of crystallization most of the surface of C_3S is covered with C-S-H phases in the reference sample (**Figure 34e**). Compared to those observed in the absence of SP (**Figure 31e**) C-S-H phases occur as spheroidal clusters when SP is added to the solution. Similar observations were evidenced by Sowoidnich[136,137]. Changes in structural arrangement of the C-S-H phases caused by PUS treatment could not be distinguished. After approximately 11 h of crystallization a decrease in the el. conductivity was detected for the sonicated sample (**Figure 33**). SEM images verify that this decrease can be correlated with portlandite precipitation (**Figure 34f**). At the same period in the reference sample only the presence of C-S-H phases is observed.

In summary effects induced by PUS application on the crystallization process (nucleation/growth) of C-S-H in the presence of SP are comparable to those determined in absence of SP. A significant prolonged induction period is observed by the addition of a very small amount of SP in the case of crystallization from clear to the eye aqueous Ca/Si-solution. However, a further variation of the primary nucleation process could not be determined by an additional PUS treatment. In other words, an acceleration of primary nucleation process due to sonication is not observed. Thus, also in the presence of SP PUS effects based on the formation of “hot spots” (increased diffusion coefficients, radical formation) are not significant. In stirred diluted suspensions the addition of a very small amount of SP also causes a prolongation of induction period. But compared to experiments in the absence of particles (primary nucleation) C_3S hydration process is accelerated by PUS treatment. SEM examination reveals an accelerated dissolution accomplished enhanced C-S-H formation/growth. Additionally same microstructural investigations clearly show the

influence of SP on the morphology of C-S-H (becoming spheroidal clusters). In contrast changes in the morphology of C-S-H phases caused by PUS treatment could not be observed.

Influence of PUS on hydration of concentrated C_3S suspensions (l/s = 0.5)

Whereas the influence of PUS on the dissolution/precipitation process during C_3S hydration in stirred diluted suspension is documented, in the next section the accelerated hydration of concentrated C_3S suspensions (l/s = 0.5) induced by PUS application has to be validated. Therefore microstructural SEM investigation (Nova NanoSEM, FEI, Netherlands) and additionally QXRD analyses (D5000, Siemens, Germany; Rietveld analyses) were performed.

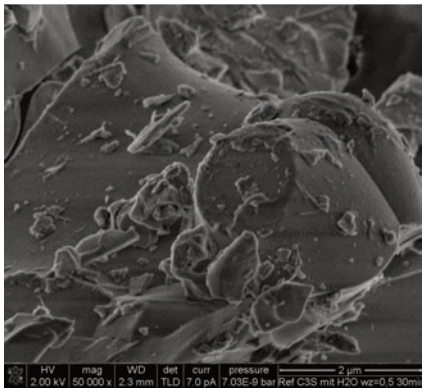

a) Reference, 30 min hydration time: smooth C_3S surfaces.

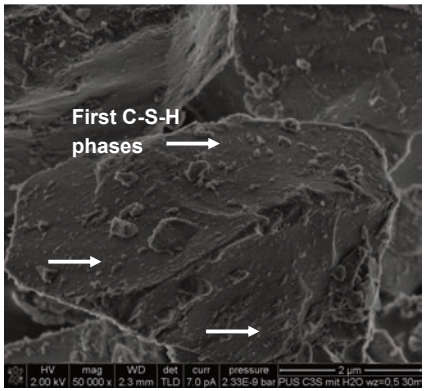

b) Power ultrasound, 30 min hydration time: first C-S-H phases are visible.

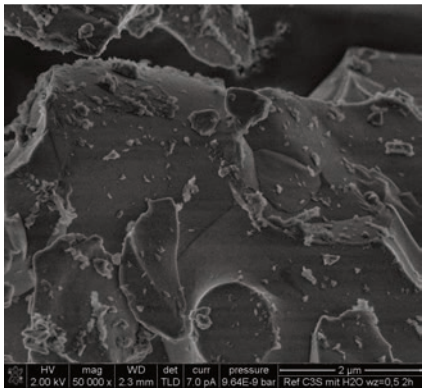

c) Reference, 2 h hydration time: mainly smooth surfaces of C_3S.

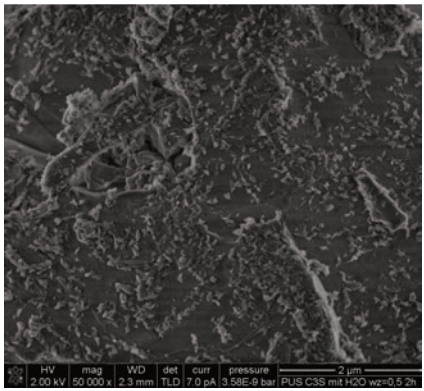

d) Power ultrasound, 2 h hydration time: significant growth of C-S-H phases.

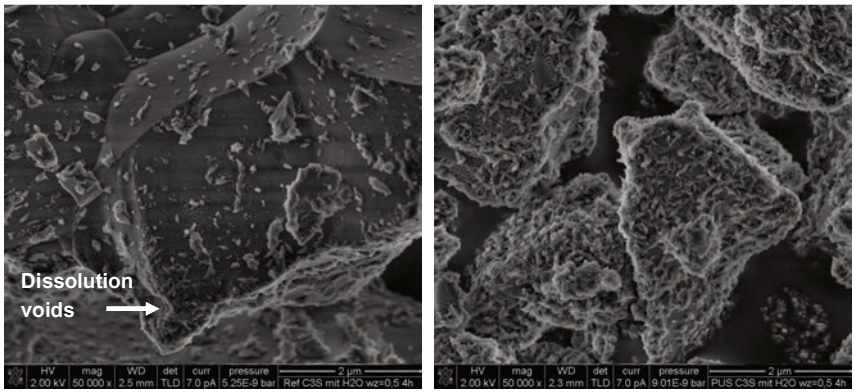

e) Reference, 4 h hydration time: typical dissolution voids (etch pits) and first C-S-H phases on C_3S surface.

f) Power ultrasound, 4 h hydration time: C_3S particles are fully covered with C-S-H phases

Figure 35: Microstructure of C_3S (hydrated in de-ionized water at l/s = 0.5) in dependence of hydration time and PUS application. Images were recorded in a SEM (Nova NanoSEM 230, FEI, the Netherlands) equipped with a Trough the Lens Detector (TLD) at approx. 10-6 mbar (high vacuum) at 2 kV acceleration voltages.

Microstructural characterization of solids (C_3S) after a hydration period of 30 minutes (**Figure 35a&b**) reveal that already after this time an ultrasonic treatment causes an enhanced hydration process. At this time first C-S-H phases are observed in the sonicated sample (arrow **Figure 35b**). Compared to that, the C_3S particles in the reference sample posses a smooth surface at similar period (**Figure 35a**). Significant changes in the microstructure of reference sample cannot be detected even two hours after water addition (**Figure 35c**). However, C-S-H phases in the PUS treated sample show a significant growth after 2 h of hydration. Only after 4 h of hydration first precipitates (C-S-H phases) and typical etch pits are observe in the reference sample (**Figure 35e**). At the same time in sonicated sample surface of the C_3S particles are fully covered with C-S-H phases (**Figure 35f**).

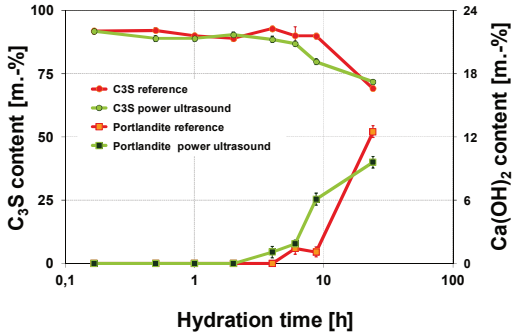

Figure 36: Phase content of C_3S paste (hydrated in de-ionizied water at w/s = 0.5) determined by QXRD in dependence of hydration time and PUS application.

To verify results documented by SEM investigations phase content was quantified by QXRD (Rietveld method, external standard method). Results are displayed in **Figure 36**. Relevant period of time concerning the strength development of cement is in between 4 h and 8 h of hydration. For this period a significant decrease of C_3S content due to PUS application could be documented by QXRD. Simultaneously increased portlandite content was determined. Thus the accelerated hydration process determined by SEM investigations is confirmed.

5.1.4. Conclusions

Results of **Chapter 5.1** documenting the influence of PUS on the initial setting and the hardening of OPC suspensions and the nucleation of C-S-H represent the first experiences gained in the field of accelerated cement hydration induced by PUS application. At the beginning, the optimal PUS parameter (amplitude and specific energy input) were identified in compliance with practical requirements (short sonication duration, restricted temperature increase of suspension and significant acceleration of cement hydration). For sonication at ambient pressure it was found that large amplitudes (43 µm) transmitted via large front face diameter of ultrasonic horn and moderate specific energy inputs (75 J/ml) are the most suitable parameters that meet all aforementioned requirements. Results obtained by several methods working independently of each other (determination of initial setting time, isothermal heat conduction calorimetry, non-destructive ultrasound testing, compressive strength of mortar) clearly evidence a significantly accelerated cement hydration induced by PUS treatment. SEM investigations indicated an accelerated alite hydration coupled with accelerated C-S-H formation. Thus, the influence of sonication on hydration process of alite phase itself was investigated in more detail using the model substance C_3S. Results of experiments focusing the primary and heterogeneous precipitation (nucleation and growth) of C-S-H reveals that the most probably effect leading to the accelerated C_3S hydration is the formation of shock waves induced by cavitational events. Shock waves are assumed to cause particle acceleration leading to increased particle collisions and thus erosion effects[81,82,92]. In the case of C_3S hydration that might lead to a removal of initial C-S-H precipitates away from C_3S surfaces. Therefore, on the one hand C_3S particle surfaces

remain uncovered with respect to hydrate phases. On the other hand C-S-H precipitates that are removed from C_3S surfaces provide additional regions for growth. However, other PUS effects induced by the generation of “hot spots” and “jet streams” are identified to be of minor significance or even impossible at all. Furthermore, it was demonstrated that the C_3S hydration is also accelerated by sonication in the presence of SP. Morphologically changes of C-S-H (formation of spheroidal clusters) caused by SP addition could be verified. In contrast, significant changes in morphology of C-S-H induced by PUS application were never observed.

5.2. Influence of PUS on workability of Portland cement suspensions

5.2.1. De-airing, Homogenizing, and Dispersing

In concrete production a dense microstructure is required for most applications. Disadvantageous pore structure (coarse pores: air voids and capillary pores) not only reduces the compressive strength[34,141] but also induces durability risks (especially capillary pores: infiltration of destructive media)[138,3].

A well known phenomenon from PUS application is amongst others the de-airing effect[77,80,139]. Hence, in the next section the influence of PUS on air void contents and pore structure of cement pastes is in focus of investigations.

In fresh cement pastes air void content was determined according to DIN EN 12 350-6 by de-airing cement paste at low pressure after 20 minutes of hydration. The porous structure was characterized by light microscopic investigations (VHX II 600, Keyence, Japan) on polished sections from 7 d hydrated cement pastes.

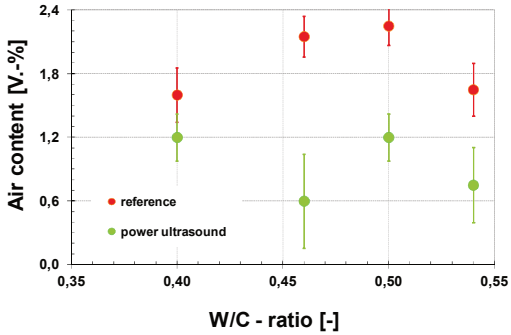

Figure 37: Air void content in fresh cement suspension in dependence of w/c ratio and PUS application.

Figure 37 displays the air void contents of fresh cement pastes in dependence of water to cement (w/c) ratio and PUS application. Obviously, results show a significant decrease in air void contents due to the PUS treatment. The determined average air void contents in the reference samples was 2 v.-%. Due to PUS application a reduction of 1 v.% air void content was measured independently of the w/c ratio.

The air void distribution in hardened cement pastes is present in **Figure 38**. Images reveal that even after 7 d of hydration the influence of PUS treatment on air void composition can be evidenced. In the reference sample air voids of 0.3 up to 1.0 mm in diameter are observed (**Figure 38a**). In the sonicated sample less and smaller (< 0.2 mm) air voids are detected (**Figure 38b**). Hence, the de-airing effect of PUS application determined in fresh cement pastes can also be proven in hardened cement paste by light microscopic investigations. With the escape of air a denser microstructure is achieved. Thus apparent density of sonicated cement pastes was determined to be approximately 20 kg/dm³ (≈ 1 m.-%) higher than the corresponding reference, i.e. 1.88 kg/dm³ for reference vs. 1.90 kg/dm³ for PUS.

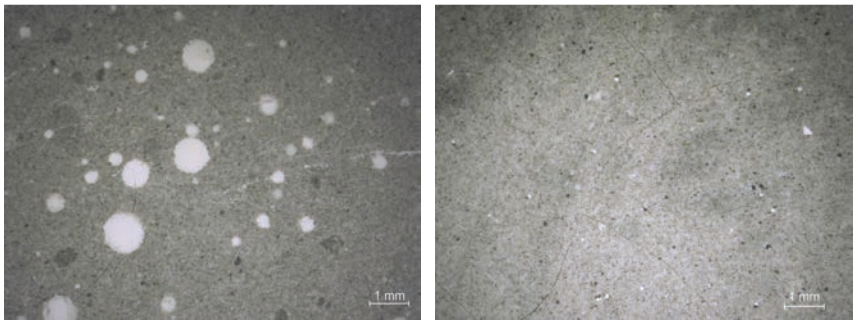

a) Reference **b) Power ultrasound**

Figure 38: Air void distribution in cement suspension (w/c = 0.4) after 7 d of hydration, images taken by light microscopy on polished sections.

Besides the de-airing obtained by PUS the most common application of PUS in industry is to homogenize and disperse liquids and suspensions/emulsions[97,98]. If cement suspensions are treated with PUS homogenizing and dispersing effects can also be observed. From the photographs of cement pastes shown in **Figure 39** the homogenizing effect (i.e. equally distribution of all constituents throughout the suspension[140]) becomes obvious. Whereas in the reference cement suspension lumpy structures (cluster of cement particles) are visible (arrows **Figure 39a**) the sonicated sample appears as smooth homogeneous suspension (**Figure 39b**).

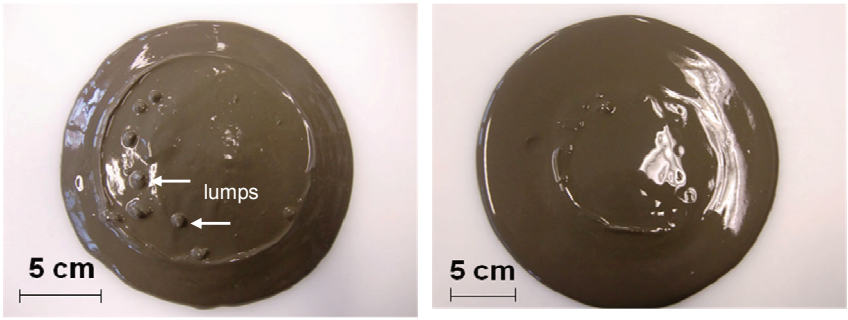

a) Reference **b) Power ultrasound**

Figure 39: Homogenizing effect of PUS on cement suspensions (w/c = 0.43).

Furthermore, the dispersing effect of PUS on cement suspensions was evidenced by sedimentation experiments[141,142]. For this purpose cement suspensions (w/c = 0.4 and PUS application if necessary) were produced. After 10 minutes of hydration 25 g cement suspension were introduced into a settling cylinder that was subsequently filled up to 100 ml with de-ionized water. Afterwards all samples were agitated in the same manner. After given periods of time (e.g. three minutes) the sedimentation volumes were measured (**Figure 40**). Since sedimentation velocity is linked with the fines of particles (Stokes´ law, **Eq.19**)[143]

$$v = \frac{2 \cdot a^2 \cdot g \cdot (\rho' - \rho)}{9\eta} \qquad \textbf{Eq. 10}$$

where v is the sedimentation velocity, a is the radius of spherical particle, g is earth´ gravity, ρ' and ρ are the density of particle and fluid, respectively, and η the viscosity of the fluid; the dispersing effect is assessed by determining the sediment volume of cement particles after given times (the finer the particle the lower the sedimentation velocity and thus the greater the sediment volume). The greater the sediment volume, the greater the dispersing effect.

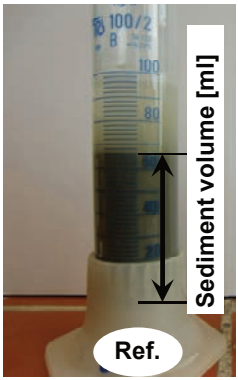

Figure 40: Sediment volume of cement suspensions

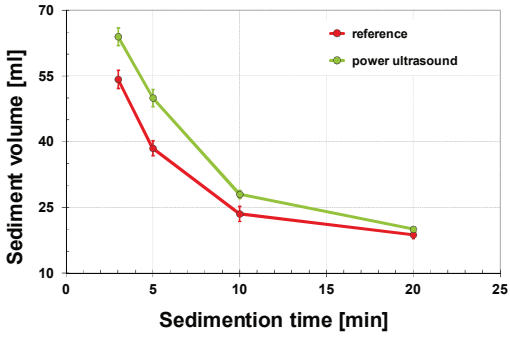

Figure 41: Sediment volume of cement suspension in dependence of time and PUS application.

Results in **Figure 41** demonstrate the dispersing effect of PUS application. Up to ten minutes of sedimentation (i.e. 20 min of total hydration time) PUS induces a substantially increased dispersion of particles (**Figure 41**). The dispersing effect due to sonication itself vanishes after 20 minutes of sedimentation (i.e. 30 minutes of hydration). The sediment volumes of the references and the sonicated samples become equal. From these results it is concluded, keeping in mind that PUS is applied within the first minutes of mixing, that the dispersing

effect induced by PUS is limited in time, i.e. up to approximately 30 minutes after water addition.

In addition to sedimentation experiments the dispersing effect of PUS application was also estimated by cryo-SEM investigation (Nova NanoSEM 230, FEI, Netherlands). Characteristic microstructures of cement pastes 15 minutes after water addition are present in **Figure 42**. These images (**Figure 42a&b**) show the "close-to-native" distribution of cement particles in the concentrated cement suspension (w/c = 0.4).
In the reference sample (**Figure 42a**) large cement particles (> 10 µm) are observed. Smaller particles (2 < 10 µm) are in between the larger ones. Additionally agglomerates of very small particles (< 2 µm) are visible in the pore solution. However, the particle distribution of samples becomes clearer when grey scaled images are converted into binary images. In these binary images (**Figure 42c-f**) red regions represent cement particles and black regions are attributed to the frozen and partially sublimated pore solution structure. At higher magnification agglomeration of particles smaller than 2 µm is obvious in the reference sample (**Figure 42e**). In contrast in PUS treated sample particles of similar size are better dispersed (**Figure 42b,d&f**). Agglomerates could not be observed in the sonicated sample.

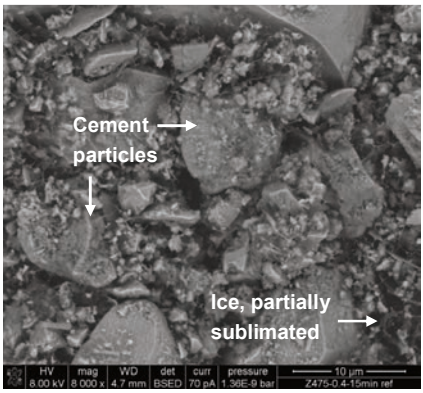

a) **Reference.**

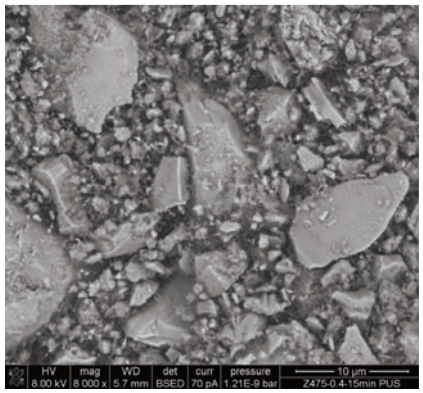

b) **Power ultrasound.**

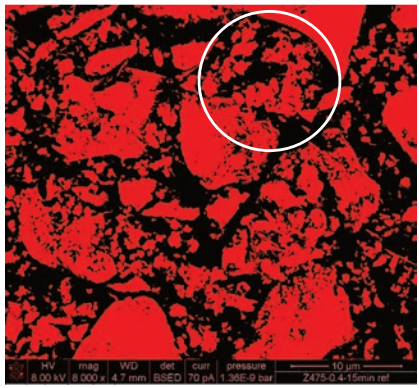

c) Microstructure of reference as binary image: Cement and hydration products as red regions.

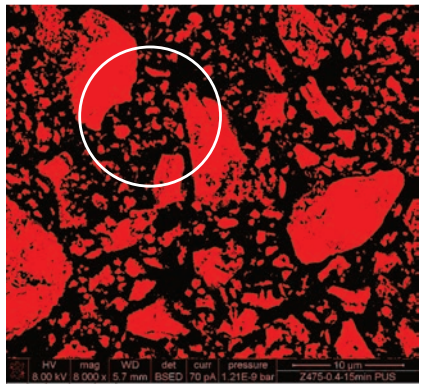

d) Microstructure of PUS treated cement suspension as binary image.

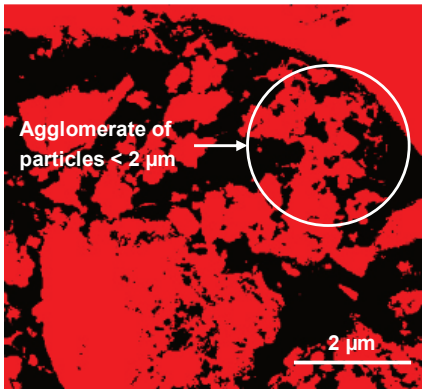

e) Microstructure of reference; agglomeration of particles < 1 µm.

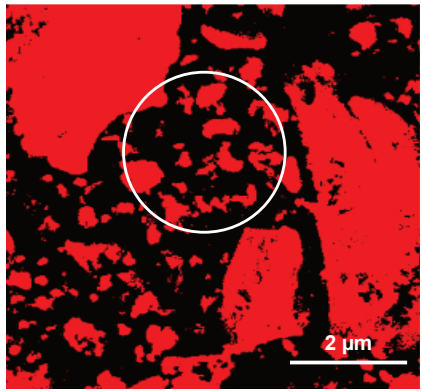

f) Microstructure of PUS treated cement suspension; well dispersed very small particles.

Figure 42: Microstructure of cement suspension (CEM I, w/c = 0.4) showing the dispersing effect of PUS on small cement particles (< 1 µm), imaged by cryo-SEM after 15 minutes of hydration, partially sublimated. BSE images were recorded at approx. 10^{-6} mbar (high vacuum) at 8 kV acceleration voltages.

5.2.2. Influence of PUS on fluidity of cement pastes

To estimate the fluidity of cement suspensions the determination of mini slump flow (according to DIN EN 12 350-5 and DIN EN 12 350-8) and V-funnel flow time (according to DAfStb SCC guideline 2003-11) were performed. For current investigation the water to cement ratio of cement suspensions varied from 0.4 to 0.54. All measurements were conducted 15 minutes after water addition.

Results in **Figure 43** document spread flow diameters and V-funnel flow times of cement suspensions 15 min after water addition in dependence of the w/c ration and PUS application. In the case of mini slump flow results shown in **Figure 43a** clearly reveal that a PUS treatment causes an increase of spread flow diameters independently of the w/c ratio. This increase in mini slump flow due to sonication is equivalent to 7.5 - 10.0 m.-% of water addition respectively an increase of w/c ratio of 0.25 - 0.4. However, a greater impact of PUS can be observed for the V-funnel flow times (**Figure 43b**). For the reference cement suspension a V-funnel flow time could not be measured at w/c = 0.4 because suspension was too stiff. Nevertheless, with increasing water content V-funnel flow times decreases rapidly in the reference samples. Finally a V-funnel flow time (reference) of only two seconds was determined at w/c = 0.54. In the case of sonicated samples the situation looks quite different. Even at w/c = 0.4 a V-funnel flow time of approximately two seconds was measured. This is a similar flowability as observed in the reference at w/c = 0.5. Thus, this increase in V-funnel flow time induced by sonication is equivalent to 25 m.-% of water addition. However, with increasing w/c ratio substantial changes in the V-funnel flow times could not be detected when PUS was applied. Two seconds of flow time already rages tightly at the detection limit of the method.

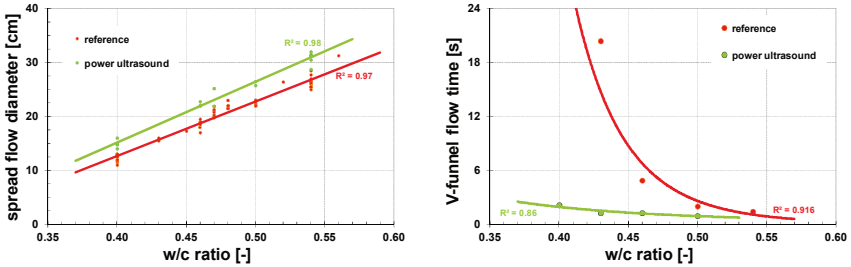

a) Mini slump flow diameter b) V-funnel flow time

Figure 43: Fluidity of cement suspensions 15 min after water addition in dependence of w/c ratio and PUS application.

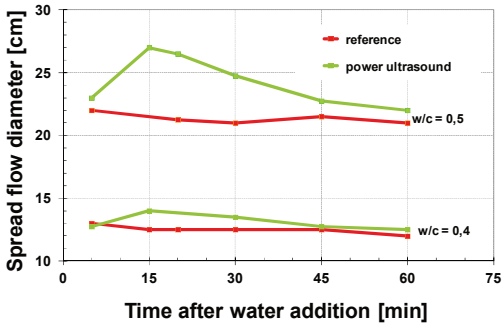

Figure 44: Development of spread flow of cement suspensions (w/c = 0.4 and 0.5, respectively) with time in dependence of PUS application.

Additionally to the determination of mini slump flow after 15 minutes of hydration the development of slump flow in dependence of time was documented. Therefore cement suspensions with w/c = 0.4 and w/c = 0.5 were produced. Corresponding spread flow diameters were detected in dependence of time and PUS application (**Figure 44**). Results in **Figure 44** confirm previously documented significant increase in fluidity 15 minutes after water addition due to PUS application. It also can be seen from **Figure 44** that the liquefying effect of PUS on cement suspension is increased at w/c = 0.5 compared to that at w/c = 0.4. Furthermore it becomes obvious that the increased flowability caused by PUS is limited in time. After longer hydration times (i.e. 45-60 minutes) sonicated samples show similar spread flow diameters compared to their references independently of w/c. These observations are in good correlation with the sedimentation experiments (**Figure 41**) where the dispersing effect was also determined to be limited in time.

5.2.3. Influence of PUS on fluidity of cement pastes in the presence of SP

To investigate the influence of PUS on cement suspensions in the presence of SP two different polycarboxylate type SPs were used. SP A is a commercial SP for precast production whereas SP B is used in ready mix concrete. SP addition varied between 0.04 m.-% to 1.2 m.-% SP dry mass referred to cement mass.

Results in **Figure 45** display the influence of PUS on the spread flow diameter (mini slump test) of cement suspensions in dependence of w/c ratio and type of SP. As expected, SP addition generally increases spread flow diameter of cement suspensions. Also additional PUS treatment liquefies the suspensions containing 0.06 m.-% SP dry mass referred to cement mass. However, the increase in fluidity strongly depends on the type of SP: In the presence of SP A (used for precast production) a distinct increase in slump flow was documented in the sonicated sample. On the contrary only a slightly increase was measured for sonicated samples in the presence of SP B (used in ready mix concrete) (**Figure 45a** vs. **Figure 45b**). Results in **Figure 45** also reveal that at increasing w/c ratio the effect of PUS

on mini slump flow is more significant. This is in good correlation with the results found for cement suspensions in the absence of SP (**Figure 44**).

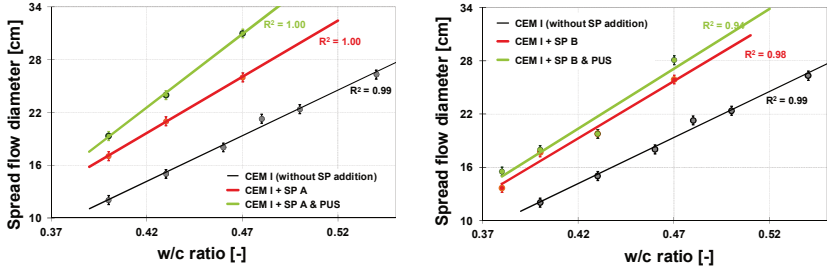

a) 0.06 m.-% (bwoc) dry SP A (ACE 30) content

b) 0.06 m.-% (bwoc) dry SP B (SP6) content

Figure 45: Spread flow diameter of cement suspension in dependence of w/c, SP addition and PUS application.

Additionally the influence of varying SP dosage at constant w/c (w/c = 0.4 and w/c = 0.5) was examined. Results are present in **Figure 46**. From these figures (**Figure 46a&b**) it becomes obvious that liquefaction is not generally observed in PUS treated suspensions. For examined SP (SP B) a critical SP dosage of approximately 0.08 m.-% (SP dry mass referred to cement mass) can be identified above which sonication has no influence on fluidity (**Figure 46b**) or even causes a reduction of fluidity. This observation was made for w/c of 0.4 and 0.5 (**Figure 46a&b**). A destruction of the polymer itself when treated with PUS was excluded by determination of molecular mass of polymers before and after sonication using gel permeation chromatography (GPC, see Appendix).

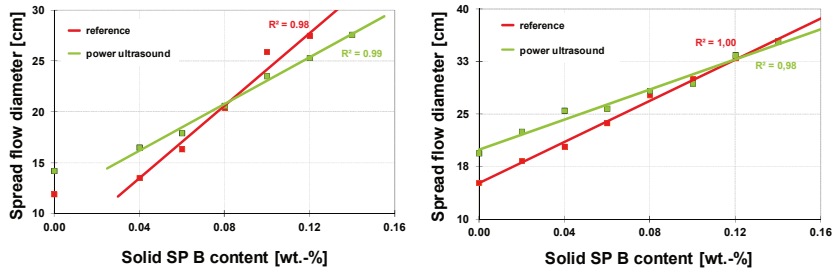

a) w/c = 0.4

b) w/c = 0.5

Figure 46: Spread flow diameter of cement suspensions in dependence of SP B content (m.-% SP dry mass referred to cement mass) and PUS application.

Therefore, in order to evaluate if the reason for this diminished fluidity lies in changes in the early hydration reactions, the microstructures of the corresponding cement suspensions

(w/c = 0.4, 0.1 m.-% SP B dry mass referred to cement mass) were imaged by SEM after 20 minutes of hydration (**Figure 47**).

In the reference cement paste the typical microstructure as described elsewhere[144] is observed after 20 minutes of hydration. The most important hydration product found at this stage is ettringite at sub-micrometer size (arrow **Figure 47a**). Comparing the microstructure of suspensions shown in **Figure 47a & b** it clearly can be seen that due to the application of PUS in the cement suspension containing increased SP B dosage nano-scaled foils occur (**Figure 47b**). The characterization of these nano-scale phases was difficult, because for both methods, SEM-EDX and QXRD analyses, the dimension and amount of these phases were too few or their crystalline nature is unknown. Thus it only can be assumed from comparative investigations on other cement and clinker[144] that most probably these foil like phases belong to the AFm group, indicating that the reaction between the aluminate clinker phase and the set regulator (calcium sulfates) is disturbed by a simultaneous application of SP and PUS at critical low w/c.

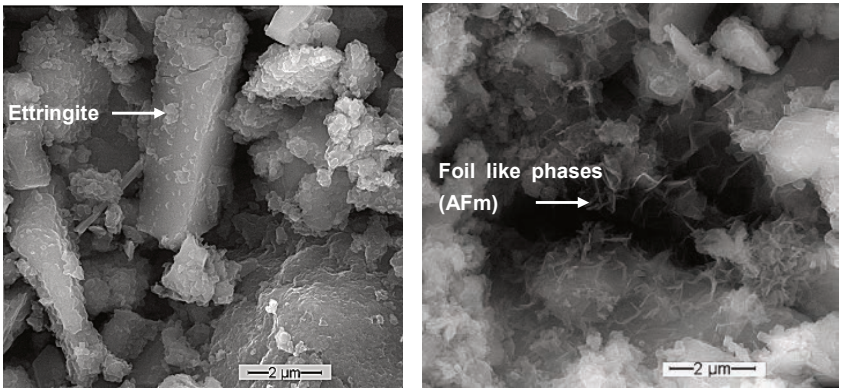

a) Microstructure of reference cement suspension; nanoscaled ettringite on surfaces

b) Microstructure of PUS treated cement suspension; additionally to ettringite (not shown here) locally foil like phases occur, assumed to be of AFm-type.

Figure 47: Microstructure (imaged by ESEM-FEG, XL 30 at 25 kV, 80 % humidity) of cement suspensions (w/c = 0.4, 0.1 wt-% dry mass SP B) after 25 minutes of hydration in dependence of PUS application.

To get more detailed information a random testing investigation of the influence of PUS on the crystallization process of ettringite in the presence of polycarboxylate based SP (0.1 m.-% dry mass of SP B in 100 ml de-ionized water) were performed.

Therefore, firstly ettringite was precipitated from a clear to the eye solution containing aluminum, calcium and sulfate ions (homogeneous nucleation, mixture from saturated solutions of $Al_2(SO)_3$: $Ca(OH)_2$: $CaSO_4$ = 1:1:0.5 [v.-%]). The results presented in **Figure 48** show no significant changes in the course of the el. conductivity during first 60 minutes of

crystallization due to PUS treatment. This was found for a PUS application immediately after mixing and for a PUS application at the end of the induction period (reduced el. conductivity) that signifies initial precipitation.

Otherwise, considering heterogeneous ettringite nucleation from a stirred diluted C_3A-HH-suspension (in proportion C_3A : HH = 1:1 [m.-%], l/s = 50) substantial differences in the development of the el. conductivity become obvious (**Figure 49**). The results displayed in **Figure 49** reveal increased values of the el. conductivity in the sample treated with PUS (suggest altered solubility of C_3A and/ or sulfate phase). Also a delay of the minimum and following maximum of the el. conductivity is observed in the sonicated sample. The minimum and subsequent maximum of the el. conductivity (related to the fast dissolution of C_3A when all sulfate is consumed by ettringite formation) is observed after approx. 11 minutes in the reference sample and delayed to approx. 14 minutes in the sonicated sample.

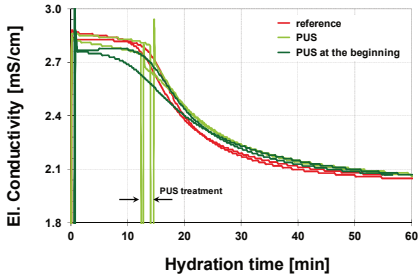

Figure 48: Development of the el. conductivity in a clear to the eye solution containing aluminum, calcium and sulfate ions in dependence of PUS application.

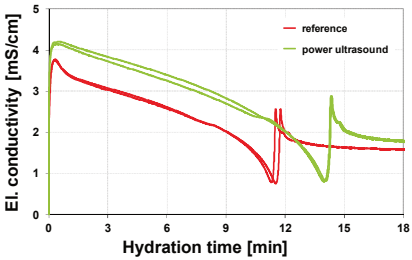

Figure 49: Development of the el. conductivity in a diluted C_3A-HH suspension in dependence of PUS application.

Microstructural characterization reveal that the ettringite, precipitated after PUS was applied, tend to occur as long-prismatic crystals (**Figure 51** and **Figure 52**). However, differences in the phase composition (occurrence of AFm phases) as observed in the cement paste were not determined for diluted suspension conditions.

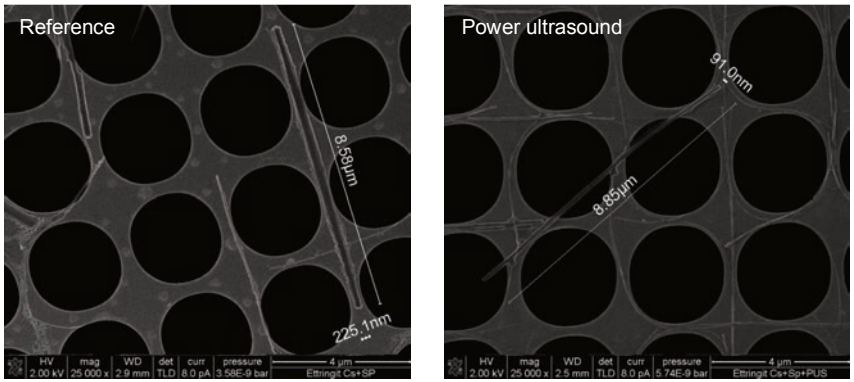

Figure 50: Microstructure of ettringite precipitated from a clear to the eye solution in dependence of PUS application.

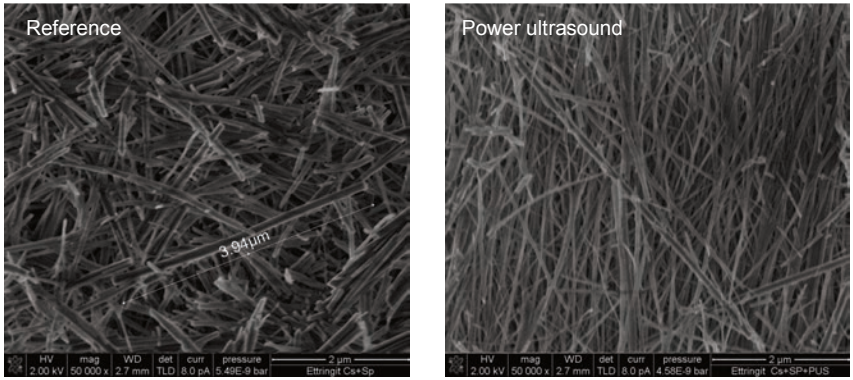

Figure 51: Microstructure of ettringite precipitated from diluted suspension in dependence of PUS application.

Finally, the results presented above provide additional evidence that PUS influences the reaction between aluminate phase and set regulator (calcium sulfate). The origin for this altered reaction progress has to be in focus of further investigations.

5.2.4. Conclusions

The influence of PUS application on the fluidity and microstructure of cement suspension was investigated. It was found that PUS reduces the air void content of cement suspensions and hardened cement pastes. Consequently, the reduction of air void content leads to a denser microstructure i.e. may increase compressive strength[141].

Moreover homogenizing and dispersing effects of PUS could also be verified for cement suspensions. Sedimentation experiments and cryo-SEM images clearly demonstrated the dispersion of very small particles (< 1 µm) by PUS application. As a result of dispersion induced by PUS application increased fluidity of cement suspension was determined. As described previously (**section 4.2.10**) rheological parameters (yield stress, viscosity) of cement suspension can be estimated on the basis of mini slump flow and V-funnel flow times. It is generally accepted that slump property is mainly related to the rheological parameter yield stress[68,145,146]. Flow time (spreading) may be related to the viscosity as proposed in[145,65,147]. Results of slump flow measurements and V-funnel flow time determination in dependence of PUS application reveal that the influence of sonication on V-funnel flow time is much more significant compared to mini slump flow. This implies that PUS mainly reduces viscosity whereas yield stress is little affected.

However, the fluidity improving effect (dispersion) of PUS may be deduced while comparing with effects observed by SP addition. As summarized by Mollah et al.[148] it is generally accepted that dispersion induced by SP addition is caused by the adsorption of SP molecules on cement particles. This leads to changed inter-particle forces (repulsion, steric hindrance)[149]. Consequently, preliminarily the yield stress is reduced[140,150]. Additionally dispersion leads to de-agglomeration of flocculated cement particles. As a result the water entrapped in agglomerates becomes liberated. This (free) excess water is accounted for reduced viscosity.[6,145] Thus also decreased viscosity of cement suspension was observed when SP was added to the mix[150,151]. Since in the case of PUS a „permanent“ change of inter-particle forces is not expected (i.e. no steric hindrance) the influence of sonication on yield stress should be less compared to the influence on viscosity. This is what was found during the current investigation. Consequently, the increased fluidity induced by PUS application can be ascribed to de-agglomeration of flocculated cement particles that increases (fee) excess water.

Additionally, results of mini slump flow reveal that the w/c of cement suspension influences yield of liquefaction resulting from PUS treatment. With increased water content of suspension an increased liquefying effect due to PUS application is observed. Given that PUS generates its effects from cavitation and cavitation is generated in the liquid phase an increased amount of water lead to increased gain in fluidity. The liquefaction due to the PUS application was also demonstrated to be a timely limited effect. After 60 minutes of hydration similar fluidity was documented for sonicated and reference sample.

However, if PUS is applied to a cement suspension containing SP liquefaction is not generally observed. Whether an increase or decrease in fluidity can be observed depends not only on the type and dosage of SP but also on the w/c of cement suspension. Results obtained by SEM investigation suggest that especially in the presence of high SP content at critical low w/c, PUS influences the hydration reaction between the aluminate clinker and the calcium sulfate phases significantly. The interaction of aluminate and the sulfate phase is known to have a great impact on early workability of cement suspensions. Rößler[152] showed that the formation even of small amounts of secondary gypsum, syngenite and foil like AFm significantly decreases fluidity. Therefore it is concluded that in some cases sonication of SP containing cement suspensions leads to the variation of early hydration composition (in

current investigation: probably occurrence of AFm phases) and thus reduces fluidity of the cement suspensions. Nevertheless, at higher w/c this influence of PUS on reaction between aluminate clinker and sulfate phase seems less important compared to the dispersing effect yielding from SP addition.

5.3. Influence of power ultrasound on hydration and fluidity of slag cement

One of the main challenges in cement production is the reduction of CO_2 emission. With every produced ton of OPC approximately 0.85 tons of CO_2 are emitted. One of the approaches to lower the CO_2 emission is to use supplementary cementitious materials (SCM). These SCM include latent hydraulic (granulated ground blast-furnace slag: GGBFS), puzzolanic (silica fume, flay ash, metakaolin), and inert (lime stone) materials. The utilization of SCM (composite cements) improves the ecological/economical balance of resulting concretes by reducing the OPC content (reduced CO_2 emission) and increasing the durability[3]. With regard to structural engineering the disadvantage of increased amounts of SCM is a delayed initial setting time and thus decreased early strength development of concrete. Consequently methods to improve the hydration progress of composite cement have to be identified.
The focus of the following chapter is to evaluate if acceleration of the hydration progress by PUS, i.e. compressive strength development, proven for pure OPC can also be obtained for GGBFS containing cements. Additionally it has to be clarified if sonication directly improves the reactivity of GGBFS.

5.3.1. Identification of optimized PUS parameter

In a first step, analogous to the investigations in CEM I 42.5 R systems, optimized PUS parameters to accelerate slag cement have to be identified. Similarly as defined for the OPC system certain requirements for PUS application (induced by applicational reasons) are:

- sonication duration as short as possible,
- limited increase of suspension temperature due to PUS treatment (maximum 45 °C) and
- significant acceleration of cement hydration process.

The initial setting time (according to DIN EN 196-1) and the continuously measured development of sample temperature were determined in dependence of varying PUS amplitudes and specific energy inputs. As mentioned before, these approaches enable the measurement of simple experimental parameters to judge which PUS parameters are suitable. Based on the substitution of OPC by GGBFS, reduced hydration temperatures were expected[3]. Cements with lower hydration heat liberation are beneficial for PUS treatment because the specific energy input can be increased (compared to parameters identified for pure OPC) without exceeding the maximum tolerable suspension temperature of 45 °C. In contrast to investigations on pure OPC system, all considered amplitudes (12, 43 & 53 µm) used for the current examinations were generated using the same ultrasonic horn (**Table 2**, page 23) to guarantee a constant front face diameter (i.e. increased amplitudes induces increased emitted acoustic power, **Figure 12**).

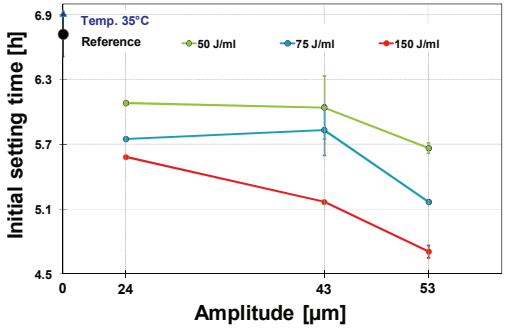

Figure 52: Initial setting time of CEM II/B-S 32.5 R in dependence of PUS parameter amplitude and specific energy input.

In **Figure 52 & Figure 53** results of precede tests (initial setting time and development of sample temperature) to identify the optimal PUS parameter are documented. From initial setting times, displayed in **Figure 52**, it becomes obvious that PUS application (in analogy to pure OPC systems) always decreases initial set of slag cement suspension. Again, major influence on initial setting time is observed to be the variation of the specific energy input. Increased specific energy input significantly decreases initial setting times of slag cements independently of used PUS amplitude (at constant front face diameter). In other words, compared to the specific energy input, the variation of PUS amplitude has a minor influence on setting times. At a lower specific energy input (e.g. 50 J/ml or 75 J/ml) using a PUS amplitude of 24 µm and 43 µm, very similar acceleration of the initial set is observed. However, at an energy input of 150 J/ml an accelerated setting is documented for increasing PUS amplitudes.

Since PUS treatment always induced a temperature increase of the cement suspension at the beginning of hydration, the influence of a temporary temperature rise is evaluated by an equivalent heated cement suspension (**Figure 52**: Temp. 35 °C). This short time heat treatment equals the PUS treatment of 150 J/ml using the 53 µm PUS amplitude. Whereas results in **Figure 52** evidence that the temporary temperature increase does not affect initial setting times (similar setting times for reference and temp. 35 °C), it influences development of sample temperature during hydration process (first 48 h, **Figure 53**). The determination of the development of sample temperature is used to estimate the hydration kinetics of cement suspensions. As mentioned before, an informative basis of the hydration progress is provided by comparing the time of maximum sample temperature (c.f. **Figure 16**). **Figure 53** presents the development of sample temperature and the time of maximum sample temperature measured in CEM II/B-S 32.5 R suspensions (w/c = 0.4 + 0.04 m.-% SP dry mass referred to cement mass) in dependence of varying PUS parameter (amplitude and specific energy input).

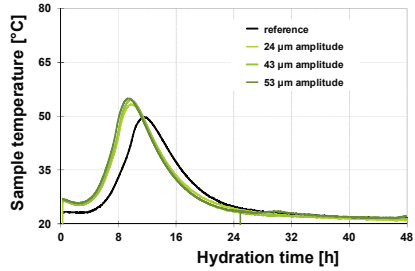

a) **Development of sample temperature in dependence of amplitude at a specific energy input of 50 J/ml.**

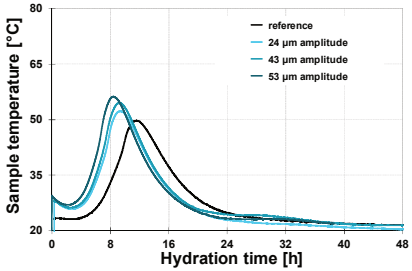

b) **Development of sample temperature in dependence of amplitude at a specific energy input of 75 J/ml.**

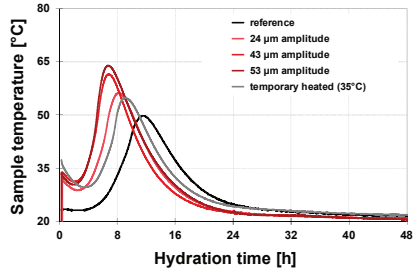

c) **Development of sample temperature in dependence of amplitude at a specific energy input of 150 J/ml.**

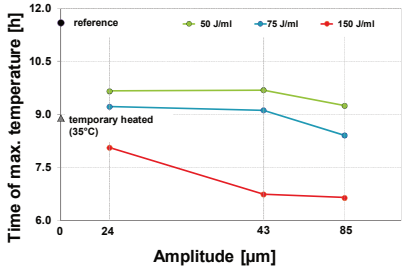

d) **Time of maximum sample temperature.**

Figure 53: Development of sample temperature (a-c) and time of maximum sample temperature during acceleration period (d) of hydrating CEM II/B-S 32.5 R pastes (w/c = 0.4 + 0.04 m.-% SP dry mass referred to cement mass) in dependence of PUS parameter amplitude and specific energy input.

From the present results (**Figure 53**) it becomes obvious that an ultrasonic treatment always causes a shift of the maximum sample temperature to earlier times compared to the unsonicated reference. As seen for the initial setting times (**Figure 52**) the specific energy input has the major influence on the occurrence of maximum sample temperature during the hydration process (**Figure 53d**). At increasing specific energy input the maximum sample temperature is shifted to earlier periods independently of the PUS amplitude. Again, an increased energy input causes an increased suspension temperature at the beginning of hydration. This initial temperature rise in suspension due to PUS application is maximal for the PUS amplitude of 53 µm and a specific energy input of 150 J/ml (i.e. 33 °C). The influence of comparable temperature increase on the occurrence of maximal sample temperature is also shown in **Figure 53c & d** (temporary heated (35 °C)). Compared to the reference a temporary heating causes a slightly accelerated main hydration and thus maximum sample temperature is determined approximately 3 h earlier in the temporary

heated sample. However, this acceleration is less compared to corresponding sonicated sample (150 J/ml and 53 µm). Therefore it is concluded that the temporary heating as well as PUS treatment both accelerate development of sample temperature. Nevertheless, the gain due to PUS exceeds the effect of the temporary heat treatment.
Finally, precede investigations show that the slag cement (CEM II/B-S 32.5 R) hydration is accelerated by PUS application. While OPC is substituted by GGBFS (leading to reduced initial heat release) it was possible to increase the specific energy input without exceeding critical suspension temperature of 45 °C. Most effective acceleration (about 2 h compared to the reference) at maintainable sonication times (max. 4 min for 1000 ml suspension) and a maximal suspension temperature of 33 °C was determined using the 53 µm amplitude and specific energy input of 150 J/ml. Consequently these PUS parameters (150 J/ml and 53 µm) are regarded as optimum PUS parameter for following investigations.

5.3.2. Influence of PUS on initial setting times of slag cement suspensions and strength development of mortars

In this section the influence of PUS treatment on the hydration progress of slag cement is examined. The investigation focuses on the question, if solely the OPC content is accelerated or the glassy phase (GGBFS) itself can also be activated by PUS application. For this reason mixtures containing different amounts of GGBFS were produced by homogenizing varying percentages of CEM I and GGBFS (i.e. up to 90 m.-% GGBFS). Homogeneous distribution of CEM I and GGBFS was achieved by using a ploughshare mixer (Type FM 50, Lödige, Germany).
The water to binder (cement + slag) ratio (w/b) = 0.4 was constant for all mixtures. A very low SP addition (0.04 m.-% SP dry mass referred to binder mass) was added for sufficient workability to enable suspension passing the PUS circuit.
The hydration progress was evaluated by isothermal heat conduction calorimetry (TrioCAL 7339, ToniTechnik, Germany). Initial setting times of cement suspensions were determined according to DIN EN 196-1. In addition compressive strength of mortars (cement : aggregates = 1:1) was tested after 24 h of hydration. The mortars were produced applying the “suspension mix design” introduced in **section 4.2.2**.

Figure 54 displays the results of isothermal heat conduction calorimetry in dependence of GGBFS content, PUS application and a temporary heat treatment. The heat release of pure OPC is shown in **Figure 54a**. Here, in the reference sample (100 wt-% CEM I = 0 m.-% GGBFS, without PUS application) the maximum heat release is observed approximately 8 h after water addition. If the sample (100 wt-% CEM I = 0 m.-% GGBFS) is treated with PUS the maximum heat release rate occurs after 6 h, i.e. at earlier period. For comparison, the sample which is only solely treated by temporary heat is also shown in **Figure 54a**. In this case (100 wt-% CEM I = 0 m.-% GGBFS, temporary heated) the hydration progress is similar to the reference.

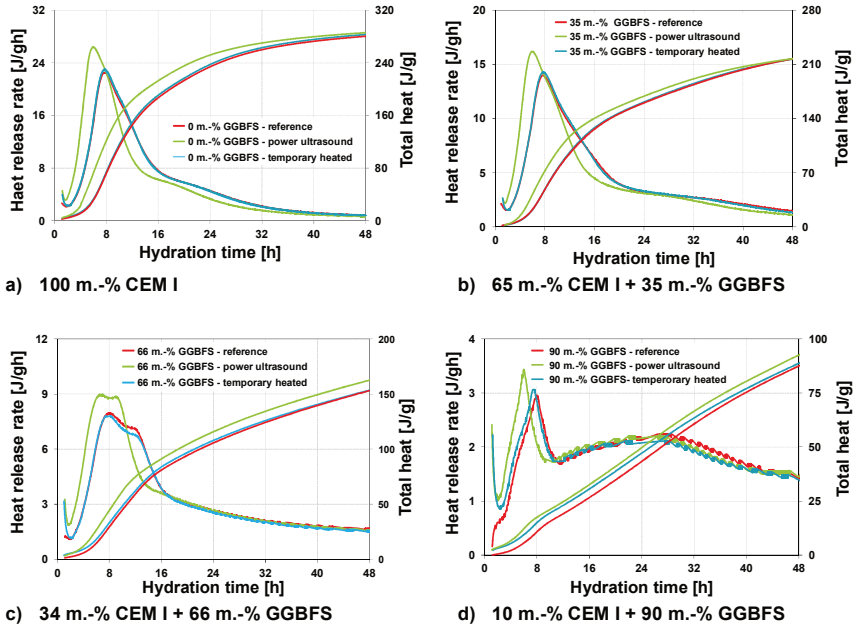

Figure 54: Heat release rate and total heat of cement containing different amounts of GGBFS in dependence of time, temperature and PUS application.

Whereas the substitution of CEM I by GGBFS has no strong effects on the early hydration kinetics (up to 10 h), PUS application generally causes an accelerated hydration process independently of GGBFS content (**Figure 54a-d**). This is documented by the other references (**Figure 54b,c & d**, without PUS). At increasing GGBFS content the maximum heat release is detected after approximately 8 h of hydration for all reference samples. In comparison, in all of the sonicated samples the maximum heat release rate during the acceleration period is observed after approximately 6 h of hydration independently of GGBFS content. Whereas the substitution of CEM I by GGBFS doesn´t lead to significant changes in the hydration kinetics up to this time, the overall reaction rate is decreased with increasing content of GGBFS. Thereby the maximum heat release rate decreases from 22.56 J/(gh) to 2.95 J/(gh) at GGBFS contents between 0 and 90 m.-%, see **Table 5**. These numbers demonstrate the slower reaction rate of GGBFS in comparison to CEM I as already known[158]. In the sample with 66 m.-% GGBFS (**Figure 54c**) the overall reaction is not only dominated by CEM I as shown by the maximum heat release rate which is broadened. At highest degree of CEM I substitution (90 m.-% GGBFS, (**Figure 54d**) the maximum heat release rate is splitted. In this case the peak which is originated by CEM I (similar to the mixtures before) is separated by the broad reaction peak (hump) induced by the reaction of GGBFS. The

broadening of the maximum heat release peak may be caused by the decreasing activation of GGBFS by a decreasing amount of CEM I. However, the separated hump reaches its maximum reaction rate after approximately 26 h for the reference sample. Nevertheless, a significant difference in the course of the curves (especially at 90 m.-% GGBFS) during this second hump due to PUS treatment could not be determined. Therefore, a distinguished acceleration of the GGBFS hydration could not be observed by isothermal heat calorimetry for current experimental constitutions.

Table 5: Maximum heat release rate of cement suspension during acceleration period in dependence of PUS application determined by isothermal heat conductivity calorimetry.

Sample	Maximum heat release rate (acceleration period) [J/gh]		Gain [%]
	Reference	Power ultrasound	
100 m.-% CEM I + 0 m.-% GGBS	22.56	26.45	+ 17.2
65 m.-% CEM I + 35 m.-% GGBS	14.02	16.20	+ 15.5
34 m.-% CEM I + 66 m.-% GGBS	7.98	8.98	+ 12.5
10 m.-% CEM I + 90 m.-% GGBS	2.95	3.43	+ 16.3

Moreover, the increase of maximum heat release of CEM I due to PUS application was calculated to roughly 15 % for all samples (**Table 5**). This again indicates that the acceleration of alite hydration induced by sonication is comparable for all mixtures independently of the amount of GGBFS.

The conclusion of lower activation of GGBFS is supported by microstructural images (Nova NanoSEM, FEI 230, Netherlands, **Figure 55**) recorded during acceleration period of paste containing largest amount of GGBFS (10 m.-% CEM I + 90 m.-% GGBFS). It becomes obvious that even when PUS is applied, only a substantial dissolution of alite can be observed. In contrast the GGBFS particles exhibit smooth surfaces without visible indication of dissolution structures (**Figure 55)**. Thus, it is concluded that primarily OPC hydration proceeds at this stage of hydration. Hence, the maximum peak during acceleration period (after 8 h for references and after 6 h for sonicated samples, respectively) is associated with alite (OPC) hydration for all samples.

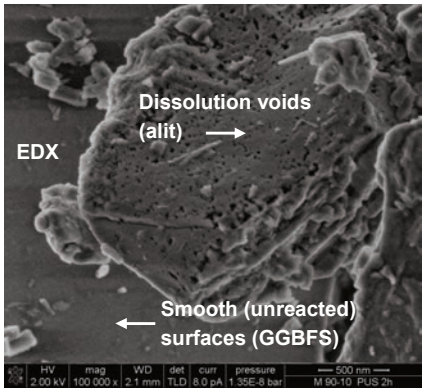

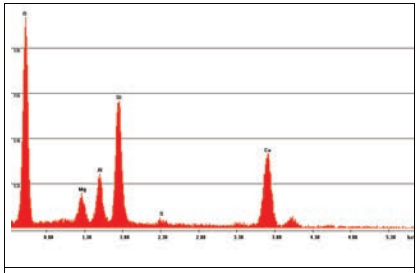

Element content [m.-%]					
O	MgO	Al	Si	S	Ca
44.63	3.91	6.61	18.66	1.05	25.14

Figure 55: Microstructure of 10 m.-% CEM I + 90 m.-% GGBFS (w/c = 0.4 + 0.04 m.-% SP dry mass referred to binder mass) after 2 h of hydration (first acceleration period) imaged by SE-SEM recorded with a Through the Length Detector (TLD) at approximately 10^{-6}mbar (high vacuum) at 2 kV acceleration voltage.

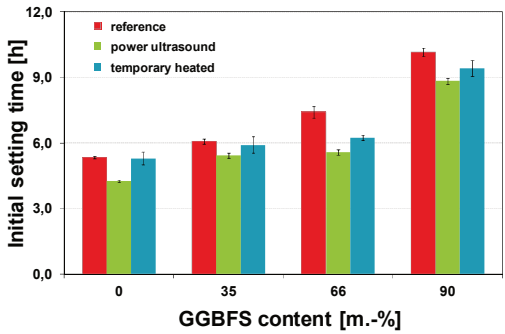

Figure 56: Initial setting time of cement paste in dependence of GGBS content, temperature, and PUS application.

The influence of a PUS treatment on the initial setting times of slag cement suspensions (**Figure 56**) was determined. Additionally compressive strength of mortars was measured (**Table 6**).

From the results shown in **Figure 56** it can be seen, that with increased GGBFS content also initial setting times increases. This is a known effect due to the lower hydraulic reactivity of the slag[158]. According to data of heat conduction calorimetry, the results in **Figure 56** reveal that a PUS application causes an earlier initial set compared to the corresponding reference cement suspension in all mixtures. Furthermore, it is obvious that a temporary heating at the beginning of hydration (comparable to the temperature rise induced by sonication) does not influence the setting times at GGBFS contents of 0 m.-% and 35 m.-% (**Figure 56**). However, at GGBFS contents of 66 m.-% and 90 m.-% a temporary heating of suspension after mixing accelerates setting as well what is in good correlation with results known from literature[153,154]. But the acceleration is still greater in the case of PUS application.

Considering the strength development of mortars (cement : aggregate = 1:1; **Table 6**) it is obvious that a PUS treatment causes a significant increased compressive strength after 24 h of hydration. The gain in compressive strength is about nearly 20 % for all samples except the mixture of 10 m.-% CEM I + 90 m.-% GGBFS. In this case the compressive strength could not be detected for the reference mortar after 24 h of hydration and the compressive strength of sonicated sample is quit nearly at the detection limit of the method.

Table 6: Compressive strength of mortar (cement : aggregates = 1:1) after 24 h of hydration in dependence of GGBS content and PUS application.

Sample	Compressive strength after 24 h of hydration [N/mm²]		Gain [%]
	Reference	Power ultrasound	
100 m.-% CEM I + 0 m.-% GGBS	31.7	37.3	+ 17.7
65 m.-% CEM I + 35 m.-% GGBS	19.8	23.8	+ 20.2
34 m.-% CEM I + 66 m.-% GGBS	6.2	7.5	+ 21.0
10 m.-% CEM I + 90 m.-% GGBS	0.0	0.3	---

Although the presented results obtained by investigations of OPC-GGBFS systems documented accelerated cement hydration, they suggest that the hydration of GGBFS could not be accelerated by PUS application. Thus, further investigation were performed on pure GGBFS in the absence of OPC (alite phase) to verify these results.

5.3.3. Influence of PUS on pure GGBFS hydration

GGBFS belongs to the latent hydraulic supplementary cementitious materials. That means it needs to be activated for hydration (alkaline or sulfatic activation)[6,155,34]. In cement pastes this activation is achieved by the alkaline aqueous phase and later by $Ca(OH)_2$ released during cement hydration[34,156,157,158,159]. To simulate the alkaline environment of cement suspension GGBFS was homogenized with 10 m.-% of CH (activation via hydroxide ions). So the influence of PUS on pure GGBFS hydration could be investigated.
Analogous to **section 5.1.3** (*Influence of power ultrasound on the nucleation of C-S-H*) the nucleation and growth process of the hydrate phases (e.g. C_2ASH_8, C_3AH_6, CSH, C_4AH_{13}) formed during the hydration of stirred diluted GGBFS suspension was in focus of the investigation. Besides the measurement of the el. conductivity during first 18 h of hydration (TetraCon®, WTW, Germany) also the heat release rate and total heat (TrioCal 7338, ToniTechnik, Germany) were recorded during 48 h after water addition. Microstructural changes were documented by SEM images (Nova NanoSEM 230, FEI, Netherlands).

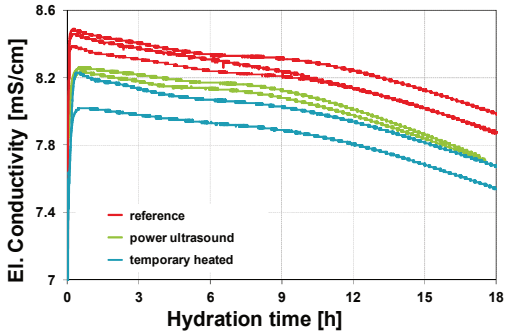

Figure 57: The el. conductivity of diluted suspension (90 m.-% GGBS + 10 m.-% CH; l/s = 50) in dependence of hydration time, PUS application and temporary heat treatment.

The development of the el. conductivity of stirred diluted suspensions (l/s = 50; 90 m.-% GGBS + 10 m.-% CH) in dependence of PUS application is present in **Figure 57**. Additionally the el. conductivity of temporary heated sample (equivalent to temperature increase induced by PUS) was recorded. Obviously significant differences between the references, temporary heated and sonicated samples can only be observed in the absolute value of the el. conductivity (hampered dissolution and/or precipitation of hydration of phases). A significant change in curve progression is not observed (only parallel translation). Thus it is concluded that the crystallization process itself is not influenced by sonication and increased temperature (similar curve progression as the reference sample) but the extent (el. conductivity value) depends on the solution temperature at the beginning of crystallization.

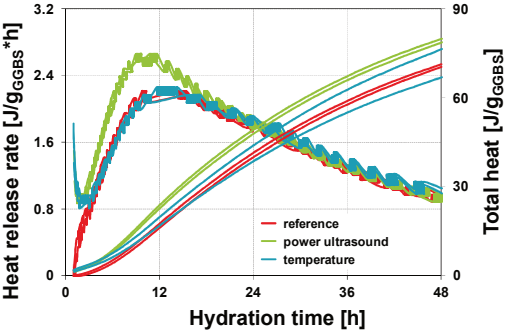

Figure 58: Heat release rate and total heat of GGBS/CH suspensions (Water/Solid = 1.0) in dependence of time, PUS application, and temporary heat treatment.

The results of the influence of sonication on hydration process in paste conditions (w/b = 1.0; evaluated by isothermal heat calorimetry) are presented in **Figure 58.** From this figure it can be seen that a PUS application slightly accelerates the pure GGBFS hydration. The maximum of heat release of PUS treated sample is observed about one hour earlier compared to the reference and temporary heated sample. Additionally, the maximum value of the heat release rate of sonicated cement suspension is increased.

A calculation of the hydration degree after 48 h of hydration (**Eq. 11**) and the dissolution rate (**Eq. 12**) of pure GGBFS (90 m.-%) hydration according to Dressel[160]

$$\alpha(t) = \frac{Q(t)}{\Delta_r H^\circ} \qquad \textbf{Eq. 11}$$

where $\alpha(t)$ is the hydration degree, $Q(t)$ the reaction heat [J/g] and $\Delta_r H^\circ$ the reaction enthalpy (810 J/g)[160]

$$R_{paste} = \frac{\alpha(t)}{dt} = \frac{(dQ/dt)(t)}{\Delta_r H^\circ} \qquad \textbf{Eq. 12}$$

where $\frac{dQ}{dt}(t)$ is the heat release rate [J/m²h] with BET - surface area of GGBFS = 1.2 m²/g and $\Delta_r H^\circ$ the reaction enthalpy (48 kJ/mol)[160];

reveals only a marginal increased dissolution rate and consequently only a slightly increased hydration degree of GGBFS (**Table 7**).

Table 7: Calculated hydration degree (Eq. 10) and dissolution rate (Eq. 11) from isothermal heat conduction calorimetric measurements according to Dressel[160].

	Max. dQ/dt [J/gh]	$Q_{(48h)}$ [J/g]	R_{paste} [µmol/m²s]	$\alpha_{(48h)}$ [%]
Reference	1.97 ± 0.03	63.8 ± 0.6	0.011	8.7
PUS	2.37 ± 0.03	71.4 ± 0.8	0.013	9.8

The characterization of growing hydrates by SEM was conducted after 5 h and 24 h of hydration. For 5 h of hydration a slightly accelerated main hydration was determined for the sonicated GGBFS sample (**Figure 58**). Images representing the microstructure at this stage are shown in **Figure 59**. However, identification of newly formed hydration products was difficult since hydration products could already be observed on “unhydrated” GGBFS surfaces (**Figure 59a**). This in combination with only a very small acceleration yield due to sonication (**Table 7**) preclude the detection of significant changes in microstructure of sonicated sample (**Figure 59b**) compared to the reference. After 24 h of hydration microstructural development are similar for the reference and the PUS treated sample: smaller particles are covered with tapered C-S-H phases and also portlandite crystals can still be observed (**Figure 59c & d**).

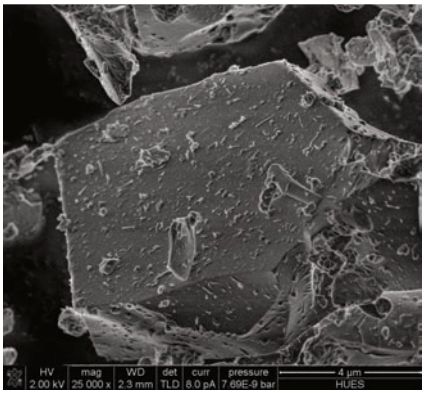

a) "Unhydrated" GGBFS with preliminarily formed hydration products on particle surface

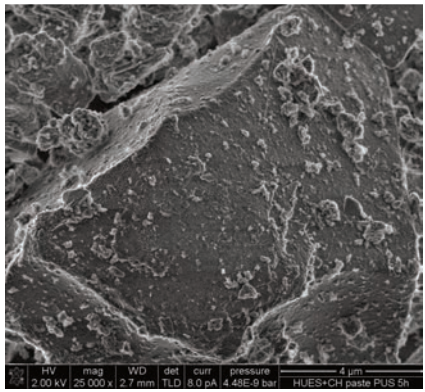

b) Power ultrasound: 5 h of hydration, hydration products on GGBFS particle surface

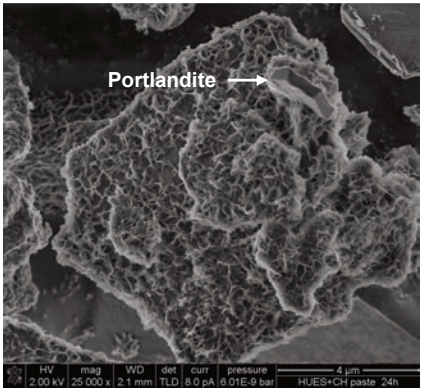

c) Reference; 24 h of hydration: smaller GGBFS particles covered by C-S-H and individual portlandite crystals

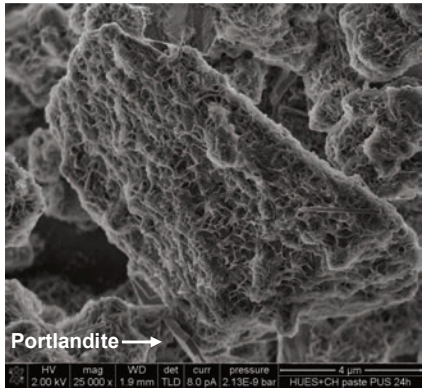

d) Power ultrasound, 24 h of hydration: smaller GGBFS particles covered by C-S-H and individual portlandite crystals

Figure 59: Microstructure of GGBFS (90 m.-%) + CH (10 m.-%) suspension (w/b = 1) in dependence of time and PUS application imaged by Nova NanoSEM 230 equipped with a Trough the Lens Detector (TLD) at approx. 10^{-6} mbar (high vacuum) at 2 kV acceleration voltages.

5.3.4. Influence of PUS on workability and fluidity of slag cements

As observed for OPC de-airing, homogenizing and dispersing effects of PUS leads to enhanced workability of cement suspension (**Chapter 5.2**). As known from literature the addition of relatively fine SCM may cause an enhancement in workability of cement suspensions as well[6,161,146,162]. Therefore, in analogy to pure OPC suspension de-airing and especially dispersion effects of PUS were also expected for slag cements. The additional aim of the following section was to verify to which extent PUS may improve fluidity of cements pastes blended with varying amounts of GGBFS.

From light microscopic investigations (VHX II 600, Keyence, Japan) on polished sections of 7 days hydrated CEM II/B-S 32.5R suspensions the de-airing effect attributed to PUS treatment was confirmed (**Figure 60**). Compared to the air voids contained in pure OPC at w/c = 0.4 (**Figure 38)** generally less air voids are visible in slag cement (**Figure 60a**) what was expected due to increased packing density by the addition of slag[3].
To compare the reference slag cement and the sonicated slag cement the difference of the air void content is as follows: Whereas in the reference air voids up to 4 mm in diameter can be observed only scattered very small air voids with maximal 1 mm in diameter are documented for the sonicated sample. In latter one also a homogeneous distribution of air voids with 0.2 mm in size is obvious. For ultrasonic fields (20 kHz) a critical size of roughly 150 µm[79] (more than 170 µm[82]) in diameter was calculated for cavitation bubbles before their collapse. Thus, it is believed that these very small air voids visible in sonicated sample are comminuted voids that could not float to the surface or even remnants of cavitation bubbles.

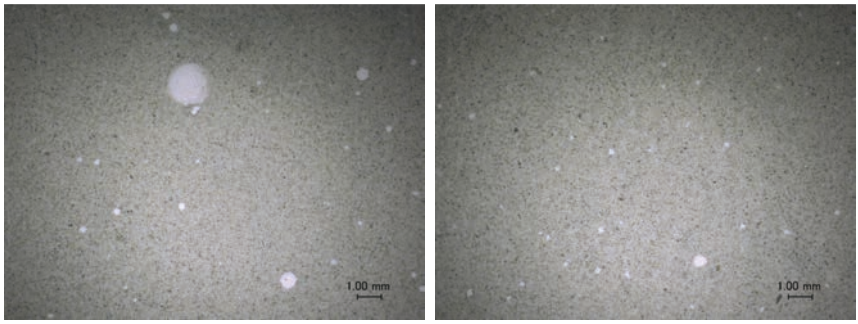

a) Reference **b) Power ultrasound**

Figure 60: Air void content and air void distribution in hardened slag cements suspension (CEM II/B-S 32.5R; w/c=0.4) after 7 days of hydration imaged by light microscopy on polished sections.

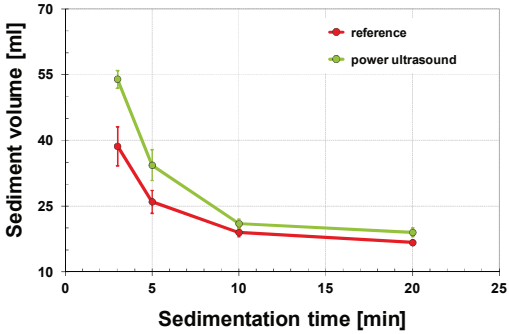

Figure 61: Sediment volume of sedimenting slag cement suspension in dependence of time and PUS application.

The dispersion in dependence of PUS application was estimated by sedimentation experiments as described in **section 5.2.1**. **Figure 61** displays the measured sediment volumes in dependence of time and PUS application. Obviously PUS treatment leads to significant increased sedimentation volumes i.e. decreases sedimentation velocity during first 10 minutes of sedimentation. Thus, it is concluded that PUS enhances the separation of finer particles and/or prevent them to agglomerate. This is in line with the result observed in pure OPC system and thereby confirms the dispersing effect of PUS in slag cement suspensions.

After the de-airing and dispersion effects of PUS is now demonstrated for slag cement the influence on fluidity of suspension is assessed on the basis of mini slump flow (DIN EN 12 350-5 & DIN EN 12 350-8) and V-funnel flow times (DAfStb SCC guideline 2003-11).

Figure 62a displays the measured spread diameters of cement suspensions (w/b = 0.4; 0.04 m.-% SP dry mass referred to binder mass) 15 minutes after water addition in dependence of varying GGBFS content and PUS application. In addition also spread flows of temporary heated samples (equivalent to temperature increase induced by PUS treatment) are visible. Results in **Figure 62a** reveal that with increasing GGBFS contents also spread flow diameter, i.e. flowability of cement suspensions, increases. This correlates with results observed in previous investigations[146,161]. Furthermore, it can be seen that at small amounts of GGBFS (0 m.-% and 35 m.-% GGBFS; **Figure 62a**) sonication induces an additional increase of spread flow diameters. At a GGBFS content of 66 m.-% no significant change in fluidity could be determined compared to the related reference suspension. However, at a GGBFS content of 90 m.-% sonication decreases the fluidity of cement suspension. Furthermore, the results in **Figure 62a** reveal that at GGBFS content of 66 m.-% and 90 m.-% a temporary heat treatment (equal to temperature increase induced by PUS application) also decreases fluidity. This is in correlation with results obtained by Živica [163]. There it was found that increased sample temperatures decreased workability of alkali-activated slag mixtures. Hence, it is concluded that at such high GGBFS content the suspension temperature seems to have a greater impact on fluidity compared to PUS application.

From documented V-funnel flow times the increased fluidity as a result of the substitution of OPC by GGBFS is also confirmed (**Figure 62b**). At w/b = 0.4 and addition of 0.04 m.-% SP dry mass referred to binder mass, pure OPC suspension was too stiff to pass the V-funnel. But already with the exchange of 35 m.-% of OPC by GGBFS a flow time of approximately

10 seconds could be measured for the reference sample (**Figure 62b**). The progressive increase of GGBFS content results in a further decrease of V-funnel flow times in the reference samples. At a GGBFS content of 90 m.-% V-funnel flow time was determined to be approximately two seconds. In contrast results in **Figure 62b** demonstrate that distinct differences in V-funnel flow times in dependence of GGBFS content could not be observed in sonicated samples. Even for the PUS treated sample with a small amount of GGBFS (35 m.-%) a V-funnel flow time of approximately two seconds was measured (**Figure 62b**). This is significantly lower as found for the corresponding reference. However, at a GGBFS content of 90 m.-% differences in the V-funnel flow time of the reference and the sonicated sample could not be detected anymore.

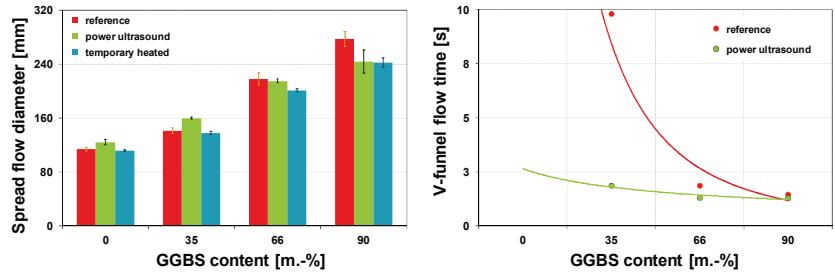

a) Mini slump flow b) V-funnel flow times

Figure 62: Fluidity of cement suspensions (w/b = 0.4; 0.04 m.-% solid SP referred to binder) 15 minutes after water addition in dependence of slag content and PUS application (for mini slump flow additionally temporary heat treatment).

5.3.5. Conclusions

The iInvestigations on slag cements containing variable GGBFS content reveal that PUS is able to accelerate the hydration progress of blended cements. Compared to the PUS parameter used for the OPC system, specific energy input can be increased due to reduced initial heat release of blended cements. From precede tests optimal PUS parameters that meet all demands (short sonication duration, restricted temperature increase, significant acceleration of hydration process) were identified to be the PUS amplitude of 53 µm and a specific energy input of 150 J/ml. With these PUS parameters (53 µm & 150 J/ml) initial setting times of cement suspension can significantly be reduced and thus early compressive strength of mortars increases up to nearly 20 % after 24 h of hydration. Furthermore results of measurements of heat release from hydrating GGBFS/ CH admixtures evidence a marginal accelerating effect of ultrasonic treatment on pure GGBFS hydration. Nevertheless this acceleration is less significant compared to that found for OPC. Consequently the main proportion of accelerated hydration process induced by sonication in slag cements is attributed to the acceleration of OPC content (accelerated alite hydration).

The workability was assessed to be influenced by the amount of GGBFS, PUS and sample temperature. Increased GGBFS content generally increase fluidity (slump flow and flow time) of the cement suspensions (what is in line with previous investigations[146,161]). On the other hand, in the case of PUS application the influence is inconsistent. The evaluation of the fluidity has to be differentiated between slump flow measurements (mainly associated with yield stress) and flow time measurements (mainly associated with viscosity). Considering the slump flow measurements it was demonstrated that a PUS treatment increases fluidity at smaller quantities of GGBFS. In contrast sonication reduces fluidity when GGBFS content increases. However, spread flow diameter also decreases at high GGBFS content when the sample temperature is increased. Thus it is concluded that with increased GGBFS content the sample temperature have a major impact on spread flow behavior compared to PUS treatment. Finally, with increasing GGBFS content the influence of sample temperature on fluidity (i.e. reduction of fluidity) becomes more significant than the increase of fluidity induced by PUS application. Nevertheless, the flowability of slag cement suspension expressed as V-funnel flow time (representing viscosity) is generally enhanced by PUS application.

5.4. Capability of applying PUS in ready mixed mortars

In previous chapters (**Chapter 5.1.**, pp. 43 and **Chapter 5.3.**, pp. 87) the positive effect of PUS application on cement hydration was demonstrated. The results clearly prove the accelerated initial setting of cement pastes as well as the increased early strength development of mortars due to ultrasonic treatment. Furthermore it was evidenced that these effects were induced by accelerated alite hydration. For slag cements besides enhanced alite hydration also the hydration of GGBFS is marginal accelerated by PUS.
Up to now an effective application of PUS to increase early strength development of mortars is expected only if pure cement suspensions are sonicated. Mixing only water and cement guarantees the availability of sufficient aqueous phase for the generation of cavitation. It is assumed that the presence of coarse aggregates in mortars may influence sound wave propagation by attenuation and the reduction of available liquid phase and thus hinders the generation of cavitational events. Consequently, considering concrete production the mixing process has to be changed. These kinds of alternative concrete mix procedures (so called "suspension concrete") are already widely discussed and partly successfully used. In special cases (when only small aggregates ≤ 4 mm are added, e.g. grouts) and when the paste content is very high (aggregates : cement = 1 : 1) it seems not to be economical to split up the mixing process. Therefore, the capability of applying PUS in ready mixed mortars will be discussed in the next section. For this reason relevant properties of sonicated ready mixed mortars and sonicated mortars obtained by suspension mix design are compared to standard mixed ones (unsonicated).

5.4.1. Properties of fresh and hardened mortars

To evaluate the capability of applying PUS in ready mixed mortars two different mixing procedures were performed. In the following, these are named the "suspension" and the "conventional" mixing procedure. In the case of suspension mix procedure first water, cement, and SP were mixed. Afterwards PUS is applied to the cement suspensions. Then during final mixing the aggregates are added. In the following, samples made by this mix procedure are called "PUS- suspension". During conventional mixing all components, i.e. water, cement, SP, and aggregates < 4 mm are added to a Hobart mixer and a standard mixing procedure is carried out. Subsequently ultrasound treatment (samples named "PUS-conventional") is applied. In conventional and suspension mixing the specific energy input induced by PUS is 150 J per ml of cement suspension for all samples using the PUS amplitude of 53 µm. Mortars of conventional mixing in the absence of PUS application are called "reference". Additionally to evaluate the effect of an initial temperature rise due to PUS treatment on mortar properties, one mortar series was temporary heated in a similar manner as PUS induces temperature rise in mortar. This mortar series is called "Temp. 45°C".
All experiments were carried out with CEM II/B-S 32.5 R at w/c = 0.4 and very low SP addition of 0.04 m.-% (SP dry mass referred to cement mass).

Table 8 shows the properties of fresh mortars (aggregates : cement = 1:1) determined 15 minutes after water addition. Considering mortar temperatures it becomes obvious that PUS application always causes a rise in mortar temperature. In PUS-conventional mixed mortars the sample temperature after sonication is much higher (43.4 °C) as in PUS-suspension mixed mortars (34.8 °C). Since the PUS energy input is the same for both mix procedures (150 J per ml of cement suspension) it becomes obvious that more energy in form of heat remains in the PUS-conventional mixed mortars.
The influence of PUS on flowability i.e. mini slump (DIN EN 12 350-6) and V- funnel flow time (according DAfStb SCC guideline 2003-11) as can be seen from **Table 8** is:
1) V- funnel flow time decreases due to sonication indicating a decrease in viscosity,
2) mini slump decreases reflecting increased yield strength of sonicated samples.
Since the application of PUS causes a temperature rise of mortars, mini slump values might be decreased due to temperature change. Thus mini slump of an equivalent heated sample (45 °C, without PUS) was tested. Results reveal a similar mini slump value compared to that of PUS treated samples. Consequently it is concluded that the decreased mini slump values in mixtures treated with PUS are caused by increased temperature of the samples (**Figure 63**).

Table 8: Properties of mortars (aggregates : cement = 1:1) in dependence of mix procedure and PUS application 15 minutes after water addition.

Property (15 minutes after water addition)	Reference (without PUS)	PUS- Suspension (with PUS)	PUS- conventional (with PUS)	Temp. (45°C)
Temperature [°C]	23.4	34.8	43.4	44.8
Mini slump [mm]	250 ± 4	237 ± 3	230 ± 2	235
V-funnel flow time [s]	2.6	1.8	1.8	--
Density [g/cm³]	2.19	2.20	2.19	--
Air void content [Vol.-%]	0.8	0.6	0.5	--

Due to the high fluidity of the mortars with actual high paste content (comparable with self compacting mortars), measurements of the density and air void contents in dependence of PUS application and mix procedure show no significant differences (**Table 8**). Therefore selected tests were repeated with mortars containing a higher amount of aggregates (aggregates : cement = 2:1). Related results are present in **Figure 63** and **Table 9**.

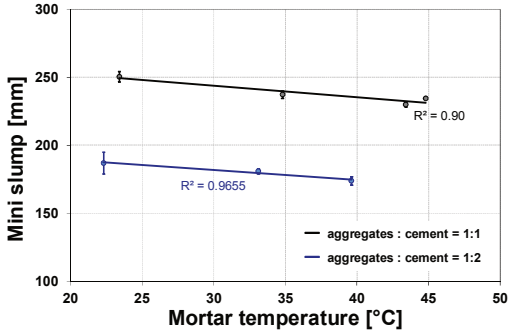

Figure 63: Mini slump values of mortars in dependence of temperature and aggregate content.

Compared to mortars with increased paste content (aggregate : cement = 1:1) a lower temperature rise is observed at reduced paste content (aggregate : cement = 2:1) keeping the PUS energy input of 150 J per ml cement suspension constant (**Table 9**). Again, decreased mini slump values are ascribed to the increased mortar temperatures (**Figure 63**). Considering the density and air void content, obviously, the PUS-conventional mixed mortar possesses a significant lower air void content compared to the reference (**Table 9** "PUS-conventional" and "reference"). Hence, a slightly higher density of PUS treated mortar (PUS-conventional) was determined. In **section 5.2.1** and **section 5.3.4** a de-airing effect of PUS on the cement suspensions was evidenced. Present results reveal that the de-airing effect of PUS is also detectable in mortars. Comparing the air void content of mortars made by suspension and conventional mix procedure (both treated with PUS) only in the PUS-conventional mixed mortar a decrease in air void content was measured. Therefore it is concluded that the addition of aggregates during the final mixing increases the air void content in the PUS-suspension mortars similar to that of the reference.

Table 9: Properties of mortars (aggregates : cement = 2:1) in dependence of mix procedure and PUS application 15 minutes after water addition.

Property (15 minutes after water addition)	Reference (without PUS)	PUS- suspension (with PUS)	PUS- conventional (with PUS)
Temperature [°C]	22.3	33.1	39.6
Mini slump [mm]	187 ± 8	181 ± 2	174 ± 3
Density [g/cm³]	2.24	2.23 (1.94)*	2.29
Air void content [Vol.-%]	4.7	4.9 (0.5)*	2.0

* cement suspension before aggregate addition

To monitor the kinetics of the hydration progress the development of temperature in the mortar samples were recorded (Almemo 2590-4S, Ahlborn, Germany). **Figure 64** displays the development of the mortar temperatures during relevant hydration time (up to 24 h). Clearly it can be seen that PUS application causes a shift of the occurrence of maximum

mortar temperatures to earlier hydration times. Thus, an acceleration of the main hydration is documented. At increased paste content (aggregates : cement = 1:1; **Figure 64a**) the maximum temperature for PUS-suspension mortar occurred 3 h 20 min and for PUS-conventional mixed mortars 4 h 25 min earlier compared to the sample without PUS treatment. Therefore an additional acceleration of PUS-conventional mixed mortar compared to PUS-suspension mixed mortars can be observed. Inferred from determined higher mortar temperature at constant ultrasonic energy input it might be possible that remaining energy (in form of heat) act as internal heat treatment to enhance hydration progress and therefore may improve very early compressive strength development.
Furthermore, to evaluate the overall effect of the temporary temperature increase induced by PUS application at the beginning of hydration, the temperature curves of the temporary heated mortars are evaluated (**Figure 64a**, Temp. 35°C and Temp. 45 °C, respectively). Analogue to results in **section 5.1.1** a slightly accelerated hydration as a result of temporary heating is detectable (**Figure 64a**). But the extent is much smaller than that observed in corresponding sonicated samples. Thus it is concluded that the major accelerating effect in mortars treated with PUS results from sonication rather than from solely temperature increase due to PUS application.

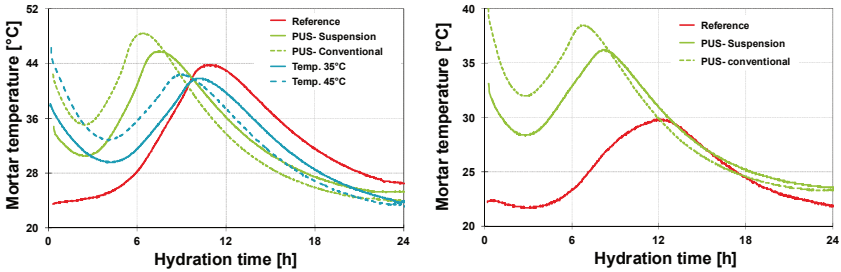

a) **Aggregate : cement = 1:1** b) **Aggregate : cement = 2:1**

Figure 64: Temperature development of mortars in dependence of time, mix procedure, and PUS application.

To confirm the acceleration of hydration in sonicated mortars, temperature development was also measured in mortar with an increased aggregates content (aggregates : cement = 2:1). Results in **Figure 64b** verify the obtained influence of PUS on the hydration progress. The appearance of the maximum mortar temperature was reduced about 3 h 45 min for PUS-suspension mortar and about 5 h and 10 min for sonicated ready mixed mortar (PUS-conventional) compared to reference.

The compressive strength development of mortars is correlated with the alite hydration and thus the formation of C-S-H phases. In a previous section (**section 5.3.2**, pp. 90) it was shown that PUS application causes an accelerated very early compressive strength development of mortars during first 24 h of hydration containing variable content of GGBFS (**Table 6**, p. 94). Additionally, results present in **Figure 65** clearly show, that with PUS application an increase of the very early compressive strength (≤ 24 h) is always detectable independently of applied mixing procedure. For instance the gain in compressive strength is about 100 % after 12 h of hydration due to PUS application. However, until 24 h of hydration statistically significant differences (Student´s t-test) in the compressive strength (at given time) of diverse sonicated samples obtained by different mixing procedures could not be verified. In other words, a more increased compressive strength of PUS-conventional mortar compared to the PUS-suspension mortar is not detected. Thus, acceleration effects from increased mortar temperatures of sonicated ready mixed mortar, that are believed to act as internal heat treatment, could not be evidenced by results of compressive strength development presented above.

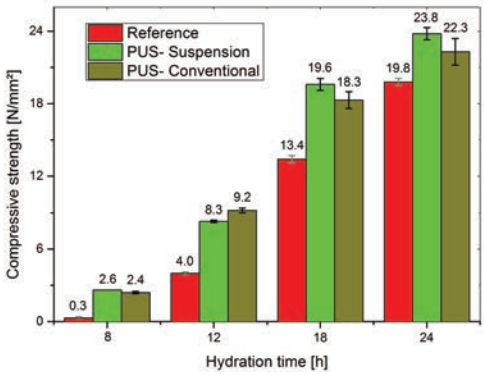

Figure 65: Compressive strength of mortars (aggregate : cement = 1:1) in dependence of hydration time, mix procedure and PUS application.

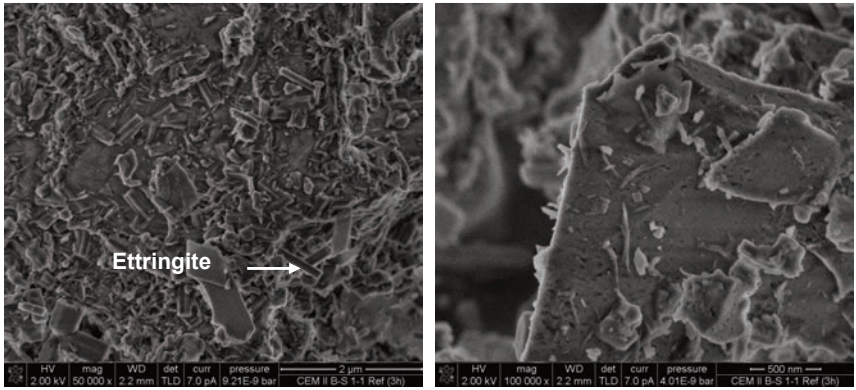

a) Reference

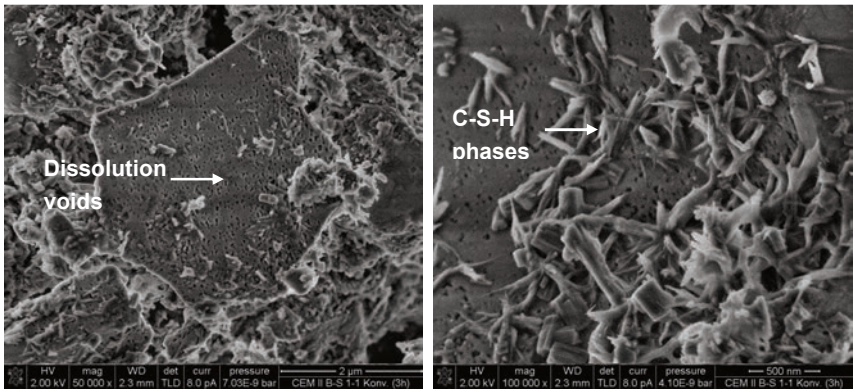

b) PUS- conventional

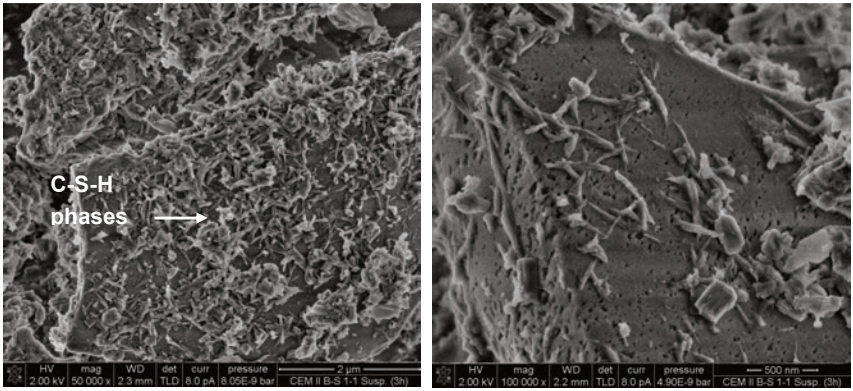

c) PUS- suspension

Figure 66: Microstructure of cement paste obtained from mortar imaged by secondary electrons after 3 h of hydration in dependence of mix procedure and PUS application. (Nova NanoSEM, 230, FEI, the Netherlands) recorded applying a Trough the Lens Detector (TLD) at approximately 10^{-6} mbar (high vacuum) at 2 kV acceleration voltages.

To characterize the microstructure during hydration of cement suspension of mortars, coarse aggregates were washed out using 2-propanol and a sieve (mesh size 63 µm) after 3 h of hydration. The images recorded by secondary electrons in the SEM (NovaNano SEM 230, FEI, Netherlands) are shown in **Figure 66**. In the reference without PUS application (**Figure 66a**) manly ettringite is detectable. Only a few sparely distributed small dissolution voids can be observed at higher magnification. **Figure 66b & c** present the microstructure of the paste of sonicated samples. There additional to ettringite tapered C-S-H phases as well as widely distributed dissolution voids on alite surface are observed. These results confirm the accelerating effect of PUS on alite hydration. Consequently, the detected increased early strength development correlates well with enhanced alite hydration, i.e. accelerated C-S-H

formation. An influence of PUS application on GGBS could not be determined from present images.

5.4.2. Conclusions

Since the positive effect of a PUS application on cement hydration progress was demonstrated by results in previous chapters (**5.1**, pp. 43 **& 5.3**, pp. 87) the question aroused if PUS treatment is also efficient in mortars. Because accelerated effect of PUS on the hydration is based on cavitation (implosion of bubbles in the liquid phase) it was arguable whether coarse aggregates (< 4 mm) influence sound wave propagation too strongly (e.g. attenuation, reduction of liquid phase). Hence, PUS was applied to two different mortar mix designs. On the one hand "common" suspension mix design (only the cement suspension is sonicated before adding the aggregates) and on the other hand a conventional mix design (ready mixed mortar inclusive aggregates is sonicated) were applied. The influence on properties of fresh and hardened mortars was compared to reference mortars (conventional mix) without PUS treatment.

As known from previous investigations on the influence of PUS application on cement suspensions, sonication causes an increase of mortar temperatures due to sonication. This temperature rise is much greater when aggregates are already present during the ultrasonic treatment (i.e. for "PUS-suspension" + 10.0 K and "PUS-conventional" + 17.3 K compared to the unsonicated reference). Because the total energy input is always the same (150 J per ml cement suspension) it is demonstrated that the additional energy (in form of heat) remains in the sonicated ready mixed mortar ("PUS-conventional") providing the possibility to act as an internal heat treatment. Measurements of the development of sample temperature during the hydration process demonstrate a more accelerated hydration in the "PUS-conventional" sample. Moreover, it has been observed that the increasing mortar temperatures cause a reduction of mini slump values. If necessary, this could be avoided by a slight increase of SP dosage and/or cooling of mortars before or during the sonication.

Results also reveal that the mix procedure influences the de-airing effect of PUS. If PUS is applied to ready mixed mortar, air void content is reduced. In contrast, in sonicated mortars made by suspension mix procedure the air void content is similar to unsonicated mortars. This is due to the suspension mixing procedure where after the ultrasonic treatment of cement suspension the aggregates are added by additional mixing, which induces air. A direct consequence of reduced air void content is a higher density that might enhance compressive strength in addition to the increased strength due to sonication. The determination of the early compressive strength development revealed a significant increase of strength due to PUS application. For instance after 18 h of hydration an increase about 50 % could be obtained. Even at earlier ages a gain of more than 100 % in compressive strength was achieved in the sonicated samples compared to the reference. Statistically significant differences (Student´s t-test) between divers sonicated mix procedures could not be evidenced. Consequently, strength improvement induced by the overall acceleration due to PUS is more significant than the effects that might be obtained by reduced air void content

(densified microstructure) and internal heat treatment. Additionally, microstructural investigation confirmed that the improved early strength development is a result of the accelerated alite hydration and thus C-S-H formation. An influence of PUS on the glass phase (GGBFS) could not be observed in the examined mixture.

Finally it is concluded that the application of PUS in mortars (aggregates < 4 mm, high cement paste content) leads to an achievement of higher early compressive strength at comparable workability. Thus, besides for suspension concrete, the PUS technique is appropriate for mortar applications.

5.5. Optimized SCC mixture in precast production

Constructional engineering with precast concrete elements has many advantages compared to placing concrete on the building site. A High quality of precast concrete (fairfaced concrete, accurate elements), the independence on weather conditions (concreting in plant, assembling on the construction site), and economic efficiency (relatively low-cost production processes, short assembly times) leads to an increasing demand of such precast concrete elements. Thus to ensure an effective production of precast concrete strict requirements on the workability and the strength development are essential. Sufficient early strength development is required to strip the formwork. To achieve the desired strength development of concrete, mixtures include cements possessing a high strength class, high cement content, and low water to cement ratio. Additional compressive strength improvement is obtained by the addition of chemical admixtures and especially by heat treatment. The advantages and disadvantages of these approaches are already discussed in **section 2.1.2**, p. 24. Furthermore the addition of high efficient SP guarantees appropriate workability but causes an undesirable delay of cement hydration progress and thus concrete strength development.

Without doubt results discussed in previous sections demonstrate the positive effect of PUSon cement hydration, accelerated strength development and partial improved workability. Therefore a successful integration of the PUS technique in precast production should give the possibility to reduce heat treatment and SP addition by keeping or even improving concrete quality. Further economic and ecologic improvement (saving energy and resources) and the reduction of CO_2 emission would be feasible.

The following section addresses the question how PUS application influences the (fresh and hardened) properties of a commercial self compacting concrete (SCC) mix. For this purpose a given SCC mixture (kindly supplied by ZAPF GmbH) is tested on the laboratory scale (adjusted to mortar scale). The influence of PUS on properties of fresh (fluidity, density, air void content) and hardened mortar properties (isothermal heat conduction calorimetry, ion concentration of aqueous phase, compressive strength development, sedimentation stability, and porosity) is characterized. Furthermore, mixture has to be optimized taking into account the practical requirements (strength development, workability). Additionally, ways to implement the PUS technique in concrete production will be discussed.

5.5.1. Materials and test methods

Cement of type CEM II/A-S 52.5 N blended with limestone powder (LSP) was used for investigation. Chemical compositions (oxide content) of raw materials were determined by inductively coupled – optical emission spectroscopy (ICP-OES, Perking Elmer Optima 3000) after dissolving solids in hydrofluoric acid (**Table 10**). Specific surface area of cement is 5520 cm²/g and that of LSP 6610 cm²/g (Blaine method). Also a polycarboxylate type SP was added to the mixture (density 1.06 g/cm³ and solid SP content 30 m.-%).

Table 10: Chemical composition of CEM II/A-S 52.5 R and limestone powder determined by ICP-OES given in m.-%.

	SiO_2	Al_2O_3	Fe_2O_3	CaO	MgO	MnO	K_2O	Na_2O	TiO_2	SO_3	loI
CEM II/A-S 52.5 R	20.9	6.2	2.8	59.5	2.0	0.14	1.29	0.21	0.27	3.3	3.0
Limestone powder	--*	--*	--*	53.2	2.7	--*	0.17	0.02	--*	--*	42.5

* not determined

The investigated mixture is a SCC for wallboard production. The water to cement ratio of the mixture was 0.6. Addition of water dissolved SP was added about 1.7 m.-% referred to cement mass. That equals an addition of 0.5 m.-% SP dry mass referred to cement mass. Cement content of the concrete mix was 360 kg/m³: Aggregates composition was given as follow: 610 kg/m^3 sand (particle size group 0/2), 470 kg/m³ split (particle size group 2/5), 470 kg/m³ split (particle size group (5/8), and 235 kg/m³ LSP, respectively.
To estimate the influence of PUS on given SCC mixture a downscale to mortar was required (due to the limitation of PUS apparatus). Downscaling the SCC mixture to a mortar means to omit coarse aggregates (> 2 mm). Thus only cement, LSP, sand (0/2) and SP were mixed to obtain self-compacting mortar.

The mix regime of mortar was kept in accordance with the production in the precast plant. Only in the case of PUS application the mixing procedure was changed to follow a suspension mix design. Therefore, in the first place cement and LSP are mixed with water and SP. Afterwards cement suspension is treated with PUS. During a final mixing step aggregates are added to the mixture.
To ensure economic production of wallboards, an early demoulding and reuse of formworks is desired. Thus, formworks are heated to achieve sufficient compressive strength (15 N/mm²) after 7 h of hydration. At the plant side parameters for actual heat treatment are an exposure time of 4.5 h with a maximum concrete temperature of 60 °C. At laboratory scale heat treatment was provided by a drying oven (60 °C). Temperature sensors (Ni Cr-Ni thermo wire type Z 190-10, Ahlborn, Germany) were used to monitor maximum mortar temperature. To avoid evaporation moulds were packed air tightly in plastic sheets. Mortar prisms remain in moulds until examination (e.g. compressive strength < 24 h).

Properties of fresh mortars were evaluated by means of temperature, mini slump flow and V - funnel flow times (according to DAfSt SCC guideline 2003-11), as well as density and air void content (DIN EN 12 350-6 and DIN EN 12 350-7 respectively).

Hydration progress was monitored by isothermal heat calorimetry (TrioCAL 7339, ToniTechnik, Germany) of cement pastes and chemical composition of aqueous phases (ICP-OES, Optima 3000, Perking Elmer, Germany). Setting time was determined according to DIN EN 196-3 (Vicat needle test), where surcharge has to be increased to 1000 ± 2 g due to mortar examination. Additionally strength development was documented by continuously

nondestructive measurement of ultrasonic P- wave velocity (ultrasonic probe CELplus, GEOTRON Elektronic, Germany) and compressive strength development (DIN EN 196-1).

Another important requirement of self-compacting mortar is structural stability, evaluated by laserultrasound and light microscopic investigations (VHX II 600, Keyence, Japan). Measurements were performed in hardened mortars.

5.5.2. Influence of PUS on properties of self-compacting mortar

The influence of PUS application on the properties of fresh mortars is presented in **Table 11**. Obviously the influence of PUS treatment is consistent to observations described in previous chapters:
1) Sonication causes an increase in mortar temperature.
2) Mini slump flow is increased despite increased mortar temperatures.
3) Also the V- funnel flow time is improved due to PUS application.
This confirms a direct influence of PUS on yield stress and viscosity. Consequently, an enhanced fluidity is responsible for decreased air void content and thus higher mortar density.

Table 11: Properties of fresh self-compacting mortars in dependence of PUS application

Property of fresh mortar	Reference	Power ultrasound
Temperature [°C]	22.0 ± 1.0	28.0 ± 1.0
Mini slump flow [cm]	30.0 ± 1.0	38.0 ± 1.0
V funnel flow time [s]	3.5	1.5
Density [g/cm³]	2.13	2.17
Air void content [%]	2.7	0.4

The influence of PUS application on hydration progress evaluated on the basis of isothermal heat calorimetric measurements (without heat treatment at constant temperature: 25 °C) and chemical composition of aqueous phase is shown in **Figure 67** and **Figure 68**, respectively.
Results of heat release rate and total heat of cement paste (**Figure 67**) verify the known acceleration effect of ultrasonic treatment. The acceleration period related to main hydration is shifted to earlier times. Considering important hydration time of 7 h (demoulding time in precast production; marked by an asterisk) it can be seen that in PUS treated sample the maximum of heat release rate has almost been reached. The total amount of heat released at this time is approximately two times of that observed in the reference.

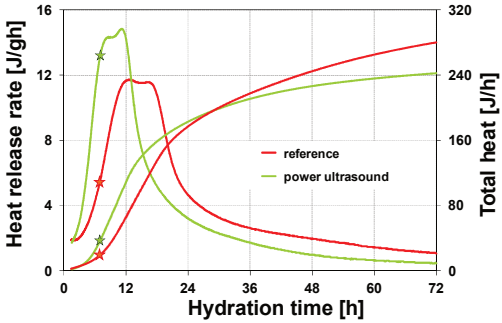

Figure 67: Heat release rate and total heat of cement paste in dependence of hydration time and PUS application.

Also the chemical composition of the aqueous phase (**Figure 68**) confirms accelerated hydration process. After 3 h of hydration a significant lower concentration of calcium and sulfate ions are detected in the sonicated sample. Whereas potassium ions and sodium ions as well as the pH value are increased at the same time compared to the reference.

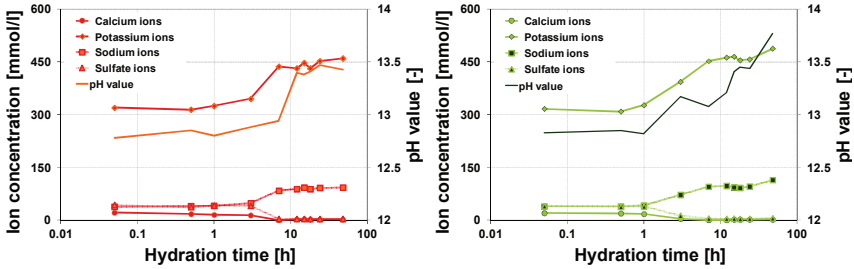

a) Reference b) Power Ultrasound

Figure 68: Chemical composition of aqueous phase in dependence of hydration time and PUS application.

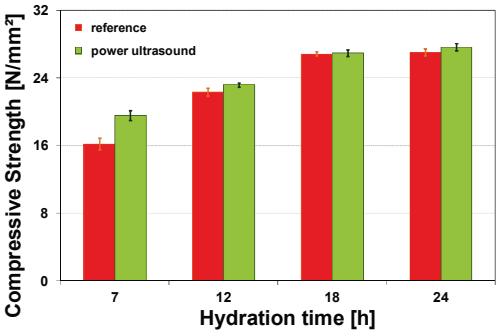

Figure 69: Compressive strength development of self-compacting mortars in dependence of hydration time and PUS application.

Compressive strength development is shown in **Figure 69**.

The maximal increase of compressive strength is detected at important hydration time of 7 h. At this time reference sample has to provide a compressive strength of 15 N/mm² after a short thermal treatment (4.5 h at 60°C). Present results reveal that this requirement was met (reference 16.2 ± 0.7 N/mm² after 7 h of hydration) for the reference sample. In comparison, the sonicated sample achieves a compressive strength of 19.6 ± 0.6 N/mm² at the same time. This is a statistical significant increase (Student´s t-test) of approximately 20 %. At later hydration times (up to 24 h) compressive strength of both mixtures are quite similar.

The sonication of cement suspension causes dispersion of small particles (**section 5.2.1**, pp. 74) and reduced air content. Thereby yield stress and viscosity of cement suspension are influenced (**section 5.2.2.**, pp. 79) One result of these effects is the sedimentation of mortar aggregates. This sedimentation is obvious in light microscopic images of longitudinal sections (**Figure 70**) as well as in results of determination of laserultrasound wave propagation velocity v_p (**Figure 71**).

The structural stability of mixture without PUS application is characterized by the homogeneous distribution of all aggregates in the whole mortar profile (**Figure 70a**). Compared to that in the sonicated sample the coarse particles are concentrated on the bottom (**Figure 70b**). A sinking of coarser/ heavy aggregates indicates a reduction of yield stress of the mixture and correlates well with observed increased mini slump flow.

In general ultrasound wave propagation velocity (v_p) through mortar is influenced by several parameters that are aggregates, cement matrix, air void content, and hydration degree[119,120,164,165]. In this context, a constant v_p all over the mortar sample indicates a homogeneous distribution of all increments. The reference mortar was evidenced to be a stable mixture (**Figure 70**).

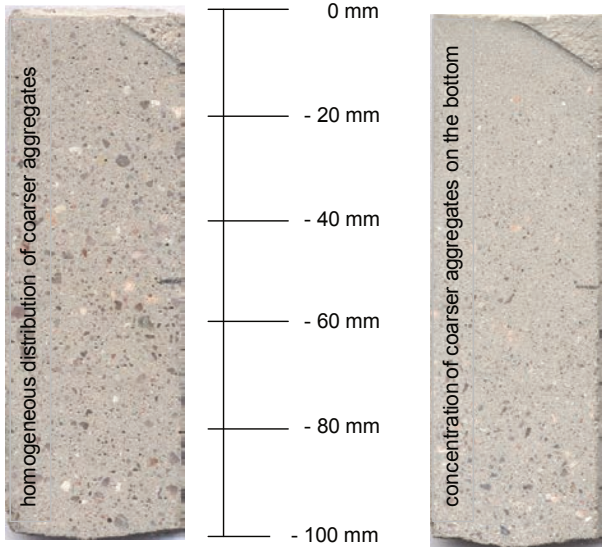

Figure 70: Longitudinal sections of self-compacting mortars in dependence of PUS application.

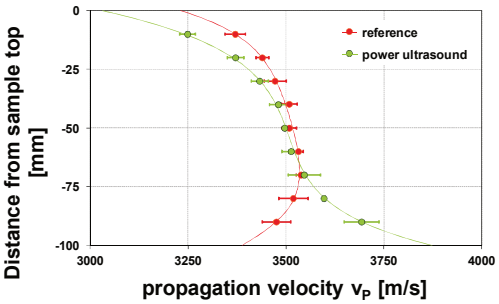

Figure 71: Wave propagation velocity v_p in mortars in dependence of sample height and PUS application.

Results in **Figure 71** demonstrate that only on the top of the reference sample (- 10 mm) a significant reduced ultrasound wave propagation velocity was determined. It can be argued that in that region the content of cement paste as well as the porosity is increased (**Table 12**) causing a decrease in wave propagation velocity. In the rest of the sample a similar P- wave velocity was measured, indicating a homogeneous distribution of all components. In the sonicated sample differences in wave propagation velocity in dependence of sample height are more significant. At the top v_p is less compared to the reference indicating even higher porosity and/ or increased cement content. In contrast at the bottom of the sample v_p is increased corresponding to the concentration of coarser aggregates (consequently higher density, cf.

Table 12). Finally results of wave propagation velocity confirm sedimentation problems (as shown in **Figure 70**) in ultrasonic treated mortar prisms.

Table 12: Density and porosity of self-compacting mortars in dependence of sample height and PUS application.

Sample height	Density [g/cm³]		Porosity [%]	
[mm]	Reference	PUS	Reference	PUS
0 … - 20	1.92	1.78	25.8	30.5
-40 … - 60	1.95	1.94	24.3	24.5
-80 … -100	1.96	2.11	23.5	19.6

5.5.3. Optimization of sonicated self-compacting mortar

The major priority of current investigation is to discover the savings that can be realized by PUS application. The focus is on economic parameters (i.e. heat treatment). Whereas demoulding periods of formworks should not be changed.
Results present in previous chapter (**section 5.5.2**, pp. 79) show that a PUS application in cement suspension for self-compacting mortar causes accelerated cement hydration linked to an increased early strength development. The simultaneous dispersion and de-airing of cement suspension cause an increase in fluidity due to PUS treatment. Keeping mixture parameters constant this results in sedimentation of aggregates. Consequently, the sonicated mixture should be optimized concerning SP addition or water content to guarantee stability. However, major goal of investigation was to reduce heat treatment. Accelerated development of very early strength development due to PUS application gives the possibility to reduce the time of thermal treatment for the desired 15 N/mm² after 7 h of hydration.

In a first step mortar composition was adjusted to avoid sedimentation. This was attained by SP reduction. The target is to obtain similar fluidity (mini slump flow) as documented for the unsonicated reference (30 cm). The stepwise SP reduction with corresponding slump flow values is shown in **Table 13**. To achieve a slump flow value of 30 cm in reference mortar (without PUS) a SP dosage of 1.7 m.-% referred to cement mass is required. To obtain similar slump flow in sonicated sample a SP addition of only 1.2 m.-% referred to cement mass is necessary. This reduction (0.5 m.-%) is equivalent to saving roughly 30 % of SP. On hydrated samples stability against sedimentation by measurements of ultrasound P- wave velocity (**Figure 72**) could be proven. Similar to the reference a stabilized mortar was obtained by reducing SP content in the sonicated mortar.

Table 13: Optimization of liquid SP addition (target = 30.0 cm)

Liquid SP addition [m.-%] bwoc	Slump flow [cm]
1.70	38.0
1.50	37.5
1.30	35.5
1.25	34.0
1.20	30.0
1.10	28.5

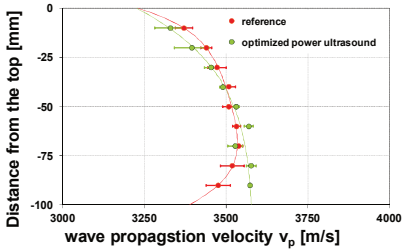

Figure 72: Wave propagation velocity in optimized sonicated self-compacting mortar.

The strength development of stabilized (reduced SP content compared to reference) sonicated self-compacting mortar was assessed by means of setting time, continuously measurements of ultrasound wave propagation velocity and compressive strength development (DIN EN 197-1).

Firstly Vicat needle test was carried out to determine the set times of reference and stabilized PUS treated mortar. In the reference initial setting was detected after 2:30 h of hydration. Compared to that the initial set of the optimized PUS treated mortar was detected after 2:00 h of hydration.

An advantageous option to monitor strength development non-destructively is the measurement of ultrasonic wave propagation velocity (v_p). Results presented in **Figure 73** of continuously measured v_p (measurements without heat treatment of mortars) verify accelerated structural development due to PUS application. Consistent with this structural development an increased strength development in mortars could be determined (reference: 16.2 N/mm² optimized PUS: 19.3 N/mm³ after 7 h of hydration, **Figure 74**). As shown, the 7 h compressive strength is increased in the sonicated stabilized self-compacting mortar without changing the duration of thermal treatment. Thus, this gives the possibility to reduce the duration of heat treatment in sonicated samples while guarantee desired compressive strength (minimal 15 N/mm² after 7 h of hydration).

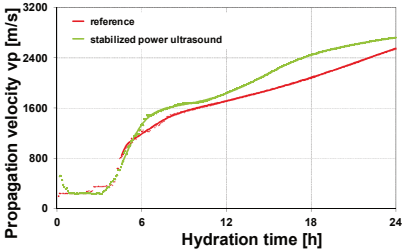

Figure 73: Continuously measurement of ultrasound p-wave velocity in stable self-compacting mortars (without heat treatment) in dependence of PUS application.

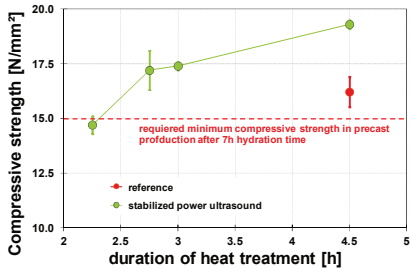

Figure 74: Compressive strength of self-compacting mortars in dependence of heating periods.

Results in **Figure 74** document compressive strength of sonicated stabilized mortars in dependence of heat treatment duration. The required compressive strength of 15 N/mm² after 7 h of hydration was measured in stabilized sonicated mortars even if heating was reduced to 2:15 h:min. However considering uncertainties it would be better to choose longer heat treatment duration. Even with a reduction of 1:45 h:min of heat treatment (i.e. heat treatment duration of 2:45 h:min) nearly 40 % of the time for formwork heating can be saved.

Consequently, investigations have shown that PUS application could reduce material usage (here SP addition) and duration of heat treatment during wallboard production. Assuming a production of 60 000 t of concrete per year (= 25 000 m³/a) and a PUS energy consumption of 8.75 kWh/m³ for current concrete mixture (75 J/ml $_{suspension}$) approximately a energy of 200 000 kWh/a is needed. Thus, the overall investment for the production of one m³ SCC with and without PUS can be calculated (**Table 14**).
Obviously the total financial effort for SCC production can be reduced by the application of PUS. Considering all parameters (raw materials, standard costs, energy) approximately 3.3 % of costs can be saved by reduced SP addition and heat treatment. This seems not to be awesome. However, SP addition and heat treatment only pay a small contribution towards the overall costs. Hence an optimization of “cement” could be more efficient. These might include, for example, the reduction of cement content, the usage of cement possessing a lower strength class and the replacement of cement by SCM.

Table 14: Financial effort to produce one m³ SCC with and without PUS application in the precast plant.

	Per m³ concrete	Investment	Conventional [€]	With PUS [€]
Sand (0/2)	610 kg	10.20 €/t	6.22	6.22
Split (2/5)	470 kg	12.70 €/t	5.97	5.97
Split (5/8)	470 kg	12.70 €/t	5.97	5.97
Cement	360 kg	121.80 €/t	43.85	43.85
Water	200 kg	6.00 €/m³	1.2	1.2
SP	6.12 kg (1.7 wt-%)	1.33 €/kg	8.14	--
	4.32 kg (1.2 m.-%)	1.33 €/kg	--	5.75
Mixing costs	---	12.75 €/m³	12.75	12.75
Heat treatment	7 l (4.5 h)	60 €/100 l	4.52	--
	4.2 l (2.75 h)	60 €/100 l	--	2.52
PUS energy	8.75 kWh	0.17 €/kWh	--	1.49
Total		∑	**88.62**	**85.72**

Nevertheless, besides reduced production costs induced by the usage of PUS, another important advantage is the reduction of CO_2 emission. Using PUS instead of heat treatment the consumption of heating oil is reduced. One liter heating oil (with a density of 0.82 kg/l possessing a heat value of approximately 36.0 MJ/l) emits about 2.71 kg CO_2 during combustion. In considered case (reduced formwork heating from 4.5 h to 2.75 h) provided that 25 000 m³ SCC are produced per year approximately 190 t of CO_2 emission would be prevented.
A prerequisite is the implementation of the appropriate PUS technique in precast production without large effort. Therefore in the next section this topic will be discussed.

5.5.4. PUS technique in precast production

Provided that it is most effective to sonicate cement suspension without aggregates the common mixing procedure has to be split. Therefore, initially cement suspension is prepared, then treated with PUS and subsequently aggregates are added. Thus the existing precast plant should provide the possibility to produce cement suspension and to connect a pumping circle. In general, the process for concrete production in a horizontal concrete mixing plant can be described as follows (**Figure 75**):

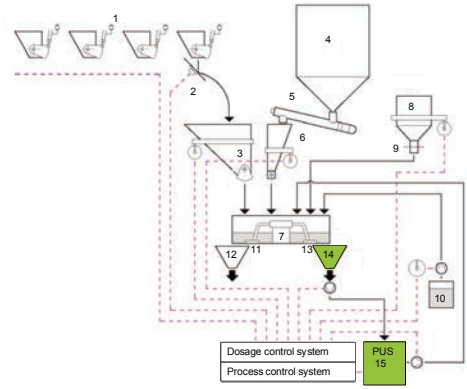

1. Aggregate scales
2. Moisture measuring of aggregates
3. Aggregate dosage
4. Cement silo
5. Screw
6. Cement scales/ dosage
7. Ring-pan mixer
8. Fresh & residual water
9. Water dosage
10. Admixture dosage
11. Discharge chute
12. Reservoir (fresh concrete)
13. Second discharge chute
14. Reservoir linked with pumps and pipeline to
15. PUS equipment linked with pumps back to ring.pan mixer

Figure 75: Schematic diagram of mixing process in common a horizontal concrete mixing plant with integrated PUS technique.

Aggregates and cement, transported from the silo (no. 4) via screw (no. 5), are weighed (no. 1 & no. 6) and subsequently homogenized (dry) in the ring pan mixer (no. 7). In accordance with the concrete formulation water is weighed (no. 9) and injected in the mixing chamber. However, variations in humidity of aggregates (no 2) have to be considered with regard to the accurate w/c of resulting concrete mix. After water addition required chemical admixtures (no. 10) can be added via a separate feed pipe directly in the mixing chamber. When the mixing process is finished, the fresh concrete is removed via a discharge chute (no. 11) on the bottom of the mixing chamber. From the reservoir (no. 12) the fresh concrete is transferred to a concrete hopper and subsequently transported to the formwork that has to be filled by crane runway. During transport a rotating shaft prevents concrete to sediment.

In the particular case an expertise of the considered plant construction reveals the present of a second (unused) discharge chute to empty the mixing chamber (no. 13). Here an additional reservoir (no. 14) should be installed. Attached pipelines equipped with optimal designed pumps convey cement paste to the PUS equipment (no. 15).

Figure 76: Series of power ultrasound generators (1) in an acoustic cabinet (2) with flow-through cell (3).

For instance PUS application could be realized in a one-time flow process. Therefore an adequate number of PUS generators have to be connected in series or in parallel (**Figure 76**). Optimal ultrasonic horn/ booster combinations have to be supplied to guarantee an efficient energy contribution. For safety secure an acoustic cabinet is required. After sonication cement suspension is transported back to the mixing chamber (no. 15). While PUS treatment proceeds aggregates can be homogenized in the mixing chamber. Thus, it is possible to complete the concrete mix with sonicated cement suspension immediately.

5.5.5. Conclusions

Up to now the application of the PUS technique was limited to laboratory mortar mixes. Hence the focus of present chapter was to evaluate the influence of PUS application on a mixture used in common precast production. The ostensible aim was to reduce cost-intensive heat treatment by accelerating cement hydration using PUS.

Thus, a SCC mixture for wallboard production was downscaled by omitting coarse aggregates to laboratory scale (self-compacting mortar). Selected properties of fresh and hardened mortars were characterized in dependence of PUS application.

Strength development and workability of current mixture were significantly influenced by PUS application. An accelerated strength development was determined. However, improved dispersion and de-airing due to PUS treatment leads to the sedimentation of coarser particles. Consequently an adjusting of sonicated mixture was performed. First structural stability has to be restored. As a result the liquid SP addition could be reduced from 1.7 m.-% bwoc (reference without PUS application) to 1.2 m.-% bwoc in sonicated mortars at constant flowability. This equals a reduction of 30 %. Additionally increased compressive strength due to PUS application leads to a reduction of the duration of heat treatment. To obtain the required compressive strength of 15 N/mm² after 7 h of hydration, a short time heat treatment

of 4.5 h (60°) was applied in reference mortar. In sonicated mortars crucial compressive strength was detected already after a heat treatment of 2.15 h. But also with a reduction only to 2.75 h heat treatment duration roughly 40 % are economized.
Finally the assessment of financial effort reveals that production costs can be reduced (3.3 %) by PUS application for actual investigation. Thus, the ambitious aim is to optimize concrete formulation and PUS parameter as such that benefit is increased. Nevertheless, the integration of PUS technique in existing precast plant is possible without large effort. The structure of concrete batching plant enables a simple attachment of PUS equipment.

6. Summary

The aim of the presented work was to gain a basic knowledge of how power ultrasound (PUS) influences the hydration process and workability of cement. Another challenge was to keep a close eye on essential requirements of practical relevance (adaptability of PUS technique). To satisfy the scope of work, it was divided in five separate parts.

In the first two parts (**Chapter 5.1.**, pp. 43 and **Chapter 5.2.**, pp. 74) the focus lies on the influence of PUS on ordinary Portland systems (OPC systems). Effects on hydration process and fluidity were examined. First of all, a general overview on the application of PUS on OPC (CEM I) suspension was documented. As expected, the major impact on cement suspension was observed to be the variation of the specific energy input. Furthermore, it was demonstrated that the usage of increased PUS amplitudes transmitted via large front face diameters of ultrasonic horns were advantageous with regard to practical requirements (short sonication duration, restricted temperature increase of sonicated cement suspension, significant acceleration of cement hydration). Consequently, optimal PUS parameters (amplitude/ specific energy input) were deduced from this pre-examination. In the following the influence of PUS application on the hydration kinetics of OPC hydration was investigated in more detail applying optimal PUS parameters (43 µm/ 75 J/ml). The hydration progress was assessed by means of measuring the initial setting times, isothermal differential conduction calorimetry, determination of non-destructive ultrasonic P-wave velocity, compressive strength development of mortars and microstructural SEM- investigations. Results indicate that the influence of PUS on cement hydration process is principally based on accelerating alit hydration (main clinker phase in OPC) and thus C-S-H formation. Consequently, for fundamental understanding, the influence of PUS on C_3S (model substance representing alite) hydration and C-S-H precipitation were investigated. Experiments addressing the precipitation (nucleation/ growth) of C-S-H (from clear to the eye aqueous Ca-Si- solution, stirred diluted C_3S suspensions) show evidence that PUS does not alter the reaction path (kinetic path) but purely accelerate kinetics of C_3S hydration. The key determining factor (for acceleration) was contained to be increased precipitation of very early C-S-H phases. Furthermore it is believed that shock wave generation is induced by cavitation. Shock waves lead to increased particle collisions that are believed to cause localized erosion effects. Thereby, at the one hand C_3S surfaces remains available for dissolution processes and on the other hand removals may give additional growth regions for C-S-H. As a consequence an accelerated C_3S hydration was determined.
Secondly, the de-airing, homogenizing and dispersing effects known for PUS applications were confirmed for cement suspensions. It was demonstrated that PUS is able to increases flowability of OPC suspensions. However, if SP is present in the mix liquefaction induced by PUS was not generally observed. As indicated by microstructural investigation, sonication may influence reaction between the aluminate phase and sulphate phase of cement. For crucial conditions (low w/c, high SP content) this may leads to a variation of early hydration composition (occurrence of AFm) and thus reduced flowability. Nevertheless, experiments (mini slump flow and V-funnel flow time measurements) reveal that PUS mainly influences

viscosity since the deagglomeration/ deflocculation of fine cement particles increase the (free) excess water content.

Investigations in **Chapter 5.3**, pp. 87 examine the transferability of observations found in OPC systems to blended cements (containing GGBFS). The main question aroused was if sonication can accelerate slag hydration. Beforehand, an adjustment of optimal PUS parameter to 53 µm and 150 J/ml was possible. With this optimal parameters accelerated slag cement hydration was evidenced as well (by means of measuring initial setting time, isothermal heat conduction calorimetry and compressive strength development of mortars). However, experiments on pure GGBFS/ CH systems showed that PUS only marginally accelerates GGBFS hydration. Consequently in blended cements acceleration is mainly attributed to the residual OPC (alite) percentage.

The last two parts (**Chapter 5.4.**, pp. 102 and **Chapter 5.5.**, pp. 110) addresses practical aspects to the application of the PUS technique in concrete production. As presumed, a satisfy usage of PUS in concrete production requires changing concrete mixing procedure. The “suspension mix design” guarantees efficient cavitation generation (availability of aqueous phase, restricted influence on wave propagation). However, in special cases an application of the “suspension mix design” seems not to be efficient (e.g. grouts, addition of aggregates ≤ 4 mm). Hence, in **Chapter 5.4.**, pp. 102 properties of fresh and hardened sonicated mortars applying “suspension” and “conventional” mix design were documented. It was found that the sonication of ready mixed mortars (“conventional mix design”) induces higher mortar temperatures, decreased air void content but also decreased fluidity compared to sonicated mortars obtained applying the “suspensions mix design”. Significant differences in very early compressive strength development (up to 24 h of hydration) were not assessed. Therefore, since mainly very early strength development is aimed to be accelerated by PUS application, it was evidenced that besides suspension concrete the PUS technique is appropriate for mortar applications with aggregates ≤ 4 mm and high pastes contents (cement : aggregates = 1:1).
Additionally to the documented capability of applying PUS in mortars, a commercial precast SCC mixture was optimized using PUS technique in **Chapter 5.5.**, pp. 110. Due to the limitations given by the technical PUS equipment a downscale to mortar was necessary. Significant changes of several properties of fresh and hardened self- compacting mortars were documented owing to the use of PUS. Flowability was increased until sedimentation of coarser particles occurs. Nevertheless, important very early compressive strength development was increased by sonication. Consequently, the re-establishment of required mortar performance enables the reduction of SP dosage and reduced heat treatment duration due to PUS application. Finally, it was shown that an implementation of the PUS technique in precast production plant is possible without many constructive efforts. A rough calculation reveals reduced concrete production costs using the PUS technique. However, calculations are based on results found for mortars using laboratory PUS device.

7. List of Figures

8. List of Tables

9. References

1 Hou, P.; Wang, K.; Qian, J.; Kawashima, S.; Kong, D.; Shah, S.P. (2012): *Effects of colloidal nanoSiO_2 on fly ash hydration.* Cement and Concrete Composites, Vol. 34 (10): pp.1095-1103.

2 Hubler, M.H.; Thomas, J.J.; Jennings; H.M. (2011): *Influence of nucleation seeding on the hydration kinetics and compressive strength of alkali activated slag paste*. Cement and Concrete Research, Vol. 41 (8): pp. 842-846.

3 Benstedt, J.; Barnes, P. (2002): *Structure and performance of cements.* Spon Press (2nd Edition), New York.

4 Stark, J. (2011): *Recent advances in the field of cement hydration and microstructure analysis*. Cement and Concrete Research, Vol. 41 (7): pp.666-678.

5 Scrivener, K.L.; Nonat, A. (2011): *Hydration of cementitious material, present and future*. Cement and Concrete Research, Vol. 41 (7): pp. 651-665.

6 Midness, S.; Young, J.F. (1981): *Concrete*. Prentice-Hall, Inc. Englewood Cliffs, NJ, U.S.

7 Rodger, S.A.; Groves, G.W.; Clayden, N.J.; Dobson, C.M. (1988): *Hydration of Tricalcium Silicate Followed by 29Si NMR with Cross-Polarization*. Journal of the American Ceramic Society, Vol. 71 (2): pp. 91-96.

8 Bullard, J.W. Jennings, H.M.; Livingston, R.A.; Nonat, A.; Scherer, G.W.; Schweitzer, J.S.; Scrivener, K.L.; Thomas, J.J. (2011): *Mechanism of cement hydration*. Cement and Concrete Research, Vol. 41 (2): pp. 1208-1223.

9 Stark, J.; Möser, B.; Bellmann, F. (2003): *Ein neues Modell der Zementhydratation*. Tagungsband der 15. ibausil, Band 1: pp. 14-31.

10 Jugovic, Z.T.; Gillam, J.L. (1968): *Early Hydration Reactions of Abnormal Setting Portland Cement*. Journal of Materials, JMLSA, Vol. 3 (3): pp. 517-537.

11 Richartz, W. (1986): *Einfluss des K_2O-Gehaltes und des Sulfatisierungsgrads auf das Erstarren und Erhärten des Zements.* Zement – Kalk – Gips, Vol. 39 (12): pp. 678-687.

12 Locher, F.W. (2000): *Zement – Grundlagen der Herstellung und Verwendung.* Verlag Bau+Technik GmbH, Düsseldorf: p.196.

13 Lothenbach, B.; Winnefeld, F. (2006): *Thermodynamic modeling of hydration of Portland cement*. Cement and Concrete Research, Vol. 36 (2): pp. 209-226.

14 Gebauer, J. (1978): *Technological possibilities of avoiding the early setting of cement.* Zement-Kalk-Gips, Vol. 31: pp. 302-304.

15 Bensted, J. (1980): *An Investigation of the setting of Portland cement.* Silic. Ind. Vol. 45, pp. 115-120.

16 Stein, H.N.; Stevels, J.M. (1964): *Influence of silica on the hydration of* $3CaOSiO_2$. Journal of Applied Chemistry, Vol. 14 (8): pp. 338-346.

17 Sujata, K.; Jennings, H.M. (1992): *Formation of a Protective Layer During the Hydration of Cement*. Journal of the American Ceramic Society, Vol. 75 (6): pp. 1669-1673.

18 Gartner, E.M.; Gaidis, J.M. (1989): *Hydration mechanism I*. Material Science of Concrete: pp. 95-125.

19 Trettin, R.; Wiecker, W. (1986): *Zur Hydratation von Trikalziumsilikat I. Ursachen der Induktionsperiode*. Silikattechnik, Vol. 37 (3): pp. 75-78.

20 Juilland, P. Gallucci, E.; Flatt, R.; Scrivener, K.L. (2010): *Dissolution theory applied to the induction period in alite hydration.* Cement and Concrete Research, Vol. 40 (6): pp. 831-844.

21 Barret, P.; Ménétrier, D. (1980): *Filter dissolution of* C_3S *as a function of the lime concentration in a limited amount of lime water.* Cement and Concrete Research, Vol. 10 (4): pp. 521-534.

22 RILEM Committee 68-MMH, Task Group 3 (1984): *The Hydration of Tricalcium Silicate.* Matériaux et Constructions, Vol. 17 (102): pp. 457-468.

23 Jin-Keun, K.; Hun, H.S., Chul, S.Y. (2002): *Effect of temperature and aging on the mechanical properties of concrete. Part I. Experimental results.* Cement and Concrete Research, Vol. 32 (7): pp. 1089-1094.

24 Thomas, J.J.; Jennings, H.M. (2002): *Effect of Heat Treatment on the Pore Structure and Drying Shrinkage Behavior of Hydrated Cement Paste*. Journal of the American Ceramic Society, Vol. 85 (9): pp. 2293-2298.

25 Erdoğdu, Ş.; Kurbetci, Ş. (1998): *Optimum Heat treatment Cycle for Cements Different in Type and Composition*. Teknik Dergi, Vol. 9 (3): pp. 1673-1685.

26 Cheung, J.; Jeknavorian, A.; Roberts, L.; Silva, D. (2011): *Impact of admixtures on the hydration kinetics of Portland cement*. Cement and Concrete Research, Vol.41 (12): pp. 1289-1309.

27 Ramachandran, V.S. (1971): *Kinetics of hydration of tricalcium silicate in presence of calcium chloride by thermal methods.* Thermochimica Acta, Vol.2 (1): pp. 41-55.

28 D.L. Kanto (1975): *Tricalcium Silicate Hydration in the Presence of Carious Salts*. Journal of Teting and Evaluation, JTEVA, Vol. 3 (4): pp. 312-321.

29 Singh, N.B.; Prabha Singh, S. (1991): *Hydration of Tricalcium Silicate*. In Hydration and Setting of Cements, Proceeding of the international RILEM Workshop, E & FN Spon, London: pp.35-41.

30 Riding, K. Silva, D.; Scrivener, K. (2010): *Early age strength enhancement of blended cement systems by $CaCl_2$ and diethanol-isopropanolamine*. Cement and Concrete Research, Vol. 40 (6): pp. 935-946.

31 Singh, N.B.; Ojha, P.N. (1981): *Effect of $CaCl_2$ on the hydration of tricalcium silicate*. Journal of Materials Science, Vol. 16 (10): pp. 2675-2681.

32 Thomas, N. L. (1987): *Corrosion problems in reinforced concrete: why accelerators of cement hydration usually promote corrosion of steel*. Journal of Material Science, Vol. 22 (9): pp. 3328-3334.

33 Angst, U.; Elsener, B.; Larsen, C.K.; Vennesland, Ø. (2009): *Critical chloride content in reinforcement concrete – a review*. Cement and Concrete Research, Vol. 39 (12): pp. 1122-1138.

34 Taylor, H.F.W. (1997): *Cement Chemistry.* 2nd Edition, Thomas Telford Publishing, London.

35 Huber H. Gantner J.; Kusterle, K. (1994): *Spritzbeton mit alkalifreier Erstarrungsbeschleunigung – umweltneutraler Spritzbeton.* Zement und Beton, Vol. 39 (1): pp. 19-21.

36 Xu, Q. (2005): *Chemische Wirkung von Erstarrungsbeschleunigern auf die frühe Hydratation des Portlandzements.* PhD Thesis, Cuvillier Verlag Göttingen.

37 Stark, J.; Wicht, B. (2001): *Dauerhaftigkeit von Beton – Der Baustoff als Werkstoff*. Birkhäuser Verlag, Basel/Boston/Berlin.

38 Escadeillas, G.; Aubert, J.-E.; Segerer, M.; Prince W. (2007): *Some factors affecting delayed ettringite formation in heart-cured mortars*. Cement and Concrete Research, Vol. 37 (10): pp. 1445-1452.

39 Bellmann, F.; Damidot, D.; Möser, B.; Skipsted, J.. (2010): *Improved evidence for the existence of an intermediate phase during hydration of tricalcium silicate.* Cement and Concrete Research, Vol. 40 (6): pp. 875-884.

40 Ludwig, H.-M.; Neumann, T. (2006): *Schnellzemententwicklung für die Fertigteilindustrie. Technische und wirtschaftliche Aspekte.* Betonwerk und Fertigteil-Technik, Vol. 72 (2): pp.112-115.

41 Ludwig, H.-M.; Neumann, T. (2006): *Entwicklung und Anwendung eines schnellerhärtenden Zementes.* Betonwerk und Fertigteil-Technik, Vol. 72 (5): pp. 28-39.

42 Ludwig, H.-M.; Neumann, T.; Rothenbacher, W. (2008): *Eigenschaften und Anwendung eines Schnellzementes für konstruktive Betonbauteile: höhere Frühfestigkeiten zur Beschleunigung des Fertigungsprozesses*. Beton, Vol. 58 (1-2): pp. 10-17.

43 Sowoidnich, T.; Peters, S.; Möser, B.; Ludwig, H.-M. (2013): *Influence of calcite variety and its modification on cement and Ca_3SiO_5 hydration*. Reactivity of Solids, Ceramika Ceramics, Vol. 115: pp. 149-155.

44 Alizadeh, R.; Raki, L.; Makar, J.M.; Beaudoin J.J.; Moudrakovski, I. (2009): *Hydration of tricalcium silicate in the presence of synthetic calcium-silicate-hydrate.* Journal of Materials Chemistry, Vol. 19 (33): pp. 7937-7946.

45 Odler, I.; Dörr, H. (1979): *Early hydration of tricalcium silicate: II. The induction period*. Cement and Concrete Research, Vol. 9 (3): pp. 277-283.

46 Nicoleau, L. (2011): *Accelerated growth of calcium silicate hydrates: Experiments and simulations.* Cement and Concrete Research, Vol. 41 (12): pp. 1339-1348.

47 Ludwig, H.-M.; Peters, S.; Dressel, D. (2010): *State-of-the-art acceleration technologies for precast concretes.* 17. Internationale IFF-Fachtagung, November, Weimar Germany.

48 Thomas, J.J.; Jennings, H.M.; Chen, J.J. (2009): *Influence of Nucleation Seeding on the Hydration Mechanism of Tricalcium Silicate and Cement.* Journal of Physical Chemistry, Vol. 113 (11): pp. 4327-4334.

[49] Korpa, A.; Kowals, T.; Trettin, R. (2008): *Hydration behavior, structure and morphology of hydration phases in advanced cement-based systems containing micro and nanoscale puzzolanic additives.* Cement and Concrete Research, Vol. 38 (7): pp. 955-962.

[50] Wu, Z.-Q.; Young, J.F. (1984): *The hydration of tricalcium silicate in the presence of colloidal silica*. Journal of Materials Science, Vol. 19 (11): pp. 3477-3486.

[51] Senff, L.; Labrincha, J.A.; Ferreira, V.M.; Hotza, D.; Repette, W.L. (2009): *Effect of nano-silica on rheology and fresh properties of cement pastes and mortars.* Construction and Buliding Materials, Vol. 23 (7): pp. 2487-2491.

[52] Garrault-Gauffinet, S.; Nonat, A. (1999): *Experimental investigation of calcium silicate hydrate (C-S-H) nucleation.* Journal of Crystal Growth, Vol. 200 (3-4): pp. 565-574.

[53] Tattersall, G.H.; Banfill, P.F.G. (1983): *The Rheology of Fresh Concrete*. PITMAN BOOKS, London.

[54] Banfill, P.F.G. (2003): *The rheology of fresh cement and concrete – a review*. 11th International Cement Chemistry Congress, Durban.

[55] Murata, J. (1984): *Flow and deformation of fresh concrete*. Matériaux et Construction, Vol.17 (2): pp. 117-129.

[56] Roussel, N.; Coussot, P. (2005): *"Fity-cent rheometer" for yield stress measurements: From slump to spreading flow*. Journal of Rheology, Vol. 49 (3): pp. 705-718.

[57] Johnson, S.B.; Franks, G.V.; Scales, P.J.; Boger, D.V.; Healy, T.W. (2000): *Surface chemistry – rheology relationships in concentrated mineral suspensions*. International Journal of Mineral Processing, Vol. 58 (1-4): pp. 267-304.

[58] Flatt, R.; Bowen, P. (2006): *Yodel: A Yield Stress Model for Suspensions*. Journal of the American Ceramic Society, Vol. 89 (4): pp. 1244-1256.

[59] Powers, T.C. (1968): *The Properties of Fresh Concrete.* Wiley, New York.

[60] Chong, J.S.; Christiansen, E.B.; Baer, A.D. (1971): *Rheology of Concentrated Suspensions*. Journal of Applied Polymer Science, Vol. 15 (8): pp. 2007-2021.

[61] Kapur, P.C.; Scales, P.J; Boger, D.V.; Healy, T.W. (1997): *Yield Stress of Suspension Loaded with Size Distributed Particles*. AIChE Journal, Vol. 43 (5): pp. 1171-1179.

62 Claisse, P.A., Lorimer, J.P., Omari, M.H. (2001): *Workability of Cement Pastes*. ACI Materials Journal, Vol. 98 (6): pp. 476-482.

63 Roussel, N.; Stefani, C.; Leroy, R. (2005): *From mini cone test to Abrams cone test: measurements of cement-based materials yield stress using slump tests*. Cement and Concrete Research, Vol. 35 (5): pp. 817-822.

64 Wallevik, J.E. (2006): *Relationship between the Bingham parameters and slump*. Cement and Concrete Research, Vol. 36 (7): pp. 1214-1221.

65 Wallevik, O.H.; Wallevik, J.E. (2011): *Rheology as a tool in concrete science: The use of rheographs and workability boxes*. Cement and Concrete Research, Vol. 41 (12): pp. 1279-1288.

66 Roussel, N.; Le Roy, R. (2005): *The Marsh cone: a test or a rheological apparatus?*. Cement and Concrete Research, Vol. 35 (5): pp. 823-830.

67 Saak, A.W.; Jennings, H.M; Shah, S.P. (2004): *A generalized approach for determination of yield stress by slump and slump flow*. Cement and Concrete Research, Vol. 34 (3): pp. 363-371.

68 Flatt, R.J.; Larosa, D.; Roussel, N. (2006): *Linking yield stress measurements: Spread test versus Viskomat*. Cement and Concrete Research, Vol. 36 (1): pp. 99-109.

69 Le Roy, R.; Roussel, N. (2005): *The Marsh Cone as a viscometer: theoretical analysis and practical limits*. Materials and Structures, Vol. 38 (1): pp. 25-30.

70 Schmidt, W. (2014): *Design Concepts for the Robustness Improvement of Self-Compacting Concrete.* PhD Thesis, Eindhoven University of Technology, The Netherlands.

71 Schowalter, W.R.; Christensen, G. (1998): *Toward a rationalization of the slump test for fresh concrete: Comparison of calculations and experiments*. Journal of Rheology, Vol. 42 (4): pp. 865-870.

72 Passhias, N.; Boger, D.V.; Summers, J.; Glenister, D.J. (1996): *A fifty-cent rheometer for yield stress measurements*. Journal of Rheology, Vol. 40 (6): pp. 1179-1189.

73 Flatt, R.J.; Schober, I (2012): *Superplasticizers and the rheology of concrete*. In: Understanding the rheology of concrete (Ed. Roussel, N.), Woodhead Publishing Limited: pp.144-208.

74 Ruecroft, G.; Hipkiss, D.; Ly, T.; Maxted, N.; Cains, P.W. (2005): *Sonocrystallization: The Use of Ultrasound for Improved Industrial Crystallization*. Organic Process Research & Development, Vol. 9 (6): pp. 923-932.

75 Noble, T. (2002): *Ultrasound - Coming Over Loud and Clear*. Chemical Engineering Progress, September 1: pp.10-12.

76 Lord Rayleigh O.M. F.R.S. (1917): *VIII. On the pressure development in a liquid during collapse of a spherical cavity*. Philosophical Magazine Series6 34:200: pp. 94-98.

77 Richards, W.T.; Loomis, A.L. (1927): *The chemical effects of high frequency sound waves in a preliminary survey*. Journal of American Chemical Society, Vol. 49 (12): pp. 3086 – 3100.

78 Suslick, K.S. (1990): *Sonochemistry*. Science, Vol. 247 (4949): pp.1439 – 1444.

79 Suslick, K.S. (1988): *Ultrasound - Its Chemical, Physical, and Biological Effects*, VCH Publisher, New York.

80 Henglein, A. (1987): *Sonochemistry: historical developments and modern aspects.* Ultrasonics, Vol. 25 (1): pp. 6-16.

81 Mason, T.J; Lorimer, J.P. (2002): *Applied Sonochemistry*. Wiley-VCH Verlag GmbH, Weinheim.

82 Suslick, K.S. (1989): *The chemical Effects of Ultrasound*. Scientific American, Vol. 260 (2): pp.80 – 86.

83 Doktycz, S.J., Suslick, K.S. (1990): *Interparticle Collisions Driven by Ultrasound*. Science, Vol. 247 (4946): pp. 1067 – 1069.

84 Hem, S.L. (1967): *The effect of ultrasonic vibrations on crystallization processes*. Ultrasonics, Vol. 5 (4): pp. 202-207.

85 Flint, E.B.; Suslick, K.S. (1991): *The Temperature of Cavitation*. Science, Vol. 253 (5026): pp. 1397-1399.

86 Riesz, P.; Kondo, T. (1992): *Free radical formation induced by ultrasound and its biological implications*. Free Radical Biology & Medicine, Vol. 13 (3): pp. 247-270.

87 Ando, T.; Sumi, S.; Kawate, T.; Ishihara, J; Hanafusa, T. (1984): *Sonochemical switching of reaction pathways in solid-liquid two phases reactions.* Journal of the Chemical Society, Chemical Communications, (7): pp. 439-440.

88 Ando, T.; Bauchat, P.; Foucaud, A.; Fujita, M.; Kimura, T.; Sohmiya, H. (1991): *Sonochemical Switching from Ionic to Radical Pathways in the Reactions of Styrene and* trans-*β-Methylsterene with Lead Tetraacetat.* Tetrahedron Letters, Vol. 32 (44): pp. 6379-6382.

89 Suslick, K.S.; Casadonte, D.J. (1987): *Heterogeneous Sonocatalysis with Nickel Powder.* Journal of the American Chemical Society, Vol. 109 (11): pp. 3459-3461.

90 Lindley, J.; Mason, T.J.; Lorimer, J.P. (1987): *Sonochemically enhanced Ullmann reactions.* Ultrasonics, Vol. 25 (1): pp. 45-48.

91 Suslick, K.S.; Price, G.J. (1999): *Applications Of Ultrasound To Materials Chemistry*. Annual Reviews Material Science, Vol. 29: pp. 295 – 326.

92 Thompson, L.H.; Doraiswamy, L.K. (2000): *The rate enhancing effect of ultrasound by inducing supersaturation in a solid-liquid system.* Chemical Engineering Science, Vol. 55 (16): pp. 3085-3090.

93 Portenlänger, G.; Heusinger, H. (1996): *Mechanische Effekte und Radikale als Auslöser chemischer Reaktionen durch Ultraschall: Intersuchungen an Dextranen als Modellsystem.* Abschlußbericht RCM 00397.

94 Luche, J.-L. (1994): *Effect of ultrasound on heterogeneous systems.* Ultrasonics Sonochemistry Vol.1 (2): pp. 111-118.

95 Ley, S.V.; Low, C.M.R. (1989): *Ultrasound in Synthesis.* Springer Verlag Berlin Heidelberg.

96 Farmer, A.D.; Collings, A.F.; Jameson, G.J. (2000): *The application of power ultrasound to the surface cleaning of silica and heavy mineral sands.* Ultrasonics Sonochemistry; Vol. 7 (4): pp. 243-247.

97 Pohl, M.; Hogekamp, S.; Hoffmann, N.Q.; Schuchmann, H.P. (2004): *Dispergieren und Desagglomerieren von Nanopartikeln mit Ultraschall.* Chemie Ingenieur Technik, Vol. 76 (4): pp. 392-396.

98 Sato, K.; Li, J.-G.; Kamiya, H.; Ishigaki, T. (2008): *Ultrasonic Dispersion of TiO2 Nanoparticles in Aqueous Suspension.* Journal of the American Ceramic Society, Vol. 91 (8): pp. 2481-2487.

99 Pétrier, C.; Francony, A. (1997): *Ultrasonics waste-water treatment: incidence of ultrasonic frequency on the rate of phenol and carbon tetrachloride degradation.* Ultrasonics Sonochemistry, Vol. 4 (4): pp. 295-300.

100 Hoffmann, M. R.; Höchemer, I. H. (1996): *Application of ultrasonic irradation for the degradation of chemical contaminants in water.* Ultrasonics sonochemistry; Vol. 3 (3): pp. 163-172.

101 Margulis, M.A. (2004): *Sonochemistry as a New Promising Area of High Energy Chemistry*. High Energy Chemistry, Vol. 38 (3): pp. 135-142.

102 Riera, E.; Golás, Y.; Blanco, A.; Gallego, J.A.; Blasco, M.; Mulet, A. (2004): *Mass transfer enhancement in supercritical fluids extraction by means of power ultrasound.* Ultrasonics Sonochemistry, Vol. 11 (3-4): pp. 241-244.

103 Virone, C., Kramer, H.J.M.; van Rosmalen, G.M.; Stoop, A.H., Bakker, T.W. (2006): *Primary nucleation induced by ultrasonic cavitation.* Journal of crystal growth, Vol. 294 (1): pp.9-15.

104 Luque de Castro, M.D.; Priego-Capote, F. (2007): *Ultrasound-assisted crystallization (sonocrystalization).* Ultrasonics Sonochemistry, Vol. 14 (6): pp. 717-724.

105 Li, H., Wang, J.; Bao, Y.; Guo, Z.; Zhang, M. (2003): *Rapid sonocrystallization in the salting-out process.* Journal of Crystal Growth, Vol. 247 (1-2): pp. 192-198.

106 McCauseland, L.J., Cains, P.W., Martin, P.D. (2001): *Use the Power of Sonocrystallization for Improved Properties.* Chemical Engineering Progress, Vol. 97 (7): pp. 56-61.

107 Amara, N.; Ratsimba, B.; Wilhelm, A.-M.; Delmas, H. (2001): *Crystallization of potash alum: effect of power ultrasound.* Ultrasonics Sonochemistry, Vol. 8 (3): pp. 265-270.

108 Li, H.; Li, H.; Guo, Z.; Liu, Y. (2006): *The application of power-ultrasound to reaction crystallization.* Ultrasonics Sonochemistry Vol. 13 (4): pp. 359-363.

109 Guo, Z.; Jones, A.G.; Li, N. (2006): *The effect of ultrasound on the homogeneous nucleation of BaSO4 during reactive crystallization.* Chemical Engineering Science, Vol. 61 (5): pp. 1617-1626.

110 Guo, Z.; Jones, A.G.; Li, N. (2006): *Interpretation of the ultrasonic effect on induction time during BaSO4 homogeneous nucleation by a cluster coagulation model.* Journal of Colloid and Interface Science, Vol. 297 (1): pp. 190-198.

111 Lyczko, N., Espitalier, F.; Louisnard, O.; Schwartzentruber, J. (2002): *Effect of ultrasound on induction time and the methastable zone width of potassium sulphate.* Chemical Engineering Journal; Vol. 86 (3): pp. 233-241.

112 Nishida, I. (2004): *Precipitation of calcium carbonate by ultrasonic irradiation.* Ultrasonics Sonochemistry, Vol. 11 (6): pp. 423-428.

113 Dalas, E. (2001): *The effect of ultrasonic field on calcium carbonate scale formation.* Journal of Crystal Growth, Vol. 222 (1-2): pp. 287-292.

114 Boels, L.; Wagterveld, R.M.; Mayer, M.J.; Witkamp, G.J. (2010): *Seeded calcite sonocrystallization.* Journal of Crystal Growth, Vol. 312 (7): pp. 961-966.

115 Santos, R.M.; Ceulemans, P.; van Derven, T. (2012): *Synthesis of pure aragonite by sonochemical mineral carbonation.* Chemical Engineering Research and Design, Vol. 90 (6): pp. 715-725.

116 Enomoto, N.; Katsumoto, M.; Nakagawa, Z. (1994): *Effect of Ultrasound on the Dissolution – Precipitation Process and the Aluminum Hydroxide-Water System.* Journal of the Ceramic Society of Japan, Vol. 102 (2): pp. 1105-1110.

117 Lui, J.; Chen, J.; Yin, Z.; Zhang, P.; Chen, Q. (2004): *Effect of Ultrasound Frequency on the Precipitation Process of Saturated Sodium Aluminate Solution.* The Chinese Journal of Process Engineering, Vol. 4 (2): pp.130-135.

118 Wilding, C.R. (1984): *A combined conduction calorimeter and ultrasonic pulse velocity technique for monitoring the hydration/setting of Portland cement.* Journal of Material Science Letters, Vol. 3 (1): pp. 13-14.

119 Tatarin, R.; Erfurt, W.; Stark, J. (2004): *Continuous ultrasonic investigations during the hydration of cement paste, mortar and concrete*. ZKG International, Vol. 57 (8): pp.69-78.

120 Reinhardt, H.W.; Grosse, C.U. (2004): *Continuous monitoring of setting and hardening of mortar and concrete*. Construction and Building Materials, Vol. 18 (3): pp. 145-154.

121 Chotard, T.; Gimet-Breart, N.; Smith, A.; Fargeot, D.; Bonnet, J.P.; Gault, C. (2001): *Application of ultrasonic testing to describe the hydration of calcium aluminate cement at the early age*. Cement and Concrete Research, Vol. 31 (3): pp. 405-412.

122 Robeyst, N.; Gruyaert, E.; Grosse, C.U.; De Belie, N. (2008): *Monitoring the setting of concrete containing blast-furnace slag by measuring ultrasonic p-wave velocity*. Cement and Concrete Research, Vol. 38 (10): pp. 1169-1176.

123 Trtnik, G.; Gams, M. (2014): *Recent advances of ultrasonic testing of cement based materials at early ages*. Ultrasonics, Vol. 54 (1): pp. 66-75.

124 Keating, J.; Hannant, D.J.; Hibbert, A.P. (1989): *Comparison of shear modulus and pulse velocity techniques to measure the build-up of structure in fresh cement pastes used in oil well cementing*. Cement and Concrete Research, Vol. 19 (4): pp. 554-566.

125 Wedler, G.; Freund. H.-J. (2012): Lehrbuch der Physikalischen Chemie. Wiley-VCH, Weinheim, Germany.

126 Rietveld, H.M. (1969): *A profile Refinement Method for Nuclear and magnetic Structures*. Journal of Applied Crystallography, Vol. 2 (2): pp. 65-71.

127 Hillr, R.J.; Howard, C.J. (1987): *Quantitative Phase Analysis from Neutron Powder Diffraction Data using the Rietveld Method.* Journal of Applied Chrystallography, Vol. 20: pp. 467-474.

128 Jansen, D. (2011): *The hydration of an Ordinary Portland Cement (OPC) and the influence of selected polymers: A mineralogical study using an external standard method for quantitative Xray Diffraction*. PhD Thesis, Universität Erlangen-Nürnberg, Erlangen.

129 Users manual UIP1000hd Hielscher, Germany.

130 Guo, Z.; Zhang, M.; Wang, H.L.; Kougoulos, E. (2005): *Effect of ultrasound on anti-solvent crystallization process*. Journal of Crystal Growth, Vol. 273 (3-4): pp. 555-563.

131 Garrault, S. Finot, E; Lesniewska, E.; Nonat, A. (2005): *Study of C-S-H growth on C_3S surface during its early hydration*. Materials and Structures, Vol. 38 (4): pp. 435-442.

132 Damidot, D., Nonat A. (1991): *The First Hours of Hydration.* In: Hydration and Setting of Cement. Proceedings of the International RIILEM Workshop, E&FN Spon, London: pp. 23-34.

133 Damidot, D.; Nonat, N. (1994): *C_3S hydration in diluted and stirred suspensions (II): properties of C-S-H precipitated during the two kinetic steps.* Advances in Cement Research, Vol. 6 (22): pp. 83-91.

134 Damidot, D.; Nonat, A.; Barret, P. (1990): *Kinetics of Tricalcium Silicate Hydration in Diluted Suspensions by Microcalorimetric Measurements.* Journal of American Ceramic Society, Vol. 73 (11): pp. 3319-22.

135 Damidot, D; Nonat, A. (1994): *C_3S hydration in diluted ans stirred suspensions. (I) study of two kinetic steps.* Advances in Cement Research, Vol. 6 (21): pp. 27-35.

136 Sowoidnich, T. (2015): *A study of retarding effects in cement and tricalcium silicate hydration induces by superplasticizers*. PhD Thesis, Bauhaus-Universität Weimar, Germany.

137 Sowoidnich, T.; Rößler, C. (2009): *The influence of superplasticizers on the dissolution of C_3S.* Proceedings of the 9th ACI International Conference, Seville (Spain): pp. 335-346.

138 Bertolini, L.; Elsener, B.; Pedeferri, P.; Redaelli, E.; Polder, R.B. (2013): *Corrosion of Steel in Concrete – Prevention, Diagnosis, Repair.* Wiley – VCH, Weinheim Germany.

139 Noble, T. (2002): *Ultrasound – Coming Over Loud and Clear*. Chemical Engineering Progress, September 1: pp. 10-12.

140 Wallevik, J.E. (2003): *Rheology of Particle Suspensions – Fresh Concrete, Mortar and Cement Paste with Various Types of Lignosulfonates*. NTNU, Trondheim: p. 12.

141 Powers, T.C. (1968): *The properties of fresh concrete.* New York: Wiley.

142 Aitcin, P.-C. (1998): *High performance concrete.* E&FN SPON, London and New York.

143 Lamb, H. (1993): *Hydrodynamics.* Dover paperback edition (6th Edition), New York: p. 599.

144 Rößler, C.; Eberhardt, A.; Kučerová, H.; Möser, B. (2008): *Influence of hydration on the fluidity of normal Portland cement pastes*. Cement and Concrete Research, Vol. 38 (7): pp. 897-906.

145 Kong, H.-J.; Bike, S.G.; Li, V.C. (2003): *Development of a self-consolidating engineered cementitious composite employing electrosteric dispersion/stabilization*. Cement & Composites, Vol. 25 (3): pp. 301-309.

146 Park, C.K.; Noh, M.H.; Park, T.H. (2005): *Rheological properties of cementitious materials containing mineral admixtures*. Cement and Concrete Research, Vol. 35 (5): pp. 842-849.

147 Vahdani, M.; Mehdipour, I.; Yousefi, S. (2010): *Effects of viscosity modifying admixtures in the rheological properties and stability of self consolidation cementitious materials.* 35th Conference on OUR WORLD IN CONCRETE & STRUCTURES, CI-Premier PTE LTD, Singapore.

148 Mollah, M.Y.A.; Adams, W.J.; Schennach, R.; Cocke, D.L. (2000): *A review of cement – superplasticizer interactions and their models*. Advances in Cement Research, Vol. 12 (4): pp. 153-161.

149 Uchikawa, H.; Hanehara, S.; Sawaki, D (1997): *The role of steric repulsion force in the dispersion of cement particles in fresh paste prepared with organic admixtures*. Cement and Concrete Research, Vol. 27 (1): pp. 37-50.

150 Yamada, K.; Takahashi, T.; Henehara, S.; Matsuhisa, M. (2000): *Effects of the chemical structure on the properties of polycarboxylate-type superplasticizer*. Cement and Concrete Research, Vol. 30 (2): pp. 197-207.

151 Asaga, K.; Roy, D.M. (1980): *Rheological Properties of cement mixes: IV. Effects of superplasticizers on viscosity and yield stress*. Cement and Concrete Research, Vol. 10 (2): pp. 287-295.

152 Rößler, C. (2006): *Hydratation, Fließfähigkeit und Festigkeitsentwicklung von Portlandzement – Einfluss von Fließmitteln, Alkalisulfaten und des Abbindereglers*. PhD Thesis, Bauhaus-Universität Weimar, Germany.

153 Barnett, S.J.; Soutsos, M.N.; Millard, S.G.; Bungey, J.H. (2006): *Strength development of mortars containing ground granulated blast-furnace slag: Effect of curing temperature and determination of apparent activation energies.* Cement and Concrete Research, Vol. 36 (3): pp. 434-440.

154 Escalante-García, J.I.; Sharp, J.H. (2001): *The microstructure and mechanical properties of blended cements hydrated at various temperatures*. Cement and Concrete Research, Vol. 31 (5): pp. 695-702.

155 Regourd, M. (1980): *Structure and behaviour of slag Portland cement hydrates*. 7th International Congress on the Chemistry of Cement (Paris), Vol. 1: pp. III-2/10-III/2-26.

156 Diamon, M. (1980): *Mechanism and kinetics of slag Cement Hydration.* 7th International Congress on the Chemistry of Cement (Paris), Vol. 1: pp. III-2/1-III-2/9.

157 Stark. J.; Wicht, B. (2000): *Zement und Kalk – Der Baustoff als Werkstoff*. Birkhäuser Verlag, Basel.

158 Chen, W. (2006): *Hydration of Slag cements – Theory, Modeling and Application.* PhD Thesis, Univerity of Twente, The Netherlands.

159 Chen, W.; Brouwers, H.J.H. (2007): *The hydration of slag, part 2: reaction models for blended cement*. Journal of Material Science, Vol. 42 (2): pp. 444-464.

160 Dressel, D. (2016): *Reaktivität des Hüttensandes – Thermodynamische Grundlagen und Anwendung*. PhD Thesis, Bauhaus-Universität Weimar, Germany.

161 Khan, K.M.; Ghani, U. (2004): *Effect of blending of Portland cement with ground granulated blast furnace slag on the properties of concrete*. 29th Conference on OUR WORLD IN CONCRETE & STRUCTURES, Singapore.

162 Gerlicher, T.; Heinz, D.; Urbonas, L. (2008): *Effect of Finely Ground Blast Furnace Slag on the Properties of Fresh and Hardened UHPC.* Ultra High Performance Concrete (UHPC), Kassel, No. 10: pp. 367-374.

163 Živica, V. (2007): *Effects of type and dosage of alkaline activator and temperature on the properties of alkali-activated slag mixtures*. Construction and Building Materials. Vol. 21 (7): pp. 1463-1469.

164 Tatarin, R., Erfurt. W. (2006): *Laser-Based Ultrasonic Evaluation of Cement Hydration*. Proceedings: Advances testing of fresh cementitious materials, Stuttgart, Germany, CD-ROM.

165 Krautkrämer, J. Krautkrämer, H. (1969): *Ultrasonic testing of materials.* Springer, Berlin.